Avalanche Runout Prediction for Short Slopes

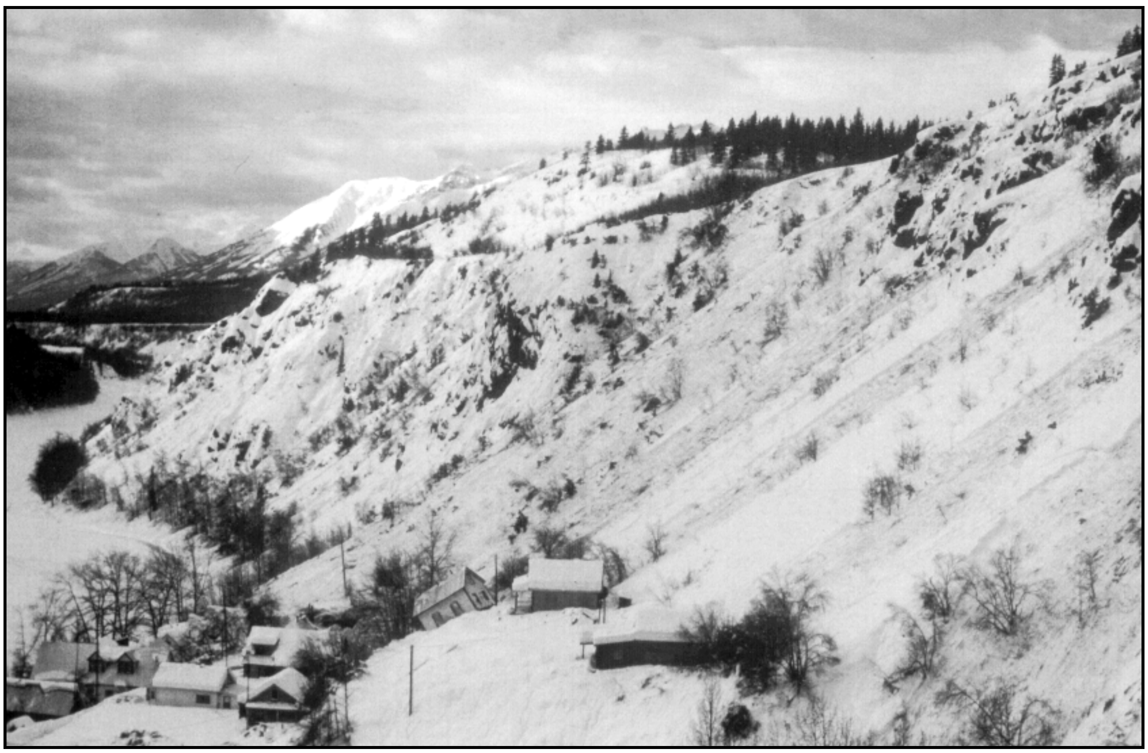

Alan S.T. Jones

UNIVERSITY OF CALGARY

Avalanche Runout Prediction for Short Slopes

by

Alan S.T. Jones

A THESIS

SUBMITTED TO THE FACULTY OF GRADUATE STUDIES

IN PARTIAL FULFILMENT OF THE REQUIREMENTS FOR THE

DEGREE OF MASTER OF SCIENCE

DEPARTMENT OF CIVIL ENGINEERING

CALGARY, ALBERTA

JULY, 2002

ABSTRACT

Avalanche experts recognize that short slopes have different runout characteristics when compared to taller slopes. There have been several residential avalanche accidents in Canada on or near short slopes, yet little research has been conducted in this field.

Data were collected at 48 short slope paths in four Canadian mountain ranges, including the Coast, Columbia, Rocky Mountains and Quebec ranges. Field studies included topographic surveys and estimation of extreme runout distance in each path.

Statistical runout models were developed using the runout ratio and multiple regression methods. Regional differences between mountain ranges were not apparent in the models. Probabilistic runout estimates are provided by these models, which are best applied to avalanche paths less than 275 m high.

A model was developed using multiple regression methods to estimate the average friction coefficient for use in an avalanche dynamics model. This model relates the average friction coefficient to two topographic variables.

ACKNOWLEDGEMENTS

I am indebted to Dr. Bruce Jamieson for providing countless hours of guidance and expertise, and for facilitating financial support for this project. His support and encouragement have made this project possible and enjoyable.

For financial support I am grateful to the British Columbia Ministry of Transportation, the Association of Professional Engineers, Geologists and Geophysicists of Alberta, the Department of Civil Engineering at the University of Calgary, members of the BC Helicopter and Snowcat Skiing Operators Association, the Avalanche Control Section of Parks Canada, and to Canada's Natural Sciences and Engineering Research Council.

For their contributions to this project in providing advice, guidance and identifying field sites, I am greatful to Chris Stethem, Peter Schaerer, Jack Bennetto, Gordon Bonwick, Peter Kimmel, Robin Siggers, Herb Bleuer, Doug Clapp, Karstein Lied, Marc Deschenes, Ladean McKittrick, Dave McClung, Phil Hein, Dave Skjonsberg, Bruce McMahon, Jeff Goodrich, Lawrence Nkemdirim, Peter Jordon, Blair McCleod, Rick Shroeder, Christoph Diezfelbinger, Daniel Germain and Bernard Hétu. For providing field assistance I am grateful to Karen Paulig, Greg Johnson and Bruce Jamieson. Thanks to Doug Wilson for providing photographs and the figure showing the location of the field sites, and to Jack Bennetto for providing the photograph of Telegraph Creek on the cover.

Thanks go out to Greg Johnson, Ben Johnson, Tom Chalmers, Michelle Gagnon, Kyle Stewart, Paul Langevin, Torsten Geldsetzer, Jill Hughes, Bruce Jamieson, Adrian Wilson, and the crew from the Avalanche Control Section of Parks Canada for good snowpit conversations and good turns during three winters at Rogers Pass.

My thanks for helpful discussions on field work and various aspects of avalanche runout to Chris Stethem, Peter Schaerer, Dave McClung and Bruce Jamieson. I am especially grateful to these men for their work and dedication to the study of avalanches in Canada and for providing a framework without which this project would not have been possible.

Finally, I would like to thank my family, friends and especially Karen Paulig for their support and encouragement over the years.

Thank you to all of the above and others who contributed to or supported this project.

TABLE OF CONTENTS

LIST OF TABLES

LIST OF FIGURES

LIST OF SYMBOLS

α	Average slope angle of the avalanche path measured from the extreme runout position to the starting position (º)
α_P	Prediction interval for α as a function of non-exceedance probability, P (º)
β	Average slope angle of the avalanche track meaured from the reference β point (location where the slope first decreases to 10º) to the starting position (º)
β_i	Coefficient that determines the contribution of an individual variable x_i to a regression model
δ	Angle defined by sighting from the extreme runout position to the β point (location where the slope angle first decreases to 10º) (º)
ε	Residual, or random, error in a regression model
μ	Basal friction coefficient used in some avalanche dynamics models
ρ	Average slab density or avalanche flow density ($kg \cdot m^{-3}$)
ρ_t	Density of snow-dust-air mixture in a flowing avalanche ($kg \cdot m^{-3}$)
σ	Population standard deviation
σ^2	Population variance
ξ	Friction parameter related to turbulence in some avalanche dynamics models ($m \cdot s^{-2}$)
θ	Average inclination of the starting zone in degrees (º)
ψ	Average slope angle in an avalanche path segment (º)
Δx	Horizontal reach from the β point to the extreme runout position (m)
Δx_P	Probabilistic horizontal reach (runout) expressed as a function of non-exceedance probability, P (m)
$\Delta x/X_\beta$	Runout ratio, a dimensionless measure of runout distance
$a, b, c, \ldots$	Empirical constants
$A, B, C, \ldots$	Empirical constants
A'	Inverse $(k + 1) \times (k + 1)$ matrix for the data used to build a regression model
b	Scale parameter in a Gumbel distribution
C	Categorical variable describing the degree of confinement in a path
C_D	Drag coefficient for turbulent flow used in the Leading Edge Model

d Test statistic used in the Kolmogorov-Smirnov test of normality and in the Durban-Watson test of serial correlation

D_0 Turbulent resistive force coefficient in the Leading Edge Model (m^{-1})

g Acceleration due to gravity (9.81 $m \cdot s^{-2}$)

G_0 Dynamic Coulomb resistive force used in the Leading Edge Model ($m \cdot s^{-2}$)

h Slab thickness (measured vertically) or avalanche flow height measured perpendicular to the slope in the Leading Edge Model (m)

h_0 Average flow depth of an avalanche on entering the runout zone (m)

H_α Vertical distance measured from the starting position to the extreme runout position (m)

H_β Vertical distance measured from the top of starting position to the β point (m)

H_0 Vertical distance measured from the top of starting position to the low point of the parabola fitted to an avalanche path profile (m)

H_0y'' Scaling parameter that is the product of H_0 and y''

i Whole number in a sequence from i through N

k_P Coefficient of passive snow pressure

M/D Mass-to-drag ratio resistance parameter used in some avalanche dynamics models (m)

n Number of experimental units (sub-sample) selected in a limited portion of the total sample, N

N Number of experimental units (sample) selected from a population

p Probability associated with a statistic, significance level

P Non-exceedance probability

Q_0 Minimum

Q_1 Lower quartile

Q_2 Median

Q_3 Upper quartile

Q_4 Maximum

R Spearman rank correlation coefficient

R^2 Coefficient of determination, square of the correlation coefficient

adjusted R^2 Coefficient of determination adjusted to account for the sample size and

	the number of parameters in a regression model
RF	Categorical variable describing whether or not the extreme runout position is located within a mature forest
RZ Elev	Elevation above sea level of the bottom of the runout zone (extreme runout position) (m)
SE	Standard error of estimate that measures the dispersion of observed values about a regression line
S_o	Length of an avalanche path measured along the slope (m)
SZ Elev	Elevation above sea level of the starting position on an avalanche path
SR	Average surface roughness of an avalanche path measured in metres
T	Categorical variable describing the topography of the starting zone
TP	Ordinal variable for classifying the terrain profile of an avalanche path
u	Location parameter in a Gumbel distribution
ν	Velocity ($m \cdot s^{-1}$)
v_0	Initial or incoming velocity of an avalanche entering a segment in the Leading Edge Model ($m \cdot s^{-1}$)
W	Average width of the starting zone of an avalanche path (m)
WI	Ordinal wind index describing the availability of drifting snow to the starting zone
x	Horizontal distance measured from the starting position (m)
$x_i, x_1, x_2, \ldots, x_k$	Independent variables in a regression model
x_0'	Condition vector forming part of the prediction interval for α_P using multiple regression methods
X_α	Horizontal distance measured from the starting position to the extreme runout position (m)
X_β	Horizontal distance measured between the starting position and the β point (m)
X_R	Runout distance measured along the slope calculated by the Leading Edge Model (m)
y	Vertical distance measured from the extreme runout position (m)
y'	First derivative of the slope function $y = ax^2+bx+c$
y''	Second derivitive of the slope function $y = ax^2+bx+c$, radius of curvature

z_P z-statistic representing standard deviations from the mean for a normal distribution

1 INTRODUCTION

Beware the pine tree's withered branch!
Beware the awful avalanche!

Henry Wadsworth Longfellow, Excelsior

1.1 Effects of snow avalanches

In Canada, snow avalanches affect both people and the results of their industry including roads, residential developments, industrial facilities, mines, railways, power and communication transmission lines, ski resorts, forestry operations and backcountry recreation operations. In areas where avalanche terrain and human activities overlap, it is often essential to define where avalanches can occur and how far they will run on and near the bottom of a slope. The *runout* of an avalanche can be defined as the point of farthest reach of an avalanche deposit within an avalanche path (McClung and Schaerer, 1993, p. 115). The specification of the runout distance for the largest, or *extreme*, avalanche expected within a path is of great importance for land-use planning and zoning in snow avalanche prone areas. Accurate specification of the runout distance is of greatest importance in terms of minimizing the risk to people and structures in avalanche prone terrain. Additionally, there are important economic considerations involved when specifying runout distances, since certain types of land uses may be excluded due to zoning restrictions based on avalanche risk studies.

There are more than a dozen research papers on statistical avalanche runout methods. These methods use terrain parameters to predict extreme avalanche runout positions, and are based on fitting extreme runout positions in a particular mountain range to either extreme value or normal distributions. While the research to date has typically focused on taller slopes with fall heights greater than 300 metres, short slopes are also recognized by avalanche experts as a very important topic, both from a research and a practical engineering perspective (McClung and Lied, 1987; Schaerer, 1991; McKittrick and Brown, 1993; Jamieson and Stethem, 2002). Since 1950, avalanches have killed 31 people in and near residential or public buildings in Canada in six avalanche events (Stethem and

Schaerer, 1979, p. 89-93; Stethem and Schaerer, 1980, p. 19-23; Schaerer, 1987, p. 14-15; Jamieson and Geldsetzer, 1996, p. 171-173, 178-179; Government of Quebec, 2000). Sixteen of these fatalities and three of the avalanche events occurred in either Quebec or Newfoundland, illustrating that avalanche problems affecting residential areas are not confined to western Canada (Canadian Avalanche Association [CAA], 2002a, p. 2). Of this number, twenty fatalities (65%) occurred at the base of slopes with vertical fall heights of 150 m or less (B. Jamieson, personal communication, 2002). These numbers illustrate the importance of the understanding of avalanche runout for short slopes. Knowledge of avalanches from short slopes is also very important for transportation corridors and resource industries, including forestry and mining. These industries often have facilities or operations situated in or passing through terrain with potentially hazardous short slopes for which there is little or no documentation of historical avalanche activity. The ability to estimate runout distances for short slopes that affect these industries can potentially reduce economic losses to these industries and increase worker and public safety.

Avalanche consultants are acutely aware that the existing statistical models for estimating avalanche runout are not very effective for short slopes. These models typically *underestimate* the runout distances when compared to field observations for short avalanche paths (McClung and Lied, 1987). Consequently, practitioners typically apply very conservative margins of error to runout estimates when using these models for short slopes. This additional margin of error is coupled with the intuition and experience of the avalanche consultant to obtain runout estimates within acceptable risk levels. For at least a decade, the eminent Canadian avalanche researcher, Peter Schaerer of Vancouver, Canada has called for research on avalanche runout for short slopes (Schaerer, 1991). European researchers have also acknowledged this gap in the research (B. Jamieson, personal communication, 2002), but to date, limited research in this area has been conducted. This project aims to fill in this gap in the research, and provide some answers to some of the scale problems noted in previous avalanche runout studies (e.g. McClung and Mears, 1991; Nixon and McClung, 1993).

1.2 Types of snow avalanches

A *snow avalanche* can be defined as a volume of snow, usually more than several cubic metres, moved by gravity at perceptible speed (CAA, 2002a, p. 3). Snow avalanches may or may not contain other materials such as rock, soil, or ice. Avalanches release in two distinct ways: *loose snow avalanches* (Figure 1.1) and *slab avalanches* (Figure 1.2).

Figure 1.1. Loose snow avalanche (B. Jamieson photo)

Loose snow avalanches initiate at or near the surface when a small volume of low cohesion snow (typically less than 1 m^3) fails and starts moving down a slope (CAA, 2002a, p. 3). This mass of snow spreads outwards in an inverted v-shape on the slope, *entraining* (accumulating) additional snow as it moves down the slope. Loose snow avalanches, also known as *point releases*, are typically small, but occasionally involve large masses of snow, particularly when the snow is wet. Slab avalanches are initiated by a failure at depth in the snowpack, followed by the sliding movement of a cohesive slab down the slope. This slab initially moves as a cohesive unit, but then breaks up into smaller particles. Most of the larger and more destructive avalanches initiate as slab avalanches, and are considered the more dangerous of the two types of avalanches (McClung and Schaerer, 1993, p. 61). This study is primarily concerned with runout of the largest avalanche event within an avalanche path,

Figure 1.2. Slab avalanche (B. Jamieson photo)

which is typically associated with dry snow slab avalanches.

1.3 Avalanche terrain

An *avalanche area*, or *avalanche terrain*, is defined as a location with one or more avalanche paths (McClung and Schaerer, 1993, p. 89). An *avalanche path* is defined as a fixed location within an avalanche area where avalanches move. Sometimes, evidence of avalanche activity is very obvious, with numerous avalanche paths affecting a particular feature such as a highway (Figure 1.3). However, avalanche terrain is sometimes difficult to identify because evidence of avalanche activity may be obscured by vegetation, avalanche paths are above treeline, there are no *trimlines* (boundaries between vegetation of different age classes) or vegetation in the paths, or paths are overlooked because of their small size (Figure 1.4). The size of avalanche paths can vary from small paths with a vertical fall height of approximately 50 m (e.g. large road cuts, river banks) to very large paths with

Figure 1.3. Numerous avalanche paths affecting the Bear Pass, British Columbia, Canada (British Columbia Ministry of Transportation photo)

Figure 1.4 Smaller avalanche paths that are obscured by vegetation. The full width of this slope is considered avalanche terrain and capable of producing destructive avalanches (B. Jamieson photo)

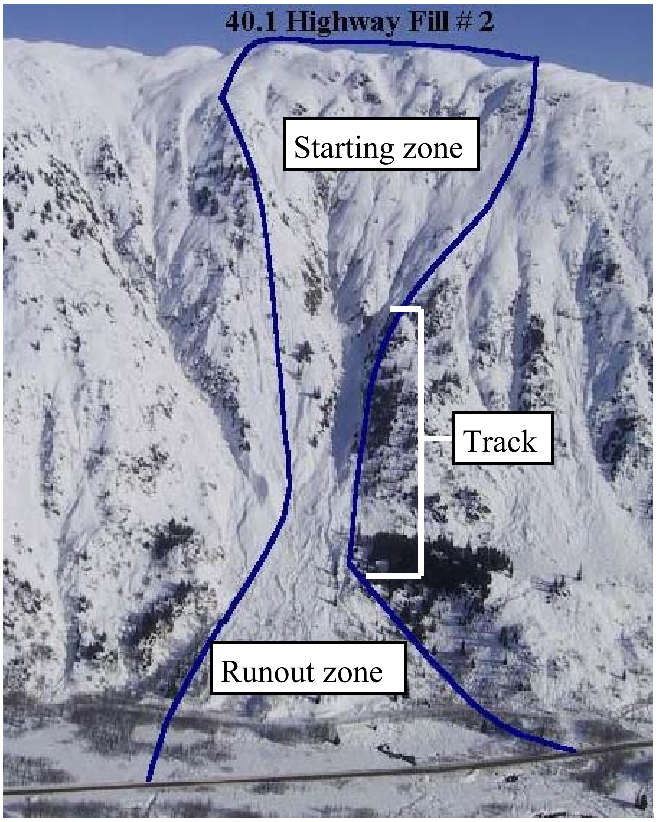

Figure 1.5 An avalanche path showing the three distinct zones: starting zone, track and runout zone. Black line shows the outline of the avalanche path from the starting zone to the highway (British Columbia Ministry of Transportation photo)

vertical fall heights on the order of 2000 to 3000 m (Figure 1.3). While larger paths can be easy to identify on the ground and their runout zone mapped, smaller paths are often difficult to identify. Consequently, short avalanche paths are often the ones where problems arise due to human activities in avalanche terrain.

An avalanche path is typically divided into three distinct zones: a *starting zone*, a *track* and a *runout zone* (Figure 1.5). These zones may be difficult to distinguish, particularly for small paths. The starting zone is the location where unstable snow fails and begins to move down slope. The starting zone typically has slope angles exceeding 25°. Small avalanches may stop in the starting zone. The track is the part of the avalanche path that connects the starting zone with the runout zone, and is sometimes referred to as the transition zone. The track is often poorly defined for short slopes, and may not exist in some cases. The slope angle in the track is typically between 15° and 25°. During larger (extreme) avalanche events, avalanches typically attain a maximum velocity in the track, and have the smallest speed variations there (McClung and Schaerer, 1993, p. 89). Small to medium size avalanches may stop in the track. The runout zone is defined as the part of an avalanche path where avalanches rapidly decelerate, deposit avalanche mass and stop moving. The slope angle in the runout zone is typically less than 15°. Sometimes, the largest avalanches in a path may runout on a lake or the valley bottom, or may run up the opposite side of the valley.

1.4 Examples of residential avalanche accidents on short slopes

To illustrate the importance of avalanches on short slopes in Canada, two examples of residential areas impacted by avalanches are discussed below.

Blanc Sablon is a small village located in eastern Quebec, near the Labrador border (Figure 1.6). Prior to 10 March, 1995 a blizzard had deposited 82 cm of snow in a period of 24 hours, with winds in excess of 100 kilometres per hour (Jamieson and Geldsetzer, 1996, p. 178-179). Several houses were situated near the bottom of an approximately 85 m high slope that accumulated large amounts of snow during the blizzard. On the night of 10 March, an avalanche released on this slope and impacted a house at the base of the slope, tearing off the roof and pushing it to the other side of the street. The avalanche mass buried a man, woman and son, and only the woman survived. In addition to damage to the house, two sheds were destroyed, a power line was damaged and a pick-up truck was partially buried. Total property damage from this avalanche was estimated at $80,000, but additional costs since the avalanche (e.g. investigations, legal fees, mitigation) have greatly exceeded this value. Following this accident, a 3 m high by 1 km long snow fence was constructed along the top of the cliff above Blanc Sablon to reduce the build-up of snow drifts and reduce the likelihood of similar events. More than a dozen houses,

Figure 1.6 Houses located near the bottom of a short slope at Blanc Sablon, Quebec. Two fatalities occurred in a house located near these houses on 10 March, 1995. These houses have since been relocated (B. Jamieson photo).

Figure 1.7 Short slope located adjacent to residential buildings in Kangiqsualujjuaq, northern Quebec. School that was impacted by an avalanche on 1 January, 1999 can be observed at the far right of the photo. Buildings at left are sheds (B. Jamieson photo).

including those shown on Figure 1.6, were not impacted by this avalanche but have since been relocated (Jamieson and Geldsetzer, 1996, p. 179).

A second fatal avalanche accident occurred in the village of Kangiqsualujjuaq, located in northern Quebec. On 1 January, 1999, approximately 500 people were gathered at the local school for New Year's Eve festivities (Government of Quebec, 2000). The school is located near the base of an approximately 85 m high slope on which an avalanche released while people were gathered in the school (Figure 1.7). The avalanche continued beyond the base of the slope and struck the school gymnasium, killing 9 people and injuring another 25.

These examples illustrate the potential serious consequences of having residential areas located near the base of short slopes, and the need for improved knowledge of potential runout distances from short slopes.

1.5 Avalanche motion

An understanding of avalanche motion and dynamics is important to determine the potential avalanche velocities within a path, and to relate these velocities to potential impacts to buildings and other structures or resources in the path. Being able to estimate velocities in the runout zone is also important for zoning purposes since most avalanche zoning methods incorporate a velocity dependent criterion, usually in the form of impact pressure (e.g. Switzerland, 1984; Höller and Schaffhauser, 2001; CAA, 2002b, p. 16).

Describing the dynamics of avalanche motion is a complicated process that involves aspects of fluid, particle and soil mechanics (Harbitz, Issler, and Keylock, 1998). The mathematical problem of describing avalanche motion over complicated terrain is far from solved, and many different avalanche dynamics models are used by experts around the world. Some of these models have a theoretical basis, involve solving differential equations for mass, energy or momentum, and treat avalanches as granular material, a fluid, or a combination of the two (Harbitz et al., 1998). Others are based on a combination of theoretical mathematical models and empirical input parameters (e.g. Salm, Burkard, and Gubler, 1990). Presently, all of these models require a degree of expert judgement to determine the appropriate input parameters for realistic modelling of velocity and runout.

When compared to *wet snow avalanches* (those containing large amounts of liquid water between snow particles) dry snow avalanches typically attain the highest velocities, often produce the largest impact pressures and travel farthest in the runout zone (Mears, 1992, p. 9). Consequently, dry snow slab avalanches are typically used as the design case avalanche for engineering purposes. Only the effects of dry snow slab avalanches are considered in this study.

Dry snow avalanches (Figure 1.8) consist of a mix of snow particles and air (called a *dense core*) at the bottom of an avalanche. This is sometimes accompanied by a powder component, or *powder avalanche*, which usually travels in front of and above the dense core and, sometimes, by an associated *air blast* which travels in front of the dense core or powder component. These two components are typically associated with large, dry flowing avalanches that attain sufficiently high speeds during transport over long distances. The powder component and air blast are not typically associated with shorter slopes and are thus not considered in this study.

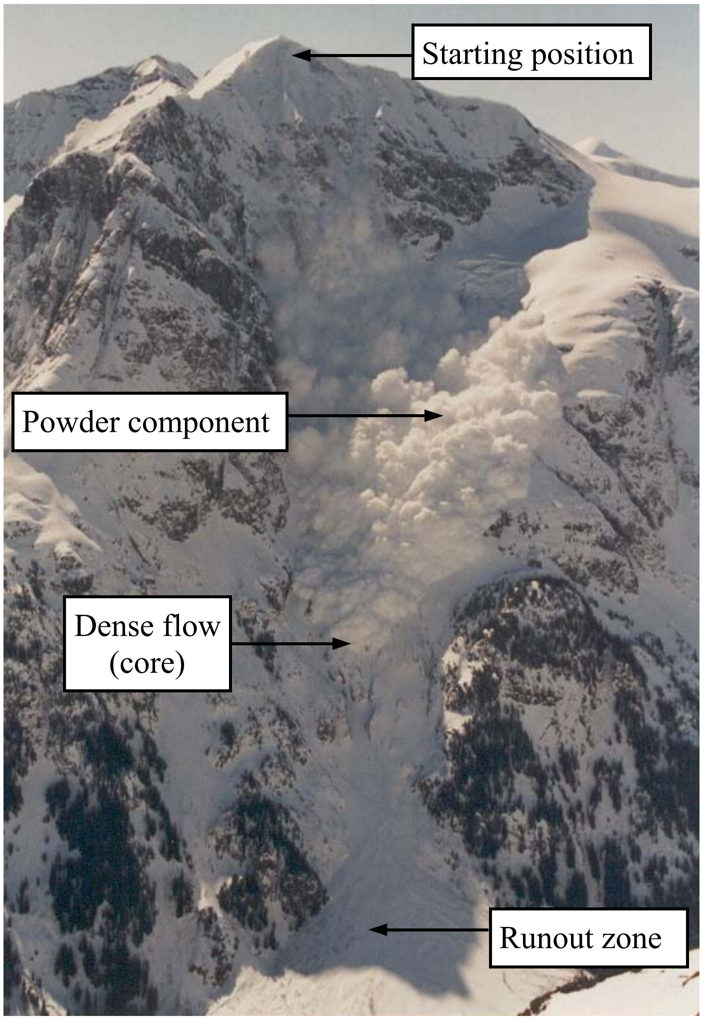

Figure 1.8 Large avalanche in motion. Note the airborne powder component and dense flow at the front of the mass (British Columbia Ministry of Tranportation photo)

With dry slab avalanches, after release of snow in the starting zone, the slab breaks into blocks or particles. As the avalanche moves farther downslope in the path, these particles become smaller due to particle-to-particle collisions and interaction with the ground or snow surface on which the avalanche moves. Eventually, this mass will evolve into a relatively high-density mixture of snow particles and air, and the motion can be described as sliding, flowing, airborne powder, or mixed (Mears, 1992, p. 9). As the flow reaches a velocity greater than approximately 10 $m \cdot s^{-1}$, the smaller particles in this mixture become suspended by the turbulence of the entrained air and forms a low-density powder cloud on the exterior of the dense material, or core. As this mass flows down slope, new snow is entrained (added to the avalanche mass) near the front of the avalanche while mass sometimes drops out of the back of the avalanche.

When an avalanche reaches a sufficiently low angle slope, deceleration and deposition increase, and the avalanche comes to a rest. Depending on the size of the avalanche and the terrain, this may occur in the starting zone, track or runout zone but, for the extreme events, will be in the runout zone. In the case of short slopes, the transition from broken blocks of the slab to a dense flow may or may not occur, depending on the length of the path, amount of snow involved and the terrain characteristics. On very short slopes, the slab blocks may remain partially intact well into the runout zone.

Table 1.1 Typical dry snow avalanche maximum velocity estimates (From Mears, 1992, p. 13)	
Vertical fall height (m)	**Velocity range (m/s)**
100 - 200	20 - 35
200 - 500	35 - 55
500 - 1000	55 - 70

Traditional studies of larger avalanches define the location where the slope angle first decreases to 10° as the start of the runout zone, and define the runout distance as the horizontal distance measured from this point to the extreme runout position (McClung and Schaerer, 1993, p. 117). However, many avalanches do not reach a 10° point before coming to a stop, leaving this definition open to discussion. Avalanches that do not reach the 10° slope angle position would thus be described as having a "negative" runout distance. For short slopes, runout likely begins at slope angles higher than 10°, and the deceleration phase of flowing snow avalanches may begin on slope angles less than 25° (Gubler, Hiller, Klausegger, and Suter, 1986).

Estimates of the maximum velocity that may be attained by dry snow avalanches on paths with variable vertical fall heights are shown on Table 1.1. These data are based on limited velocity measurement data, destructive effects of avalanches and avalanche dynamics calculations (Mears, 1992, p. 11). Field studies have shown that relatively high velocities (e.g. $> 25\ m \cdot s^{-1}$) can be attained by avalanches with vertical fall heights of less than 200 m (McClung and Schaerer, 1993, p. 105; Gubler et al., 1986), implying that the destructive potential of small avalanches can be quite high, despite the limited vertical fall height.

Although a powder cloud component can form for avalanche speeds greater than $10\ m \cdot s^{-1}$ (Mears, 1992, p. 9), the powder component for short slopes is usually not important since there is limited time for a large powder cloud to form ahead of and above the dense flow. Thus, for short slopes, only the dense flowing core component of the avalanche is typically considered for engineering applications.

1.6 Indicators of avalanche size and frequency

There are several ways to estimate both the size and frequency of large avalanches within a given avalanche path, and for estimating runout distances. Oral and written history and direct observations of avalanches are the most reliable method for determining the runout of avalanches in a path. Oral information about the extent of past avalanches can come from local avalanche experts or others who have lived in the area for years and may have observed events. Written history may come from newspapers, historical records, books, diaries or photographs (CAA, 2002a, p. 9).

Vegetation within and adjacent to avalanche paths can provide clues about the maximum extent of extreme avalanches, and the return period of smaller events within the path (Martinelli, 1974). Avalanche motion can damage vegetation such as trees and bushes, and leave evidence of impacts for decades. Table 1.2 shows some vegetation indicators as a function of avalanche frequency.

Analysis of aerial photographs and topographic maps can aid in identifying the extent of avalanche activity. Such analyses can be used to define the starting zones, tracks and runout zones, and estimate the extent of damage to vegetation from avalanches. Where several time series of aerial photographs are available, inferences about the return periods of avalanches can sometimes be made.

Weather and snow records can be used to estimate how much snow may accumulate in an avalanche area, and provide clues about the largest avalanches that may be expected in a path. Variables such as the maximum 3-day storm snow accumulation can be used in combination with avalanche dynamics models to estimate extreme runout distances (e.g. Gubler, 1994).

Surficial materials can sometimes be used to estimate extreme runout and frequency of avalanches in a path. Materials such as vegetation, rock and soil can be transported by large

Table 1.2. Vegetation as an avalanche-frequency indicator (From Mears, 1992, p. 21)

Return period (years)	Vegetation indicators
1 - 10	Track supports grasses, shrubs, flexible trees up to 2 m high; broken timber on ground and at path boundaries
10 - 30	Predominantly pioneer species; young trees similar to adjacent forest; broken timber on ground at path boundaries
30 - 100	Old uniform-aged trees of pioneer species; young trees of local climax species; old and partially decomposed debris
100 - 300	Mature, uniform-aged trees of local climax species; debris completely decomposed; increment core data required

avalanches and deposited in the runout zone. The location of this material can provide clues as to the location of the extreme runout for larger avalanche events. Organic material, such as peat, in the runout zone can sometimes be carbon-dated to provide estimates of return periods for large avalanches (Boucher, Hétu, and Filion, 1999).

1.7 Conventional or dynamics avalanche runout models

Numerous models have been developed since the mid-1950s to simulate the motion of dry, dense flowing avalanches (e.g. Voellmy, 1955; Perla, Cheng, and McClung, 1980; Perla, Lied, and Kristensen, 1984; Norem, Irgens, and Scheildrop, 1987; Salm et al., 1990; McClung, 1990; McClung, Nettuno, and Savi, 1994; McClung and Mears, 1995). These models differ significantly from each other, demonstrating the complexity of avalanche dynamics and lack of detailed knowledge of avalanche flow mechanisms (Keylock and Barbolini, 2001). Harbitz et al. (1998) summarize many of the dynamics models used in practice and some of the theoretical models that have yet to be used for practical purposes (Table 1.3). All of these models require input of terrain characteristics and avalanche material properties, and provide output on avalanche velocity and runout distance. Some models also provide information on flow depth, deposit depth and the lateral extent of the avalanche deposit.

Terrain measurements for input into dynamics models are typically obtained from topographic maps and/or field measurements, and include measurements of slope angles in the starting zone, track and runout zone. Avalanche characteristics such as slab thickness in the starting zone and friction at the base of the avalanche are typically obtained by combining published values, local experience and expert judgment.

The basic concept behind most dynamics models is that the snow accelerates in the starting zone, reaches a maximum velocity in the track, and subsequently decelerates and stops in the runout zone. While the terrain measurements in these models are fixed for a particular path, some models are highly sensitive to changes in the material properties, and thus the velocity and runout estimates can vary significantly. Additionally, some models with more than one input parameter for material properties (e.g. models with both basal and turbulent flow friction coefficients) can have non-unique solutions for runout distance. For this reason, caution must be applied when using dynamic avalanche models, and they

Table 1.3. Summary of some commonly used dense flow avalanche dynamics models

Common Model Name	**Author(s)**	**Model description**
Voellmy	Voellmy (1955)	One-dimensional fluid flow model; force-momentum equation for centre-of-mass; two friction parameters; no entrainment; simple spreadsheet application
PCM	Perla, Cheng and McClung (1980)	One-dimensional fluid flow model; force-momentum equation for centre-of-mass; two friction parameters; no entrainment; based on Voellmy (1955); simple spreadsheet application
PLK	Perla, Lied, and Kristensen (1984)	One-dimensional fluid flow particle simulation model; force-momentum equation for avalanche front; two friction parameters and a random particle velocity parameter; entrainment included; personal computer (PC)-based program
NIS	Norem, Irgens and Schieldrop (1987)	Two-dimensional non-linear visco-elastic granular model; no entrainment; five input parameters; PC-based finite-difference program
Swiss Method	Salm, Burkard and Gubler (1990)	One-dimensional fluid flow model; force-momentum equation for centre of mass; two friction parameters; no entrainment; based on Voellmy (1955); requires input slab thickness; simple spreadsheet application
McClung, 1990	McClung (1990)	One-dimensional granular flow model; mathematically similar to PCM (1980); one speed dependent friction parameter and one frictional limit term; no entrainment; simple spreadsheet application
VARA	McClung, Nettuno and Savi (1994)	Two-dimensional hydraulic-continuum model; mass-momentum equation for avalanche front; two friction parameters; requires avalanche fracture height and volume; no entrainment; PC-based finite difference program
Leading Edge Model (LEM)	McClung and Mears (1995)	One-dimensional granular flow model; force-momentum equation for avalanche front; two friction parameters; no entrainment; simple spreadsheet application

are often used in conjunction with statistical models for runout, field evidence of runout and expert judgment.

The main limitation of using the dynamics method is that the parameters required for the models are typically difficult to estimate, and usually require an intuitive feel and experience of the modeler to provide a reliable estimate of runout. Advantages of using the dynamics method include the ability to model atypical and complicated paths that cannot be modelled by statistical methods. Other advantages include the ability to relate runout estimates in terms of return intervals and risk, a requirement for some jurisdictions (Jónasson et al., 1999)

1.8 Statistical avalanche runout models

Bovis and Mears (1976) and Lied and Bakkehøi (1980) introduced an entirely different method for calculating runout distances based on statistical methods rather than avalanche dynamics models. These researchers found that extreme runout measurements for a particular mountain range can be used to estimate the runout for a particular path within this range by applying methods from probability and statistics. The methods of Bovis and Mears (1976) and Lied and Bakkehøi (1980) use topographic terrain parameters to estimate runout distances, and introduced the reference *β point* in the runout zone from which to measure runout distances (Figure 1.9). They defined the β point as the position at which the slope angle first reaches 10° when proceeding downslope from the starting zone. The corresponding β angle is defined as the angle (measured from the horizontal) at the β point to the starting position of the avalanche path. It is common to quantify extreme runout distances by using the *α angle*, defined as the angle (measured from the horizontal) at the extreme runout position observed in the field to the starting position of the avalanche path. The parameter α is similar to that used by Scheidegger (1973) to estimate the average friction coefficient for large landslides. By the use of multiple regression procedures, Lied and Toppe (1989) showed that using various topographical terrain parameters in addition to the β angle, only the β angle was statistically significant. Subsequently, Lied and Toppe (1989) developed regression equations relating the α angle to β angle for mountains in Norway, and similar expressions have been developed for mountain ranges in Canada and the United States (McClung, Mears, and Schaerer, 1989),

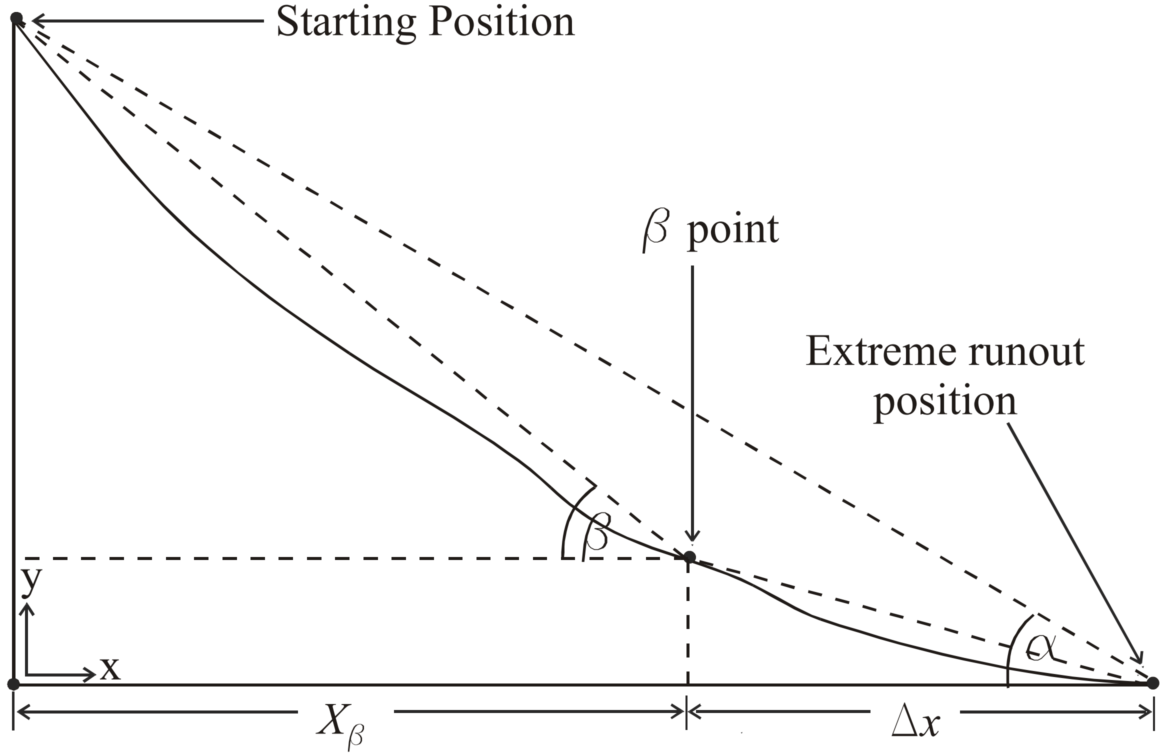

Figure 1.9 Geometry of example avalanche path used for statistical avalanche runout models

Iceland (Johannesson,1998) and Austria (Lied, Weiler, Bakkehøi, and Hopf, 1995).

A second statistical method used for estimating extreme runout distances is known as the *runout ratio method*. McClung and Mears (1991) found that the extreme runout positions for avalanche paths in a particular mountain range fit an extreme value probability density function similar to that used for water discharge from floods. With this method, a non-dimensional runout ratio is plotted versus the probability of avalanches not exceeding a given point on a path (non-exceedence probability). The *runout ratio* is defined as the ratio of the horizontal distance from the β point to the extreme runout position, Δx, to the horizontal reach from the starting position to the β point, X_β (Figure 1.9). The runout ratio can take on values ranging from -∞ to +∞, with a negative value indicating that the extreme runout position is located upslope of the defined β point location (typically 10º slope angle) The non-exceedence probability, P, is defined as the fraction of runout ratios in a particular mountain range that do not exceed a given ratio. Studies conducted by researchers for several ranges around the world (e.g. McClung and

Mears, 1991; Nixon and McClung, 1993) have found significant statistical relationships between the runout ratio and non-exceedence probability (e.g $R^2 > 0.95$) when applied to paths in a single mountain range (Mears, 1992, p. 26). Their results also show that each mountain region consists of a different population and thus each range should be analyzed separately.

It has been found in practice that short slopes tend to run propotionally farther than large slopes, and therefore the models developed for particular mountain ranges using the runout ratio method may not be applicable to short slopes (McClung and Lied, 1987; Nixon and McClung, 1993). It is this finding that has provided the impetus for the current study.

One benefit of statistical runout models over dynamics models is that the errors in runout distances are quantified in standard statistical terms. Thus, a degree of reliability of the statistical runout estimation can be applied with this type of model. The main disadvantage of statistical methods is that they do not work for atypical paths or paths with run-up the opposite side of the valley, or where dataset parameters are not available for a mountain range. Atypical paths may include paths with unusually steep or small starting zones, unusually confined paths, paths that turn corners, or where paths that include two or more merging paths. Other limitations that have been identified (McClung, 2001a) include: paths with more than one β point; paths that have steep runout zones; and paths with no β point in the runout zone. Additionally, most statistical methods do not incorporate return intervals and do not directly give the risk. Recent research by McClung (2000) makes it possible to relate statistical estimates of extreme runout to return periods, providing both spatial and temporal estimates of extreme avalanche runout.

1.9 Influence of terrain and climate on runout

It is generally accepted that avalanche frequency is a function of both terrain and climate (McClung and Schaerer, 1993, p. 121). Terrain factors that affect avalanche frequency include: slope incline of the track, shape of the track, ruggedness or roughness of the track, vegetative cover in the path, exposure to sun and wind, and starting zone size and steepness (McClung and Schaerer, 1993, p. 121). The climate variables with the greatest influence on avalanche frequency include: magnitude, frequency and rate of

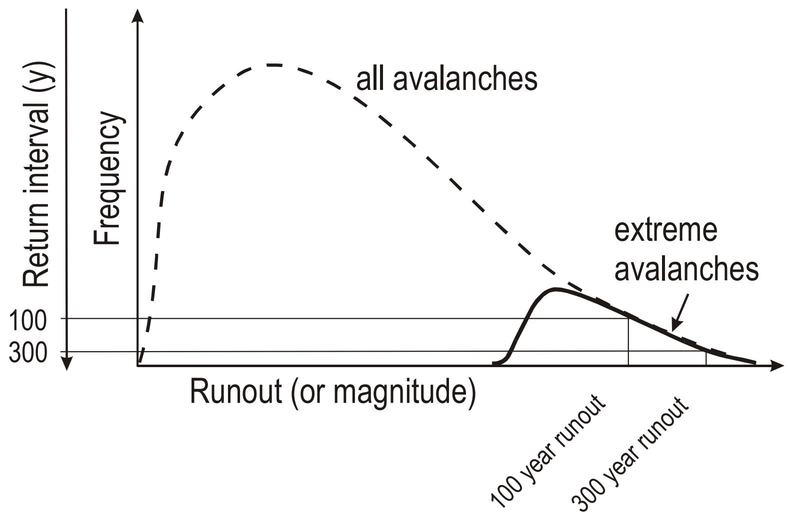

Figure 1.10. Relationship between avalanche frequency and magnitude (After Jamieson, 2001)

snowfall; air temperature; and wind speed and direction (McClung and Schaerer, 1993, p. 121). Numerous studies have been conducted that attempt to relate avalanche activity or frequency to climate variables for operational avalanche forecasting (e.g. Judson and Erickson, 1973; Buser, 1983; Salway, 1976). However, operational avalanche forecasting is mostly concerned with day-to-day changes in meteorological variables, while engineering studies for runout distances need to consider long term climate extremes common within a mountain range.

The relationship between avalanche frequency and either runout or magnitude is shown schematically on Figure 1.10. In this diagram, magnitude and runout are plotted on the same axis, although these terms are not interchangeable. Runout distance is the variable that is typically used in engineering applications to assess the size, or magnitude of an avalanche. Avalanche volume or mass may also be used, but is of limited usefulness in avalanche zoning applications because of the difficulty of modelling avalanche mass balance (Sovilla, Somavilla, and Tomaselli, 2001). It can be observed in Figure 1.10 that avalanche events range from high-frequency low-magnitude avalanches to low-frequency low-magnitude avalanches. For engineering applications, one is interested in the low frequency-high magnitude or runout events, known as the “tail” events on the F-M (frequency-magnitude) graph shown in Figure 1.10. In practice, avalanche events with return periods of 100 to 300 years are typically used for zoning and design of structures. Occasionally, very low frequency events such as those with return periods of 1000 years are used (e.g. Kristensen, Harbitz, and Harbitz, 2000), although this is an exception rather than a usual practice.

Although the relationship between avalanche frequency, terrain and climate is relatively well understood and is used as a basis for avalanche forecasting programs throughout the world, there exists little quantitative research on the relationship between avalanche magnitude and climate. Most studies relate avalanche runout to terrain variables, and assume that for longer return periods (e.g. 100 to 300 years), climatic conditions resulting in extreme avalanches will occur within most avalanche prone mountain ranges. This argument is complicated by the observation that statistical runout models from one mountain range are not applicable to other mountain ranges (Mears, 1992, p. 25). The combined effect of terrain and climate variables is thus accounted for in statistical models by developing different models for individual mountain ranges.

1.10 Applications to avalanche hazard planning and mitigation

In Canada, avalanche hazards to structures, transportation corridors and residential areas are often mitigated by hazard or risk mapping, whereby the element at risk is situated in an area where avalanche return periods are acceptably low, and/or potential impact pressures are acceptably small (CAA, 2002b, p.16). When the risk from avalanches cannot be reduced to acceptable levels by location planning, mitigation measures such as avalanche control programs or defense structures may be applied. In Canada, avalanche control programs are not considered acceptable for permanently occupied structures such as residential developments (CAA, 2002a, p. 18), so avoidance of the hazard is typically applied and, failing this, defense structures may be used.

The hazard or risk mapping process includes several steps in defining the avalanche problem and hazard areas. Some of the following methods may be applied: terrain analysis of maps and air photos; field studies of terrain; study of vegetation for signs of past avalanches; use of oral and written records of avalanches; weather and snow records; study of surficial materials; application of statistical models; and application of dynamic avalanche models (CAA, 2002a, p. 9-10). While not all of the methods listed above may be suitable for a particular problem, experts will typically combine several of these methods in their analysis, weighting the methods in which they have greater confidence. Thus, application of statistical and dynamic avalanche models is only one part of the avalanche problem. Both of these methods are explored in this thesis for their applicability to a dataset consisting of avalanche paths with small vertical fall heights.

1.11 Objectives and Outline

The objectives of this thesis are:

- to develop models based on existing statistical methods for estimating runout for short slopes in the Canadian Coast, Columbia, Rocky and Quebec mountain ranges;
- explore the applicability of avalanche dynamics models for modelling short slopes and develop some practical tools for defining model input parameters;

With regard to the first objective, it should be emphasized that the purpose of this research is to assess a new dataset for short slopes using existing methods for statistical runout modelling. Many alternate methods could potentially prove useful to analyze the dataset, but are considered beyond the scope of this research.

This research provides new tools for avalanche researchers and consultants to better estimate runout distances for short slopes in Canada. By using existing methods to analyze the data, these tools will be presented in a form already familiar to practioners and will hopefully result in easier application of the models. Urban and residential development, forestry and mining industries may also benefit from the results of this research.

Chapter 2 of this study reviews relevant literature on statistical and dynamics runout models, and extreme value statistics. Chapter 3 describes the field methods undertaken for this study, including descriptions of the study areas, site selection, field equipment, survey procedures and type of data collected. Limitations and sources of error from the field program are also discussed in Chapter 3. In Chapter 4, statistical models are used to relate runout distances to terrain parameters. In Chapter 5, a method for estimating friction parameters for the Leading Edge dynamics model is presented and the applicability of this model to short slopes is discussed. Chapter 6 presents the conclusions from this study and suggestions for future research.

2. LITERATURE REVIEW

2.1 Introduction

This review focuses on models of avalanche dynamics and of statistical runout estimation, application of extreme value statistics to runout estimation, and the affect of climate on runout distances. Section 2.2 reviews the extensive literature that exists for dynamic runout models. The application of statistical methods for estimating runout is reviewed in Section 2.3. A review of previous work on the relationship between climate and runout is presented in Section 2.4. The results of the literature review are summarized in Section 2.5.

2.2 Models of avalanche dynamics

The traditional method for determining runout distances involves selecting friction parameters as input into a dynamics model, and using this model to simulate the motion of dense flow avalanches in a particular avalanche path (McClung and Schaerer, 1993, p. 115). Most dynamics models initiate avalanche movement at the top of the starting zone (Figure 1.8), with the avalanche material starting at rest, typically in the form of a dense slab. After initiation of avalanche motion, the avalanche material quickly accelerates down the slope as a result of gravitational force, with larger dry avalanches having two principle flow components: dense and powder (Figure 1.8). Frictional forces at the boundaries of the avalanche material, and internal shear of flow in some models, provide resistance to avalanche movement. In theory, the frictional parameters in dynamics models are physical parameters. In practice, their values are based on fitting the models to real avalanches, resulting in typical ranges of empirical values for the friction parameters. The mass of the avalanche is assumed to remain constant throughout the avalanche path in early models, while some more recent models allow for entrainment of additional mass into the front of the avalanche and deposition of mass from the back of the avalanche in the track and runout zone. The runout position is defined either as the centre or tip of the mass that is farthest from the starting zone.

Most avalanche dynamics models output the runout position and a velocity profile of an avalanche in a path. Some models also provide additional information such as the flow height and width of the avalanche.

Voellmy's (1955) pioneering work on avalanche dynamics included equations of avalanche motion that are still the basis for many modern dynamics models. The Voellmy model describes the movement of the dense flow component of an avalanche as a turbulent fluid, and assumes that snow deforms freely under shear. This model is based on a Coulomb dry friction term and a dynamic term proportional to the square of the velocity (Keylock and Barbolini, 2001). In its simplest form, the fundamental equations from the Voellmy model for the maximum velocity, v and the runout distance, s are:

$$v^2 = \xi h\ (\sin\psi - \mu\cos\psi) \tag{2.1}$$

$$s = \frac{v^2}{2g\ (\mu\cos\psi - \sin\psi) + (v^2 g / \xi h)} \tag{2.2}$$

where ξ represents turbulence in the flow and has units of acceleration (m·s^{-2}) and μ represents basal friction and is dimensionless. Both of these coefficients are thought to depend on the shape of the track and the volume of the avalanche, and are assigned values based primarily on Swiss experience and fitting runout distances to observed avalanches (Mears, 1992, p. 29). The variable h represents the height of the dense avalanche flow, ψ is the slope angle and g is the gravitational constant. Avalanche velocities are calculated segment-by-segment along the path profile, and the avalanche stopping position is calculated in the last segment where the mass has insufficient velocity to surpass the end of the segment.

Salm et al. (1990) expanded and refined the Voellmy model based on Swiss experience and many have used their model extensively for avalanche hazard mapping in Switzerland (Salm, 1997) and elsewhere. Their model uses the same principles and assumptions as the Voellmy model, but provides separate formulations for both unconfined and laterally confined avalanche paths, and uses a modified expression for runout distance. Also, model inputs such as the initial slab thickness and the friction parameters are based on Swiss experience and must be extrapolated to other mountain ranges.

The next important development in avalanche dynamics modelling was the introduction of the PCM model (Perla et al., 1980), which is a simple extension of the Voellmy (1955) model. This model makes several important assumptions, including:

modelling motion at the centre-of-mass of the avalanche; constant mass with no entrainment or deposition; viscous shear is ignored; and the resistive force terms are assumed to be proportional to the combined sliding friction and dynamic drag (Mears, 1992, p. 27). This model uses friction coefficients similar to the Voellmy (1955) and Salm (1990) models, with μ representing basal friction and a mass to drag ratio, M/D being similar to the ξ parameter in the Salm (1990) model.

The model of Perla et al. (1984), commonly known as the PLK model, described avalanche motion as a flow of several hundred particles released from a starting position. This marked a move away from modelling an avalanche as a single mass continuum, instead modelling avalanche motion as a collection of particles that move randomly and independently under the influence of gravity and resistive forces at the base, lateral and top boundaries of the avalanche (Perla et al., 1984). The PLK model used a similar force-momentum equation to that used in the PCM (Perla et al., 1980) and Salm (1990) models, with the addition of a random velocity parameter that allows for a range of particle velocities at each point in the simulation. Entrainment of additional snow particles into the flow was accounted for by adding one new particle per metre of length. Deposition of mass from the flow was accounted for by allowing particles to drop out of the flow when their velocity reached zero.

The NIS model (Norem et al., 1987, 1989) was developed by the Norwegian Geotechnical Institute (NGI) as a two-dimensional model that simulates avalanche motion as a granular continuum that behaves as a non-linear, visco-elastic material. This model is relatively complicated when compared to previous models, with constitutive equations that include: normal stress, shear stress, pore pressure, effective pressure, velocity, Coulomb friction, viscosity, cohesion, and the density of the granular material. This model uses physical input parameters as compared to empirical friction coefficients used by most other models, yields a velocity distribution with avalanche flow height, and has been calibrated using field experiments (e.g. Gubler et al., 1986).

Pioneering work in the field of avalanche motion as granular flow was conducted by Dent (1986) and Savage and Hutter (1989) . The model of McClung (1990) further moved away from modelling avalanche motion as fluid, instead assuming that dense avalanche material behaves as a granular material. McClung (1990) derived an expression for avalanche velocity that was mathematically similar to the PCM model (Perla et al., 1980), with several importance differences. First, only one resistance term, μ, was assumed in the model, located at the base of the flow. This resistance term is assumed to increase as a function of the avalanche position down the path, and consequently varies with velocity. In this model, μ does not explicitly incorporate plowing, entrainment and deposition of snow but these are implicitly accounted for by calibrating the model with field data (McClung, 1990). A second resistance term, D_0, represents turbulent (air/dust) drag at the top of the flow, but is much less important in the model than basal resistance.

The model of McClung and Mears (1995) further developed the idea of avalanche flow as a granular material, expanding the simple theory of McClung (1990) into a more sophisticated model known as the Leading Edge Model (LEM). The LEM was designed for calculating run-up and runout in the deceleration phase of avalanche motion. Important aspects of this model include:

- initial conditions for incoming avalanche velocity must be assumed
- the stopping position of the avalanche deposit is calculated for the tip of the avalanche, as opposed to many other models that estimate runout as the stopping position of the centre-of-mass of the avalanche
- the model estimates the mean deposition depth
- passive snow pressure is included in the model which indirectly accounts for slope-angle dependence
- a slope angle correction is applied to account for momentum losses at slope angle changes

Possibly the most important advantage of this model is that runout is calculated for the leading edge (tip) of the dense flow which is very important when specifying runout distances for land-use planning. When compared to centre-of-mass models, the LEM predicts longer runout distances (McClung and Mears, 1995).

All of the models discussed above have a strong dependence on poorly constrained resistance terms. Without *tranference* or good local datasets (e.g. Switzerland), runout estimates from dynamic models exhibit large variations due largely to the poorly constrained range of friction parameters. Transference involves using information from known runout distances in other paths to estimate the friction parameters and consequently runout distances for a specific path. Sigurðsson et al. (1998) used length-scale tranference methods for the PCM (Perla et al., 1980) model, whereby α-angles were calculated as non-linear functions of the friction parameters, μ and M/D. *Nearest Neigbour* models (e.g. Buser, 1983; Lied et al., 1995) can also be used for transference in which it is possible to find the most similar avalanche paths by systematically comparing topographic parameters and thus estimate friction parameters and runout distances for a specific path.

Many other avalanche dynamics models have been developed, and significant developments are still occurring. Harbitz et al. (1998) provide an extensive review of avalanche dynamics models, including some of the more recent models. These include the VARA model (Natale et al., 1994) a one-dimensional model that takes a hydraulic-continuum approach to avalanche motion; and hydraulic-continuum models of higher dimensionality (e.g. Naaim and Ancey, 1992; Bartelt and Gruber, 1997).

2.3 Statistical runout models

The traditional method for determining runout distances since the work of Voellmy (1955) has been based on using one of the dynamic avalanche models discussed in Section 2.2. The work of Bovis and Mears (1976), Lied and Bakkehøi (1980) and Bakkehøi et al. (1983) introduced a different method for predicting avalanche runout distances. Their work was based on regression analyses of topographic (terrain) parameters for a set of avalanche paths in a mountain range, for which the α angle defines the runout position and is the dependent variable to be determined. Based on an analysis of 206 avalanche paths in Norway, Lied and Bakkehøi (1980) and Bakkehøi et al. (1983) found that runout distances, or α, could be related to four easily measured parameters: the β angle (see Section 1.8 for definitions); H, the vertical distance from the starting point to the low point in a parabola that best fits the path longitudinal profile; θ, the average slope angle of the top 100 vertical metres of the starting zone, and; y'', the second derivitive of the polynomial function

$$y = ax^2 + bx + c \tag{2.3}$$

best fitted to the path profile (i.e. $\alpha = f\,[\beta, H, \theta, y'']$). Perhaps the most important result of this work was the definition the of the β point, a reference point from which to measure runout distances that has been used in all subsequent work on statistical runout prediction.

Further analysis of the Norwegian data by Bakkehøi et al. (1983) showed that the variable β could explain most of the variation in the regression equation for α, and that the α angle could be related to the β angle by the simple expression

$$\alpha = 0.92\,\beta - 1.4° \qquad SE = 2.3° \quad R = 0.92 \tag{2.4}$$

where *SE* is the standard error of regression and *R* is the correlation coefficient. The standard error is an estimate that measures the dispersion of observed values about a regression line. The correlation coefficient is a measure of the strength of the linear relationship between two variables (Mendenhall and Sincich, 1996, p. 127), in this case α and β. The coefficient of determination, R^2 is the square of the correlation coefficient in simple linear regression, and represents the proportion of the sum of squares of deviations of the predictor variable about its mean that can be attributed to a linear relationship between two variables (Mendenhall and Sincich, 1996, p. 134), in this case α and β. The adjusted multiple coefficient of determination, *adjusted* R^2, is similar to R^2 but takes into account both the sample size and number of parameters in the regression model (Mendenhall and Sincich, 1996, p. 192). These terms are defined at this point as they will be used throughout this thesis.

Subsequent work by Martinelli (1986), McClung and Lied (1987) and Nixon and McClung (1993) confirmed the applicability of using topographic parameters to estimate maximum, or extreme, runout distances, and that the β angle is – for most datasets – the only statistically significant parameter for predicting α. Nixon and McClung (1993) found that other topographic parameters in their study were not statistically significant and did not improve their model beyond levels attributable to measurement error in their data.

Research conducted by Mears (1988; 1989) and McClung et al. (1989) found that the regression equation developed by the Norwegian Geotechnical Institute for avalanche paths in Norway was not consistantly applicable to mountain ranges in other parts of the world, and consequently that each distinct mountain range has a unique population of extreme avalanches that needs to be analysed separately (Mears, 1992, p. 26). This led to different regression parameters being developed for other mountain ranges, including: the Purcell, Rocky Mountain and Coast Ranges in Canada (McClung and Mears, 1991; Nixon and McClung, 1993); Coastal Alaska, Colorado Rockies and the Sierra Nevada in the

United States of America (McClung and Mears, 1991); the Austrian Alps (Lied et al., 1995); and mountain ranges in Iceland (Jóhannesson, 1998).

The work of McClung and Lied (1987) presented an alternative method for estimating extreme runout, one that is also based on topographical parameters. Instead of using regression analyses on topographic parameters, McClung and Lied (1987) introduced the concept of a dimensionless runout ratio and applied concepts from probability theory and extreme value statistics to analyse their data. McClung et al. (1989) and McClung and Mears (1991) extended and expanded upon this theory, whereby they found that extreme runout distances fit an extreme value probability distribution, or Gumbel distribution (Gumbel, 1958), similar to that used to describe extreme values for other natural hazards such as discharge from floods. They found that the runout ratio, $\Delta x / X_\beta$ (Figure 1.9), follows an extreme value distribution with respect to a reduced variate, or a non-exceedence probability expressed in the form of the equation:

$$\Delta x / X_\beta = u + b\ (-\ln(-\ln P)) \tag{2.5}$$

where Δx is the horizontal distance from the β point (where the slope first decreases to 10º) to the extreme runout position, X_β is the horizontal distance from the starting position to the β point, P is the non-exceedence probability or the fraction of runout ratios that do not exceed a given value, and u and b are location and scale parameters in a Gumbel distribution, respectively. In this equation, the variables Δx and X_β are determined either during field studies or from maps, and the variables u and b are determined by regression analyses for a set of avalanche paths. Rank order statistical methods are used to assess the significance of the regression (e.g. Watt et al., 1989).

McClung and Mears (1991) presented analyses using the runout ratio method for several mountain ranges, including: the Canadian Rockies and Purcells; Western Norway; Coastal Alaska; the Colorado Rockies; and the Sierra Nevada in California. They found that, for non-exceedence probabilities greater than 0.5, a Gumbel distribution provided a good fit to their data set of over 600 avalanche paths for each mountain range. Subsequent analyses provided location and scale parameters for the British Columbia Coast Mountains (Nixon and McClung, 1993), the combined Madison and Gallatin Ranges of southwest Montana (McKittrick and Brown, 1993), and the mountains of Iceland (Jóhannesson, 1998).

McKittrick and Brown (1993) presented, for the first time, analyses of a dataset that included mostly shorter slopes, with all the paths surveyed in southwest Montana having a vertical fall height of less than 553 m (mean of 248 m). All studies prior to this included data for mostly larger slopes, with a mean vertical fall height of approximately 700 m. Perhaps the most important result of this work was the definition of the β point as the location where the slope first decreases to 18º, rather than the value of 10º commonly used for taller slopes. By defining the location of the β point higher in the avalanche path, McKittrick and Brown (1993) obtained a better fit of their dataset using a Gumbel distribution. A possible interpretation of this finding is that extreme avalanches on shorter slopes begin decelerating on steeper inclines than extreme avalanches on larger slopes a hypothesis that is explored in this thesis.

Although McKittrick and Brown (1993) offered no physical explanation for the improved fit of their data for a β point located at 18º, other studies have found that locking of particles in the avalanche flow begins at slope angles of about 25º, and that large, dry avalanches are beginning a decelerating phase at this slope angle (Gubler et al., 1986; McClung and Mears, 1995). Thus, there may be a physical basis for using higher slope angles for definining the location of the β point, particularly for shorter slopes in which the avalanche mass may not reach a high velocity (e.g. > 30 m s^{-1}) before beginning to decelerate.

As early as 1987, McClung and Lied (1987) noted that their model likely did not apply well to short slopes with a vertical fall height of less than 350 m. McClung and Mears (1991) and Mears (1989) noted the importance of length-scale effects for data from the Colorado Rocky Mountains and Sierra Nevada Range of California. To investigate this, McClung and Mears (1991) partitioned data into two somewhat arbitrary datasets, based on X_β = 1000 m. For the Colorado data, they found that higher runout ratios (relatively longer runout distances) were associated with X_β < 1000 m, which seems to support the hypothesis that extreme avalanches on smaller slopes runout proportionately farther than on taller slopes.

Nixon and McClung (1993) also noted scale effects with the Rocky Mountains and Coast Ranges of Canada, and partitioned their data for the Rocky Mountains at X_β = 1500 m and at X_β = 2100 m for the Coast Mountains. Using a non-exceedence probability of 0.99 for the Rocky Mountain dataset, they found that runout distances are 15 % higher than the non-partitioned data for $X_\beta < 1500$ m and 28 % higher for $X_\beta > 1500$ m. These results cleary illustrate the importance of scale effects in runout modelling, and indictate that this phenomenon may be even more pronounced for short slopes.

McClung (2000), combines both temporal and spatial distributions in the prediction of avalanche runout. This work is based on extreme avalanche runout distances fitting a Gumbel distribution, as discussed above, and the avalanche arrival rate fitting a Poisson distribution (McClung, 1999). This model also provides a means of estimating the probabilistic extreme avalanche width. Although his model framework leaves open the possibility of using a distribution for runout distances other than Gumbel, his findings are supported by data from over 600 avalanche paths in eight mountain ranges.

Barbolini et al. (2000) have also presented recent work on avalanche runout prediction by integrating statistical and dynamics models for five European avalanche sites. In this paper they propose a method for avalanche hazard zoning that integrates both statistical and dynamic models and provides a level of confidence in the model output.

2.4 Climatic effects on runout

Avalanche runout is known to be dependent on numerous variables that can be classified into two main groups: terrain and snowpack (Bovis and Mears, 1976; Mears, 1984). The effect of terrain parameters on runout has been the subject of extensive research, as discussed in Section 2.3, and has resulted in several statistical models that relate α to β. The type of snow involved in the avalanche and the climatic conditions leading up to the avalanche are not explicitly included in the analysis, but are intrinsically included in these empirically derived formulae. Some dynamics models, such as the Swiss model (Salm et al., 1990), incorporate empirically developed snow depth (slab thickness) variables for the different climate regions within Switzerland, thus incorporating climate factors into the runout model.

Because statistical models are designed to be applicable to extreme avalanche events, it is assumed that, over a long time period, optimal climatic conditions will develop in each path at least once, and that avalanches will run to extreme runout positions in response to these conditions (Lied and Bakkehøi, 1980). Despite this, there are known to be distinct differences in runout characteristics that depend on regional climate variations (Mears, 1984). Consequently, there is no single model to describe runout in all avalanche paths, and different models have been developed for different climatic regions.

Although there is conclusive evidence that climate and snowpack characteristics are important components of extreme avalanche runout, few studies have attempted to separate the climate effects from the terrain effects in the runout models or identify specific climate parameters that may be important in runout prediction. Mears (1984) goes as far as stating that: “Climatically-induced variables may, in fact, be more important in determining runout potential than some easily-measured terrain variables”. Mears (1984) compared extreme runout distances for paths with the smallest α angles found in the coastal Alaska and central Colorado areas. Although he did not conduct a rigourous statistical analysis, he found that the mean α angle for the paths in Colorado was lower than in coastal Alaska and, consequently, the Colorado paths had propotionately longer runout distances. He attributed this to climatic differences between the two regions, and provided several reasons, including: the more shallow soft slabs in Colorado quickly fluidize while the thick, well-bonded Alaskan slabs encounter more resistance along the path; the lower elevation Alaskan tracks and runout zones often contain wet snow that absorbs energy from the avalanche mass; and the larger, well developed vegetation in Alaska serves to dissipate energy more quickly than the open forests in Colorado. While all of these factors are a result of climatic differences, specific climate or snowpack parameters were not identified to help quantify the climatic effect.

McClung (2001b) did analyses on climate variables for avalanche paths in western Canada, including the mean maximum water equivalent in the starting zone, a categorical Wind Index (Schaerer, 1977) which contributes to snow supply, and several vegatation parameters. However, this study only addressed avalanche frequency and avalanche size, not extreme avalanche runout distances.

2.5 Summary

Some dynamic and statistical (topographic) models for avalanche runout were reviewed in this chapter. Dynamics models were first developed to model the movement of dense flowing snow and typically provided information on avalanche velocity and runout distances. Two main types of avalanche dynamics models emerged from these studies, including those that model avalanche motion as a turbulent fluid and those that model avalanche motion as granular flow. These models have become more complicated through the years as more rigourous computational methods are available for analysis and the theoretical basis for the models incorporates more complex physical aspects of avalanche motion. Dynamics models can be used to estimate avalanche runout distances, but the estimates are highly dependent upon user experience in estimating parameters such as friction coefficients and snow slab dimensions.

Statistical models were developed that required the input of simple terrain parameters that can either be obtained from topographic maps or surveyed in the field. By regression analysis of terrain parameters collected for a set of avalanche paths in a mountain range, models were developed to provide statistical estimates of runout distance. Most notably, the β point was defined as the location in an avalanche path where the slope first decreases to 10^{o}, and it was found that avalanche runout distances could be related to the angle β measured from the β point to the top of the starting zone. Two methods for developing runout models for a given mountain range emerged from this research: the α-β (regression) method and the runout ratio method.

Both dynamics and statistical models for avalanche runout prediction incorporate regional differences between different mountain ranges. These differences are intrinsically part of the models and are empirically derived. Although the importance of climatic effects on avalanche runout has been recognized, only limited research has been conducted to quantify these effects and their relationship with extreme runout distances.

3. METHODS

3.1 Study areas

Data for this project were collected at avalanche paths located in the Canadian Coast, Columbia, and Rocky Mountains and mountain areas of Quebec during the summers of 2000 and 2001 (Figure 3.1; Table 3.1). Two sites in the Mount Baker area (Cascade Range) of Washington State are included with the Coast Range paths. Detailed field studies were conducted by the author at 46 individual sites during the 2000 and 2001 field seasons. An additional two sites located in Quebec (Kangiqsualujjuaq and Blanc Sablon) were previously surveyed by Bruce Jamieson and incorporated into this study. Thus, a total of 48 sites are included in this study.

Data were collected from four different mountain ranges in order to assess the affect of the different climate regimes in each range on avalanche runout distances. The Coast Range is classified as a maritime snow climate, and is characterized by relatively heavy snowfall and mild temperatures (McClung and Schaerer, 1993, p. 18). The Rocky Mountain Range is classified as a continental snow climate, and is characterized by relatively low snowfall and cold temperatures. The Columbia Mountain Range is classified as an intermountain (or transitional) snow climate, which is a transitional zone between maritime and continental conditions (McClung and Schaerer, 1993, p. 17-18). The Chic Choc Range and other sites in Quebec have been classified as an intermountain snow climate for this study, although they're relatively close to coastal areas.

3.2 Site selection

Sites were selected in the four study area mountain ranges based on several criteria, including: vertical fall height; reasonably good access by vehicle and foot; well defined path characteristics (e.g. starting and runout zones); well defined extreme runout position; and no run-up on the opposite side of the valley or runout into a water body. These criteria are discussed in the following sections.

It was considered important to obtain a geographically diverse sample so that the affect of climate on avalanche runout distances could be studied for the four mountain ranges. Sixteen sites were surveyed in the Coast Mountains, 10 sites were surveyed in the

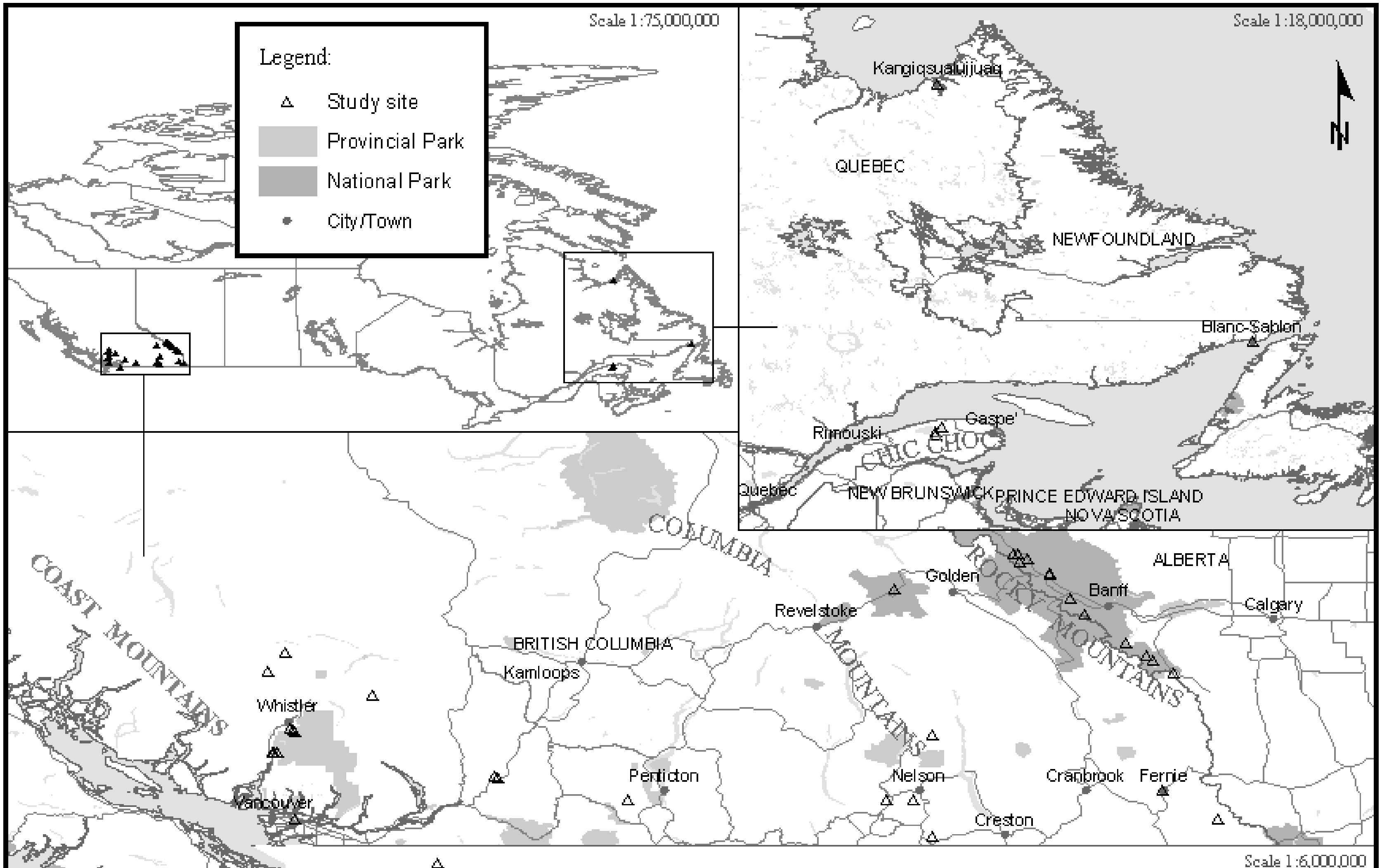

Figure 3.1 Location of study sites and mountain ranges

Table 3.1 Study sites and locations

Mountain Range	**Location**	**Study sites**
Coast Mountains	Vancouver North Shore mountains, BC	Mount Seymour
	Mount Garibaldi area, BC	Brohm Ridge, Brohm Ridge Col, Brohm Village West Slope
	Whistler, BC	Whistler East Ridge, Flute Summit NE Ridge, Franz's Run Cliffs
	Goldbridge area, BC	Donnely Creek, Green Mountain
	Near the Mount Baker Ski Area, Washington	Mount Baker Southwest, Mount Baker Northeast
	Coquihalla summit, BC	Zum Southwest Peak, Zopkios Ridge
	Duffy Lake Road area, BC	Blowdown Creek
	Near the Apex Mountain Resort, Penticton, BC	Apex Mountain Main, Apex Mountain East
Columbia Mountains	Glacier National Park, BC	Schroeder Shoulder
	Kootenay Pass, BC	Cornice Ridge North, Power Creek Ridge, Siwash East Ridge, Kootenay Pass 1, Kootenay Pass 2
	Highway 3a near Retallack, BC	Stenson Creek Headwall
	Near the Whitewater Ski Area, BC	Hummingbird Pass, Evening Ridge, Backside Ridge
Rocky Mountains	Kananaskis Country, AB	Black Prince, Shark Mountain, Quarry Mountain
	Banff National Park, Icefields Parkway, AB	Crowfoot Bumps, Pulpit Pimple, Hector Ridge North, Hector Ridge South, Bow Summit
	In the Fernie Ski Resort, BC	Knot Quite
	Southwest of Fernie, BC	Harvey Bowl

Table 3.1 (continued)		
Mountain Range	**Location**	**Study sites**
Rocky Mountains (continued)	Near the Lake Louise Ski Resort, AB	Redoubt Mountain, Wolverine Ridge
	Banff National Park, Bow Valley, AB	Copper Mountain
	Near the Sunshine Ski Resort, AB	Wawa Bowl
	Highwood Pass, AB	Highwood Ridge
Quebec	Mount Hogsback area, Chic Choc Mountains, QC	Monte Blanche LaMontagne, Mont Lyell
	Mont Jaques Cartier area, Chic Choc Mountains, QC	Mont Jaques Cartier Saddle, Mont de la Passe West, Mont de la Passe East
	Northern Quebec	Kangiqsualujjuaq
	Eastern Quebec	Blanc Sablon

Columbias, 15 sites were surveyed in the Rockies, and 7 sites were surveyed in the Chic Choc Range or other parts of Quebec, giving a small sample of sites from each range, but a reasonably large sample size (48 paths) for the combined dataset. The sites vary in latitude from approximately 48°47' to 51°38' North and in longitude from 65°55' to 123°10' West. Elevations of the starting zones of the paths range from approximately 85 m to 2500 m above mean sea level. Thus, a geographically diverse sample set was obtained both in terms of longitude and latitude, as well as in terms of elevation range.

The vertical fall height of the avalanche paths, measured from the top of the starting zone to the bottom of the runout zone, was a prime consideration in this study. Based on previous studies (e.g. McClung and Lied, 1987; McKittrick and Brown, 1993) it was decided that paths with vertical fall heights less than or equal to 350 m would be considered for the study. However, it was sometimes not possible to estimate the vertical fall height of the path accurately until the survey was complete, and consequently some paths were surveyed that exceeded 350 m in height. There was no lower limit criterion for vertical fall height, as long as the path had well defined starting and runout zones and a well defined extreme runout position. Specifically, damage to vegetation in the runout zone had to be discernable, or the path had to have a historical record of large avalanches. Practically, few slopes with vertical fall heights of much less than 100 m were found that met all of the criteria.

Paths were chosen that were reasonably accessible using a combination of vehicle and foot access. In many cases, road access to the sites was relatively good, usually requiring less than two hours approach on foot from a highway or secondary road.

Paths were chosen that had well defined starting zones and runout zones. In order to ensure accurate field surveys, it was critical that the top of the starting zone could be determined, and that the width of the starting zone could be estimated. Thus, short slopes with starting zones within densely forested terrain were not considered because it would be difficult to determine the location of the starting zone in these areas. The runout zone also had to be well defined so that the extreme avalanche position could be defined. In most cases, there was no historical data available for the extreme runout position at the study sites, so vegetation was used to estimate the extreme runout position and estimate return periods for smaller events in the path. Both channelized (confined) and unconfined paths were included in this study. Although avalanche behaviour and runout characteristics can differ significantly between confined and unconfined paths (Mears, 1992, p. 6; Lied and Bakkehøi, 1980), including both in the study made comparisons of runout for these types of paths possible.

The final criterion was that the avalanche path did not run-up onto an adverse slope or runout into a water body such as a lake or river. The statistical models that have been developed for runout estimation are not applicable when the avalanche runs up onto an adverse slope. This is particularly important when applying α-β models, in which increasing runout onto an adverse slope will result in an decreasing α angle and shorter runout, whereas the model is based on decreasing α angles being associated with longer runout distances. Some dynamics models can be used for run-up problems (e.g. McClung and Mears, 1995), but it was decided to forego the added complication of run-up and seek sites that did not have this characteristic. Where avalanche paths runout onto water bodies such as lakes or rivers, the extreme runout position usually cannot be defined from vegetation, typically requiring the use of historical records, geomorphological (e.g. Blikra and Saemundsson, 1998; Boucher et al., 1999) or paleoenvironmental methods (e.g. Caterino, 1998). Historical records were typically not available for short slopes in the study area, and the other methods are typically prohibitively expensive. Thus, these paths were excluded from this study.

Because of the difficulty of finding short slopes that meet all of the above criteria, when a suitable path was found it was usually surveyed and included in the dataset. By including sites in the dataset based primarily on the above criteria, biases in the dataset were reduced with respect to other criteria such as aspect, elevation, steepness, or other terrain factors. Although the sample is not truly a random sample, it is likely that these paths give a good representation of short slopes in their respective mountain ranges.

3.3 Equipment

Field equipment used for this study included very simple, commonly used surveying equipment, including: a fibreglass measuring tape, clinometer, compass, altimeter, hip-chain, pruning saw, and increment borer. This equipment is described below and is shown in Figure 3.2.

A 100 m fibreglass tape, commonly known as a tight-chain, was used to measure slope distance on the ground. The tape was graduated in 0.05 m increments, but was read to the nearest 0.5 m. Considering variations in ground cover and lateral deflections of the tape from the avalanche path centreline, the accuracy of the tape is considered to be approximately ± 2 m per 100 m, or 2 %.

A sighting clinometer (Suunto PM-5/360PC) was used to measure slope angles between points along the profile. The clinometer is graduated in 1° increments, and was read to the nearest 0.5°. The accuracy of the clinometer is considered to be ± 0.5°.

A magnetic compass (Silva Model 515 Ranger) was used to measure the orientation of the starting zone with respect to true north. This compass is graduated in 2° increments and was read to the nearest 1°. The accuracy of the compass is considered to be ± 1°, although the true aspect of the starting zone can vary significantly, especially when the starting zone is concave or convex across the slope.

An altimeter watch (Casio Pathfinder) was used to estimate elevations in the starting

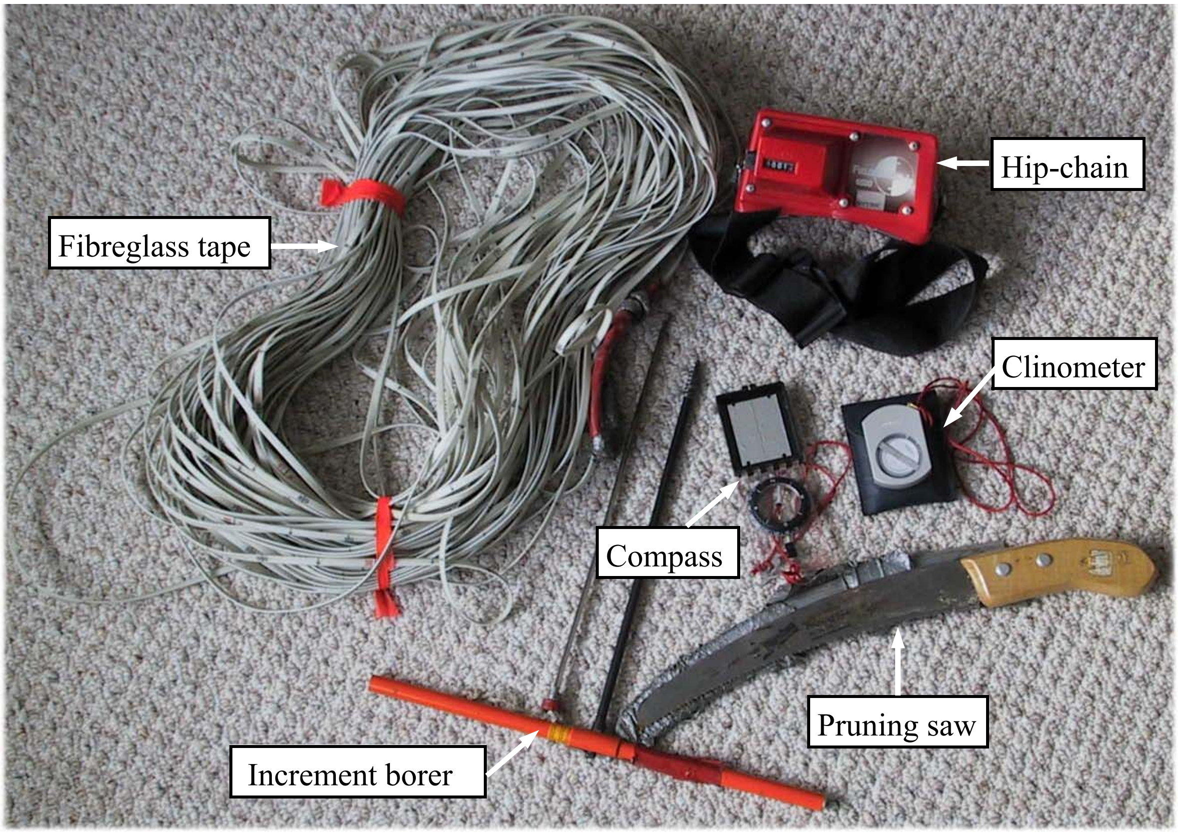

Figure 3.2 Field equipment used for surveying avalanche paths

zone, in addition to using topographic maps. The altimeter was also used as an independent check for the slope angles and distances obtained with the clinometer and fibreglass chain. The altimeter is graduated in 5 m intervals, and is considered to be accurate within 5 m (at best) when properly calibrated to a known elevation on the day of the survey.

A hip-chain (Fieldranger 6500) was usually used to measure the width of the starting zone in lieu of using the fibreglass tape. The hip-chain is used to measure distance from a point by tying a thin string to a fixed object such as a tree branch and automatically releasing string from a housing unit as one walks away from the object. A calibrated wheel mechanism located in the box measures the distance walked along the ground as a function of the amount of string released. The hip-chain is graduated in 0.1 m increments, and was read to the nearest 1 m. Because of stretch in the string and deflections from the line of measurement, the hip-chain is considered to be accurate to approximately ± 5 m per 100 m, or 5%.

A pruning saw was used for vegetation analysis in the runout. The saw was either used to cut branches to date the age of the branch, or for sectioning small trees to provide the age of the tree and date specific impacts to the tree using tree-ring analysis (see Section 3.5).

An increment borer was used to obtain core samples from trees to date the age of trees and/or impacts from avalanches. An increment borer consists of a hollow, steel bore that is threaded at one end and has at the other end a cross-piece that provides leverage for screwing the borer into a tree. Once the bore is inserted into a tree, a steel extractor is inserted into the centre of the bore, a barbed end grabs onto the tree core near the centre of the tree, and the core is subsequently removed from the bore by removing the core extractor from the steel bore.

Other field equipment included standard field data recording materials (notebooks, pencils, camera, etc.) and safety equipment (radio, bear repellant spray, first aid, etc.).

3.4 Survey procedures

All avalanche paths in the dataset were surveyed from the approximate top of the starting zone to the interpreted end of the extreme runout position in the runout zone. The paths were surveyed using a fibreglass chain and clinometer (Figure 3.2). Two surveying methods were used depending on the number of people in the survey. When two people were surveying the path, the slope was surveyed in sections, with each section representing a segment of approximately equal slope angle. The chain was extended between the two field workers to obtain the slope distance, and the average slope angle was obtained by one worker taking a clinometer reading at eye level on the other worker. Typically, measured segments varied between 10 m and 25 m in slope length, and there were typically between 10 and 25 segments per path.

When there was only one field worker, the fibreglass chain was extended down the slope to it’s full length of 100 m. The distance from the top of the starting zone was measured at each point corresponding to a notable change in slope angle. The slope angle was measured with the clinometer from these points in both the upward and downward slope directions by sighting on a feature of approximately equal height to the worker (e.g. a location on a tree or boulder), or by approximating a height equal to the surveyor’s upslope and downslope of the surveyor. The second method does not give as accurate a slope angle reading as when there are two workers. However, the average slope angle for each segment was measured at both endpoints and averaged, giving reasonably good estimates (accuracy of approximately 1º). Additionally, elevation readings were made at each point using an altimeter, which provided a secondary check on the slope angle and distance readings using simple trigonometric functions.

The position of the extreme avalanche runout for each path was deduced from vegetation damage or historical records. Similar to earlier studies (e.g. McClung and Mears, 1991; McKittrick and Brown, 1993), the goal of the runout survey was to identify the location of the "100-year" return period event, commonly referred to as the "extreme" runout position. However, the true return period for the extreme runout likely represents return periods of 30 to 300 years, introducing unavoidable random variation in the data (McClung and Mears, 1991). The cores obtained using the increment borer or sections cut with a saw were used to date trees in the runout zone using common plant dendrochronology procedures (e.g. Burrows and Burrows, 1976).

In some cases, the frequency of avalanches with differing return periods was observed as a series of steps in the ages of vegetation, commonly referred to as trimlines. In these areas, younger trees were observed in the areas affected by more frequent avalanches, while older trees grew in areas affected by larger avalanches with longer return periods. Dating the mature timber at the edge of the extreme runout position gives an approximate lower limit for return periods in this area, while younger trees and specific types of tree damage in the runout zone allow one to determine the relative frequency of smaller avalanches in the path.

3.5 Vegetative indicators of runout

Damage to trees and shrubs in avalanche paths are the result of the snow and entrained debris impacting the vegetation or from the associated wind blast which sometimes accompanies large avalanches (Hansen-Bristow and Birkeland, 1989) (Figure 3.3). The vegetation responds to these impacts in different ways and is sometimes completely destroyed. Types of vegetation disturbance that can be used to date the frequency or extent of avalanches include: variation in tree growth rings or types of

Figure 3.3 Vegetation damage caused by a large avalanche. Note large amounts of woody debris carried and deposited by the avalanche

reaction wood, tilting, scarring, growth curvature or stem indentations, stem breakage, branch trimming or breakage, tree burial or root exposure, tree removal, and tree succession. All of these disturbances except for tree succession are evident on individual trees, while tree succession is an indication of the response of an ecosystem to avalanche impacts (Hansen-Bristow and Birkeland, 1989). Burrows and Burrows (1976) and Hansen-Bristow and Birkeland (1989) provide extensive reviews of procedures using evidence of vegetation impacts for dating avalanche events. The methods used for this study are summarized below.

Dendrochronology is the method whereby tree rings within the trunks of trees can be counted to determine the age of a tree as well as date climate or avalanche impact events. A set of dark and light bands or tree rings indicate one year of growth, with the light band representing the "earlywood" grown during the spring through fall, and the dark band representing the "latewood" grown through the end of the growing season (Hansen-Bristow and Birkeland, 1989). These rings can be counted on a core or section to

Figure 3.4 Tree rings in a sectioned tree

determine the age of a tree (Figure 3.4). Advanced methods of dendrochronology use tree rings to relate tree growth to changes in climate or other ecological conditions (e.g. fires, impacts, disease) and provide specific dates for these events. These advanced methods were not used in this study.

Downslope tilting can occur when a tree is impacted by an avalanche

Figure 3.5 Tree that has responded to avalanche impact by growing upslope, up-righting itself to the vertical (B. Jamieson photo)

Figure 3.6 Large tree impacted by two smaller trees in avalanche flow showing flagging of lower branches (B. Jamieson photo)

(Figure 3.5). In response to this tilting, the tree will usually undergo a curving process to re-orient the upper part of the tree in a vertical position. Reaction wood, a type of wood that grows in reaction to a disturbance, can be observed on the downslope side of the tree where the tree is curving to a vertical position. By counting rings above and below the point of curve, the date of an impact may be estimated.

Scarring occurs when debris entrained within a flowing avalanche (e.g. rocks, trees or wood debris) impacts a tree (Figure 3.6), subsequently removing some of the bark and possibly wood. Avalanche debris typically impacts the upslope side of the tree, but may also impact the side of the tree. Rockfall may result in similar scarring to that caused by avalanche impacts, and may be difficult to differentiate in the field. After a tree is impacted, the tree responds by eventually covering the scar over with wood or bark of a younger age than the surrounding wood or bark. Wood of different ages in scarred areas may be observed in the field, particularly in cross-section, and the age of the impact can

Figure 3.7 Flagging of tree branches at the edge of an avalanche path

be dated by counting the annual growth rings from the location of the unaffected wood.

Flagging, also known as branch trimming, is common in parts of an avalanche path affected by dense flow, although powder avalanches and air blasts can inconsistently result in removal of branches (Figures 3.6 and 3.7). Typically, flagging will be evident on the upslope side of the tree, but may also be evident on the sides. Larger avalanches may also break the trunk of a tree or remove tree tops when the avalanche mass becomes airborne. Trees that survive breakage of branches or the trunk may continue to grow new sprouts which grow vertically upwards. The age of these sprouts can be dated either by core sections or by counting branch growth tiers, and the approximate date of the impact to the tree can be determined. There may be a lag time from when the damage occurred and growth initiated, and this needs to be accounted for when interpreting the age of a sprout. This lag time can be several years, depending on the growing conditions at the site. Flagging may also be used to approximate depth of flow for an avalanche, since the lower limit of the height of the undisturbed branches from the ground should relate to the depth of the dense, avalanche flow.

When trees are removed from an avalanche path, gradual succession of trees on the path will occur. Thus, there may be a younger age class of trees within the central part of the avalanche path and several different age classes of trees on the margins of the path. The boundaries between these age classes are known as trimlines (Figure 3.8). By determining the age of the oldest trees on the avalanche site, an approximate minimum time since a major avalanche can be deduced. Dating the trees in each trimline may provide an estimate of return periods for major avalanches in a path.

Accumulations of trees, branches and rocks in the runout zone may indicate the

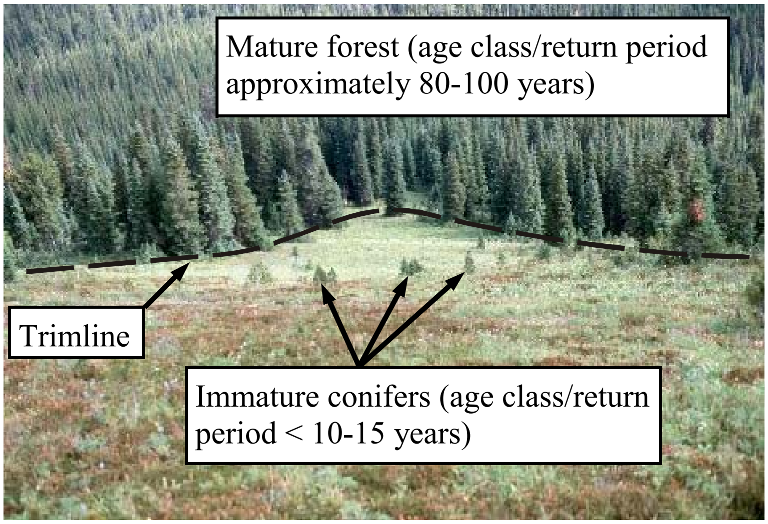

Figure 3.8 Trimline between a mature forest and regenerating conifers

Figure 3.9 Woody debris in avalanche runout zone

Figure 3.10 New tree growth growing vertically from broken tree

extent of large avalanches (Figure 3.9). Although branches will decay in a short period of time, large trees will remain on the site for a long period of time, particularly cedar trees. Soil and rock deposits will also be visible on the site for long periods of time, typically until obscured by vegetation. New trees will often grow vertically from tree debris or broken tree stems (Figure 3.10), giving an approximate date since a major avalanche. Areas where trees are lying downslope in the same direction are also good indicators of avalanche activity.

3.6 Description of data

In addition to the avalanche path survey data, various other data were collected to describe each avalanche path. These data categories are shown in Table 3.2. An example of the field notes for the Hector Ridge South path and a profile for the Schroeder Shoulder path are included in Appendix A and B, respectively.

Detailed descriptions of each of these data categories will be provided in the subsequent sections of this report as each is used in the analyses. The sections below will provide a summary of the data categories.

Each path was assigned a unique name and Path Identification (ID) number. Where a path had a known name, this was adopted for the path. Otherwise, a unique name was assigned based on the path's geographic location. The Path ID number was assigned using a letter and number combination, whereby the letter designates the mountain range in which the path is located (i.e. R for Rockies, W for (West) Coast, C for Columbias, Q for Quebec and Chic Choc mountains) and the number identifies the order in which the paths were surveyed in each range. The date that each path was surveyed is also shown.

Survey data was collected in the form of slope angle and slope distance between points, as discussed in Section 3.4. These values were translated into an x-y coordinate system that will be discussed later in this thesis.

The measured alpha and beta angles were slope angles measured from the horizontal by sighting back to the top of the starting zone from the extreme runout position and the location where the slope angle first reaches 10º in the runout zone, respectively. For some paths, these angles were not recorded either because the surveyed path did not reach a slope angle of 10º or the top of the starting zone was not visible from the runout zone.

Table 3.2 Data collected for each avalanche path

Data category	**Description**
Path ID	Identification number for each path (e.g. R1 for path 1 in Rockies)
Path name	Descriptive name for each path, either pre-existing or assigned
Date surveyed	Date path was surveyed in field
Survey data	Survey data, including slope distance and angle between points for each segment
Measured α-angle	Angle measured from runout position to top of starting zone
Measured β-angle	Angle measured from 10º slope angle point on path to top of starting zone
Starting zone data: • Average inclination • Aspect • Elevation • Average width • Topography	 Average slope angle measured in upper part of starting zone Aspect typically measured in the centre of the starting zone Elevation of the top of the starting zone Width of the upper part of the start zone Categorized topography (e.g. linear, convex, concave)
Wind index	Index relating the position of the starting zone to drifting snow potential based on a five-class system
Bottom of runout zone elevation	Elevation of extreme runout position in runout zone
Surface roughness	Surface roughness in avalanche path, measured in metres
Degree of confinement	Degree of confinement between track and runout zone (e.g. gully, unconfined)
Runs out in forest	Location of extreme runout position with respect to dense forest
Additional information	Any other pertinent information

Several measurements were made in the starting zone to obtain an average slope angle in the starting zone. This angle can have a large degree of variability depending on the configuration of the starting zone.

The starting zone aspect was measured in several locations in the central to top part of the starting zone to obtain an average value. Measurements were made using a magnetic compass adjusted for local declination.

The elevations of the top of the starting zone and the bottom of runout zone were measured using a calibrated altimeter and were compared to a topographic map for accuracy.

The average width of the starting zone was measured at the top of the starting zone, and is an estimate of the maximum width of avalanche that could initiate within a particular avalanche path. The boundaries are typically defined by either a topographic feature (e.g. gully sidewall, rock band) or a vegetative feature (e.g. dense forest).

The topography of the starting zone was described qualitatively, and classified as one of several general categories. These categories include: linear (planar) slope; concave; convex; complex; and gully. More rigourous categorizations of the topography have been applied in other studies (e.g. McClung, 2001b) but it was decided that simpler categories would suffice for this study given the relatively small area of the starting zone for most of the surveyed paths

The snow supply available for each avalanche starting zone was described qualitatively in the field and then categorized according to the five-part Wind Index (Schaerer, 1977). This scale describes the access of the avalanche starting zone to drifting snow. These categories are summarized as (Schaerer, 1977): (1) starting zone completely sheltered from wind by a surrounding dense forest; (2) starting zone sheltered by an open forest or facing the direction of the prevailing wind; (3) starting zone an open slope with rolls or other irregularities where local drifts can form; (4) starting zone on the lee side of a sharp ridge; and (5) starting zone on the lee side of a wide, rounded ridge or next to a large open area where large amounts of snow can be moved by wind.

The ground surface roughness is an approximate measure of the height of irregularity in the ground surface, excluding vegetation. Features such as stumps and logging slash were included in surface roughness in areas where forest harvesting had occurred. Ground surface roughness was estimated in the field in metres, and classified in terms of the following three categories: (1) low ground surface roughness, with < 1 m relief; (2) moderate ground surface roughness, with 1-2 m relief; and (3) high ground surface roughness, with > 2 m relief (McClung, 2001b).

The degree of confinement defines the relative confinement of the path between the starting zone and the track. This is important since confined avalanche paths may create higher velocities than unconfined avalanche paths (Lied and Bakkehøi, 1980), although higher friction in confined paths may negate any such effect. The degree of confinement was described qualitatively in the field and each path was included in one of four categories: (1) unconfined; (2) partially confined; (3) strongly confined; and (4) gully.

The variable termed “runs out in forest” describes whether or not it is believed that the extreme runout position is located within mature timber, downslope of any obvious trimlines, or is within open, treeless terrain. This can be important since it differentiates between paths where the avalanche flow comes to a stop in un-forested terrain primarily due to frictional forces at the base of the avalanche flow forces from those where the avalanche flow comes to a stop primarily because of frictional forces from impacts with mature trees. The affects of forests on avalanche runout distances is a complicated subject which is currently the focus of several other studies (e.g. McClung, 2001b; Bartelt and Stöckli, 2001; Weir, In Press 2002). The paths were included in one of two categories: (1) runs out in forest; and (2) does not run out in forest.

3.7 Limitations and sources of error

It is inevitable that numerous sources of error were introduced into this study during the collection of data for the paths. Limitations and sources of error are discussed in this thesis where they are considered to have an important effect on the results. Some of the error sources in this study have been described in previous sections of Section 3, primarily with respect to errors introduced during the field survey (Section 3.3). Further discussion is provided below.

As discussed in Section 3.2, biases were introduced into this study when defining the criteria that each site had to meet for inclusion into the dataset. The sample of short slopes used in this study is not truly a random sample since each site had to meet criteria such as the vertical fall height of the path and reasonable vehicle and foot access, criteria that were constrained by geographical factors. Biases associated with factors such as aspect, elevation, steepness, vegetation type are assumed to be limited. This is due to the limited number of sites that were found to meet the basic criteria, so that when a suitable site was found it was usually included in the study regardless of the other factors.

The majority of measurement error in this study came during the field survey of each path. Rather simple surveying techniques were used during this study that introduced instrument errors into the data. The errors associated with each surveying instrument and surveying techniques were discussed in Sections 3.3 and 3.4. The most important surveying errors are likely associated with distance measurements using the tight chain (i.e. 2 m per 100 m, or 2 %) and the clinometer which has an accuracy of ± 0.5°, which is negligable in the horizontal direction, but translates to an error of approximately 2 m per 100 m, or 2 %, in the vertical direction.

The other important surveying error lies in determining the location of the extreme runout position, as discussed in Section 3.4. The choice of the "100-year" avalanche event as the "extreme" runout position, while somewhat arbitrary, has come to be accepted as the definition of "extreme runout", particularily when applied for engineering purposes. Because of the difficulty in using vegetation to define the location of the 100-year avalanche event, the true return period of the extreme runouts may vary from 30 to 300 years, but is probably more in the range of 30 to 100 years for the sites surveyed. Also, it is assumed that extreme runout positions for short slopes include only vegetation impacts from dense flow avalanches. It is possible that in some of the larger paths, impacts to vegetation may have also resulted from powder avalanches or air blasts associated with the dense flow. These impacts can exceed the location of the runout position of the dense flow.

Another limation may be that trees in some areas may only reach a maximum age on the order of 100 years while in other areas trees may not reach such an age due to environmental factors such as fires, insects or disease. For example, it may be difficult to determine the runout associated with a 100-year avalanche event in areas where trees only attain a maximum age of 50 years.

4. STATISTICAL RUNOUT MODELS

However big floods get, there will always be a bigger one coming;
so says one theory of extremes, and experience suggests it is true.

President's Water Resources Policy Commission, p. 141

4.1 Introduction

Extreme snow avalanche runout distance is a function of both terrain and climatic variables. Some previous studies have shown that avalanche runout in certain mountain ranges depends strongly on terrain parameters, particularly the β angle. In Section 4.2, the variables used in this study are defined. Section 4.3 presents the statistical distribution and variability of terrain parameters collected for this study. Models are developed to estimate runout distance for short slopes using the runout ratio and multiple regression methods in Sections 4.4 and 4.5, respectively. The purpose of these models is to be able to estimate extreme runout distances for short slopes as a function of either the runout ratio, $\Delta x/X_\beta$, or the alpha angle, α. These models are compared in Section 4.6, and Section 4.7 provides a summary of Chapter 4.

4.2 Variable definitions

As shown on Table 3.2, various categories of data were collected for the short slopes in the dataset. These data can be represented as 25 distinct terrain variables, including 3 categorical variables, 2 ordinal variables and 20 variables with interval or ratio properties. The variables used in the following analyses are shown on Table 4.1. The naming conventions for variables are based on previous studies (e.g. Lied and Bakkehøi, 1980; Bakkehøi et al., 1983; McClung and Lied, 1987), but have been modified where considered appropriate for this study. Some key terrain variables were previously defined in Section 1.8, while the remainder are defined below and are shown graphically in Figure 4.1.

The delta angle, δ, is defined by sighting from the extreme runout position to the β point, with the angle measured from the horizontal. This variable is a measure of the

Table 4.1 Descriptive statistics for the short slope database (all mountain ranges)

	Variable	n	Mean	Standard deviation	Q_0 Minimum	Q_1, Lower quartile	Q_2 Median	Q_3, Upper quartile	Q_4 Maximum
β-point at 10°	Beta angle, β (°)	46	27.5	3.4	19.1	25.8	27.5	30.0	34.1
	Delta angle, δ (°)	46	10.1	14.9	-49.4	4.3	11.5	17.9	45.4
	Reference angle ratio, α/β	46	0.97	0.14	0.72	0.86	0.99	1.04	1.29
	Runout ratio, $\Delta x/X_\beta$	46	0.051	0.285	-0.572	-0.112	0.018	0.255	0.558
	Vertical fall height to β point, H_β (m)	46	240	143	48	145	231	305	744
	Horizontal reach to β point, X_β (m)	46	457	253	94	273	441	615	1264
	Runout distance, Δx (m)	46	-16	174	-723	-41	10	58	340
β-point at 24°	Beta angle, β (°)	46	32.8	2.8	25.0	31.1	32.5	34.7	38.5
	Delta angle, δ (°)	46	15.1	4.9	5.7	11.9	15.3	16.8	29.0
	Reference angle ratio, α/β	46	0.81	0.12	0.59	0.72	0.82	0.89	1.10
	Runout ratio, $\Delta x/X_\beta$	46	0.722	0.580	-0.394	0.357	0.613	0.919	2.424
	Vertical fall height to β point, H_β (m)	46	190	125	27	98	187	242	634
	Horizontal reach to β point, X_β (m)	46	290	176	52	173	274	381	894
	Runout distance, Δx (m)	46	151	148	-353	75	119	238	568
	Alpha angle, α (°)	46	26.5	4.5	18.8	23.1	26.6	29.3	39.0
	Vertical height to runout position, H_α (m)	46	224	120	51	145	223	295	593
	Vertical height to low point on parabola, H_0 (m)	46	216	166	28	110	206	286	963
	Total horizontal distance, X_α (m),	46	441	220	124	251	445	579	1183
	Slope length of path, S_0 (m)	46	512	253	138	303	509	675	1382
	Second derivative of the slope function, y'' (m^{-1})	46	0.0023	0.0019	0.00065	0.0011	0.0018	0.0025	0.0085
	Scale parameter for path profile, H_0y''	46	0.332	0.144	0.071	0.249	0.321	0.414	0.650

Table 4.1 Continued. Descriptive statistics for the short slope database (all mountain ranges)

Variable	n	Mean	Standard deviation	Q_0 Minimum	Q_1, Lower quartile	Q_2 Median	Q_3, Upper quartile	Q_4 Maximum
Starting zone inclination, θ (º)	46	38.3	5.0	27.5	34.5	38.0	42.0	47.5
Starting zone aspect, Aspect (º)	46	139	113	2	49	97	226	360
Starting zone elevation, SZ Elev (m)	46	1773	540	85	1513	1890	2140	2490
Runout zone elevation, RZ Elev (m)	46	1480	609	0	1251	1613	1897	2381
Surface roughness, SR (m)	46	0.5	0.4	0.1	0.3	0.3	0.5	1.5
Wind Index, WI (ordinal data)	46	3.5	1.2	2	2	4	5	5
Width of start zone, W (m)	46	98	90	17	45	65	100	500
Terrain Profile, TP (ordinal data)	46	2.1	0.6	1	2	2	2	3

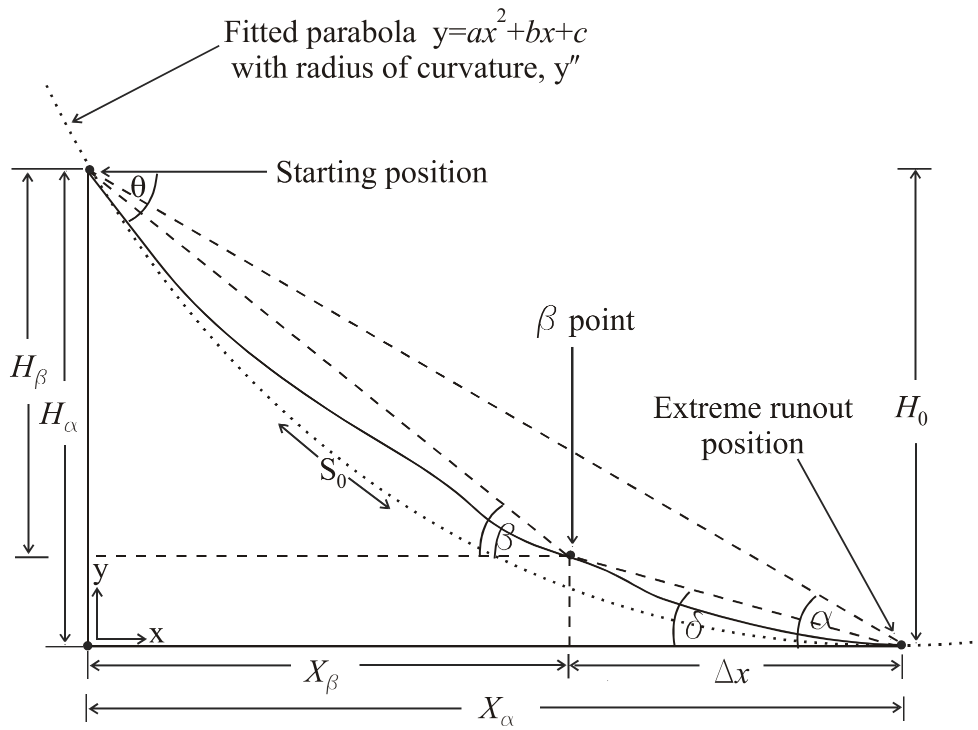

Figure 4.1 Geometry of example avalanche path showing most terrain variables used in the analyses. x-y coordinate system is shown with origin at lower left of figure.

average slope angle in the runout zone. It may be noted in Table 4.1 that unusually low values of δ were obtained in several of the paths (e.g. Q_0 = -49.4º using a β point at 10º). This can be explained by the fact that the location of the β point was found using fitted parabolas and, in several cases, the β point was located far downslope of the observed α point (the extreme runout position observed in the field). Thus, these paths are assigned negative values of δ, and these may be large if the β point was located far downslope of the α point. Similarily, very low values of Δx (e.g. Q_0 = -723 using a β point at 10º) can be observed in Table 4.1, and reflect the same reason as for unusually low values of δ. These observations illustrate that the choice of the β point at 10º may not be well suited to this dataset. As discussed later in this chapter, an alternate β point is proposed for where the slope first decreases to 24º in the path profile.

The runout ratio, $\Delta x/X_\beta$, is a dimensionless variable that relates horizontal distances Δx and X_β to the reference slope angles α, β and δ (McClung and Mears, 1991):

$$\frac{\Delta x}{X_\beta} = \frac{\tan\beta - \tan\alpha}{\tan\alpha - \tan\delta} \tag{4.1}$$

The alpha to beta angle ratio, α/β, is a dimensionless ratio of the two reference angles, α and β.

The vertical path displacement, H_α, is the vertical distance measured from the top of the starting position to the extreme runout position.

The vertical displacement to the β point, H_β, is the vertical distance measured from the top of the starting position to the β point.

The slope length of the path, S_0, is defined as the distance measured in the field along the path segments from the top of the starting position to the extreme runout position.

The terrain profile for each avalanche path was represented by fitting the polynomial parabolic curve

$$y=ax^2+bx+c \tag{4.2}$$

to the surveyed profile between the top of the starting position and the extreme runout position. The x-y coordinate system used for defining Equation 4.2 for each path is shown in Figure 4.1. This parabolic curve provided an excellent fit to the surveyed avalanche paths using regression techniques, with coefficients of determination, R^2, greater than 0.98 for every path in the dataset. The second derivative of the polynomial curve (Equation 4.2), y'', has a value of $2a$ and indicates the radius of curvature of the path profile (Lied and Bakkehøi, 1980).

The vertical displacement to the bottom of the parabola, H_0, is defined as the vertical distance measured from the top of the starting position to the lowest point on the fitted parabola (Equation 4.2), the location where the first derivative (slope) of the polynomial curve, y', is zero.

The variable H_0y'' is the product of H_0 and y'' which, according to Lied and Bakkehøi (1980), makes the path profile independent of the total vertical fall height, and thus serves as a dimensionless scale parameter.

The terrain profile variable, TP, is an ordinal variable that is related to the radius of curvature, y'', but accounts for the very abrupt change in curvature associated with *hockey-stick* profiles (Figure 4.2). A value of 1 represents a slope with a nearly linear transition from the track to the runout zone; a value of 2 represents a path with a concave parabolic shape and a relatively smooth transition from the track to the runout zone; and 3 represents

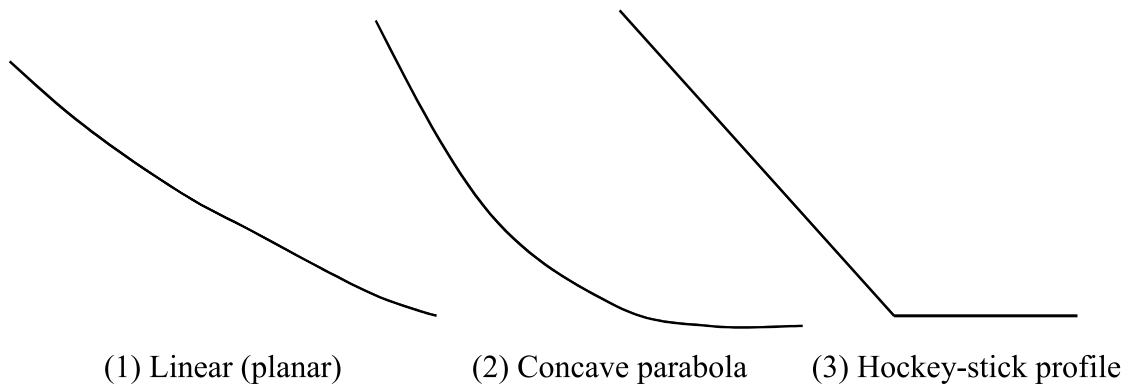

Figure 4.2 Examples of terrain profile types used for defining the TP variable

a path with a hockey-stick profile. A hockey-stick profile describes path profiles where there is an abrupt transition to a slope at or near 0º in the runout zone (Martinelli, 1986). This type of profile may be commonly found where a steep slope meets a gently sloping or flat alluvial plain in the valley bottom. An example of a path in the short slope dataset with a hockey-stick profile (Schroeder Shoulder) is included in Appendix B. Paths with hockey-stick profiles were common in this dataset, with 10 of the 48 (21 %) surveyed paths being classified as hockey-stick profiles. There were 8 (17 %) paths defined as linear (planar) and 30 (62 %) paths defined as concave parabolas.

Topography, *T*, is a categorical variable that describes the topography within the starting zone. There were 17 (35 %) starting zones classified as linear, 9 (19 %) classified as concave, 14 (29 %) classified as convex, 2 (4 %) classified as complex, and 6 (13 %) classified as gullies. Concavity and convexity are defined in the downslope direction.

The degree of confinement is a categorical variable that defines the relative confinement of the path between the starting zone and track. There were 27 (56 %) paths classified as unconfined, 16 (33 %) as partially confined, 1 (2 %) classified as confined, and 4 (9 %) classified as gullies.

The categorical variable "Runs out in forest" describes whether or not the extreme runout position was observed within a mature forest, downslope of any obvious trimlines, or was within open, relatively treeless terrain. Eleven (23 %) paths were classified as "runs out in forest" (1), and 37 (77 %) paths were classified as "does not run out in forest" (2).

4.3 Statistical distribution of variables

Descriptive statistics for the data are shown in Table 4.1, including the mean, standard deviation, median (Q_2), lower (Q_1) and upper (Q_3) quartiles, minimum (Q_0) and maximum (Q_4) values. Table 4.1 includes two separate sets of statistics for variables that depend on the defined location of the β-point. Similar to previous studies, descriptive statistics are provided for a β point defined as the position where the slope angle in the avalanche path first decreases to 10°. For reasons that will be explained in Section 4.3, descriptive statistics are also provided for the paths with the β point located where the slope angle of the path first decreases to 24°.

A total of 48 avalanche paths were surveyed for this study, 46 of which are included in the following analyses. Two paths, Mont Blanche LaMontagne located in the Chic Choc Range of Quebec and Blowdown Creek located in the Coast Range of British Columbia, were rejected on the basis that the paths did not reach a slope angle of less than 28° upslope of the interpreted location of the extreme runout position. The commonly accepted *lower* limit for dry snow avalanche initiation within the starting zone is between 25° (McClung et al., 1993, p. 92) and 28° (Gubler et al., 1994). At these slope angles, large snow avalanches should either be accelerating or attaining a steady velocity, not decelerating. According to this definition, these two paths have extreme runout positions within their respective starting zones and were consequently rejected for further analysis and excluded from the descriptive statistics. McClung (2001a) would classify these paths as continuously steep paths with no β point in the runout zone, which fits one of his discussed limitations of empirical models.

The normality of the 21 variables (excluding four categorical variables) is assessed by comparing the distribution of data to the expected normal distribution using the Kolmogorov-Smirnov (K-S) and Lilliefors tests of normality (Table 4.2) (Neave and Worthington, 1988, pp. 100-101, 149-156). The hypothesis of normality is rejected at the 1% level ($p \leq 0.01$) for 12 of the 21 variables based on the Lilliefors test of normality. The remaining 9 variables can be considered normally distributed data, including: α, β, α/β, H_α, X_α, X_β, $\Delta x/X_\beta$, S_0, and H_0y''. It is important to note that both α and $\Delta x/X_\beta$ can be considered to be normally distributed variables since they are used as response variables in the models developed in Sections 4.4 and 4.5

Table 4.2 Normality tests for terrain variables (β point defined at 24°)

Variable	n	Mean	Standard deviation	K-S		Lilliefors
				d	p	p[1]
Beta angle, β (°)	**46**	**32.8**	**2.8**	**0.076**	**>0.20**	**>0.20**
Delta angle, δ (°)	46	15.1	4.9	0.164	<0.20	<0.01
α/β ratio	**46**	**0.81**	**0.12**	**0.079**	**>0.20**	**>0.20**
Runout ratio, $\Delta x/X_\beta$ (m·m^{-1})	**46**	**0.722**	**0.580**	**0.087**	**>0.20**	**>0.20**
Vertical height to β point, H_β (m)	46	190	125	0.114	>0.20	<0.15
Horizontal reach to β point, X_β (m)	**46**	**290**	**176**	**0.105**	**>0.20**	**>0.20**
Runout distance, Δx (m)	46	151	148	0.174	<0.15	<0.01
Alpha angle, α (°)	**46**	**26.5**	**4.5**	**0.082**	**>0.20**	**>0.20**
Vertical height to runout position, H_α (m)	**46**	**224**	**120**	**0.083**	**>0.20**	**>0.20**
Vertical height to low point on parabola, H_0 (m)	46	216	166	0.121	>0.20	<0.10
Total horizontal distance, X_α (m)	**46**	**441**	**220**	**0.099**	**>0.20**	**>0.20**
Slope length of path, S_0 (m)	**46**	**512**	**253**	**0.082**	**>0.20**	**>0.20**
Second derivative of the slope function, y'' (m^{-1})	46	0.002	0.002	0.241	<0.01	<0.01
Scale parameter for path profile, $H_0 y''$	**46**	**0.332**	**0.144**	**0.074**	**>0.20**	**>0.20**
Start zone inclination, θ (°)	46	38.3	5.0	0.122	>0.20	<0.10
Start zone aspect, Aspect (°)	46	139	113	0.185	<0.10	<0.01
Start zone elevation, SZ Elev (m)	46	1773	540	0.165	<0.20	<0.01
Runout zone elevation, RZ Elev (m)	46	1480	609	0.135	>0.20	<0.05
Surface roughness, SR (m)	46	0.5	0.4	0.257	<0.01	<0.01
Wind Index, WI (ordinal data)	46	3.5	1.2	0.209	<0.05	<0.01
Width of start zone, W (m)	46	98	90	0.257	<0.01	<0.01
Terrain Profile, TP (ordinal data)	46	2.1	0.6	0.341	<0.01	<0.01

[1]Rows for which Lilliefors $p \geq 0.01$ are marked in bold

4.4 Runout ratio method

4.4.1 Introduction

The objective of the section is to develop empirical formulas to estimate the extreme runout position for avalanches within the four mountain ranges represented in this study. The hypothesis is presented that, similar to the findings of previous studies (e.g. McClung and Lied, 1987; McClung and Mears, 1991), a set of runout ratios from a mountain range conforms to an extreme value distribution, specifically a Gumbel distribution. It is further postulated that, because the terrain scale and climate effects between ranges may be relatively weak for a dataset comprising short slopes, a common model may be developed to represent all four mountain ranges and climatic effects assessed.

Section 4.4.2 describes the statistical methods used to develop models based on the runout ratio. Section 4.4.3 applies this method to develop one runout ratio model for data from all four mountain ranges. In Section 4.4.4, the runout ratio method is applied separately to the four different mountain ranges to compare the results with the combined range model. Length-scale effects are assessed in Section 4.4.5. Residual analyses are conducted for the proposed models in Section 4.4.6. Section 4.4.7 summarizes the results of the models developed in Section 4.4.

4.4.2 Description of the runout ratio method

McClung and Lied (1987) showed that a Gumbel distribution in the form,

$$P = \exp - \left(\exp - \left(\frac{(\Delta x / X_\beta)_P - u}{b} \right) \right) \tag{4.3}$$

provides a good model for extreme avalanche runout distances. In this model, the runout ratio, $\Delta x/X_\beta$, is the continuous random variable, u and b are the *location* and *scale parameters*, respectively, and P is the *non-exceedance probability* (i.e. $0 < P < 1$). A chosen value for P represents the runout ratio for which $P \times 100$ % of the values in the dataset will not exceed that given value. The above expression can be re-written as:

$$(\Delta x/X_\beta)_P = u - b\, ln(-ln(P)) \tag{4.4}$$

where the term -ln(-ln(P)) is often called the *reduced variate*. By assigning appropriate non-exceedence values P for each runout ratio in the dataset based on their rank order, it is possible to solve for u and b using least squares linear regression techniques.

In order to define non-exceedance values for each runout ratio, the commonly used procedure is to rank the runout ratios and use one of the various forms of plotting positions to define the values for P (Watt et al., 1989, p. 55). Runout ratios in the dataset are ranked in increasing order such that:

$$(\Delta x / X_\beta)_1 < (\Delta x / X_\beta)_i < (\Delta x / X_\beta)_N \tag{4.5}$$

where N is the number of paths in the dataset and $1 < i < N$.

McClung and Mears (1991) provide an extensive review of plotting position equations commonly used for small datasets. Based on this review and subsequent studies, it is apparent that the choice of the plotting position equation is not of great importance except when the focus of attention is on the one or two highest points in the dataset (Watt et al., 1989, p. 53). For this analysis, Hazen plotting positions are used (McClung and Mears, 1991):

$$P_i = \frac{i - 0.5}{N} \qquad i = 1,2,...,N \tag{4.6}$$

It should be noted here that in Section 4.3, the runout ratio, $\Delta x/X_\beta$, was shown to be normally distributed. Although analyses could be conducted treating the runout ratio as a normally distributed variable, the hypothesis that a Gumbel distribution provides a good fit to the runout ratio data will be explored in the following sections. This method is applied using methods similar to those developed for estimating runout distances in previous studies.

4.4.3 Runout ratio model for combined mountain ranges

Figure 4.3 shows the runout ratio for the combined mountain ranges plotted as a function of the reduced variate, -ln(-ln(P)), using the conventional definition of the β point located where the slope angle first decreases to 10º along the path profile. The linear regression line fit to the 46 data points has a coefficient of determination of $R^2 = 0.88$ and a standard error of $SE = 0.094$. Since the variables on both the horizontal and vertical axes are increasing functions of the runout ratio, a good fit of the regression line to the data is expected and only high R^2 values (e.g. $R^2 > 0.95$) indicate a good fit to a Gumbel distribution. While the central part of the line provides a reasonably good fit to the data, the higher and lower values of runout ratio are poorly fit by the regression line. This

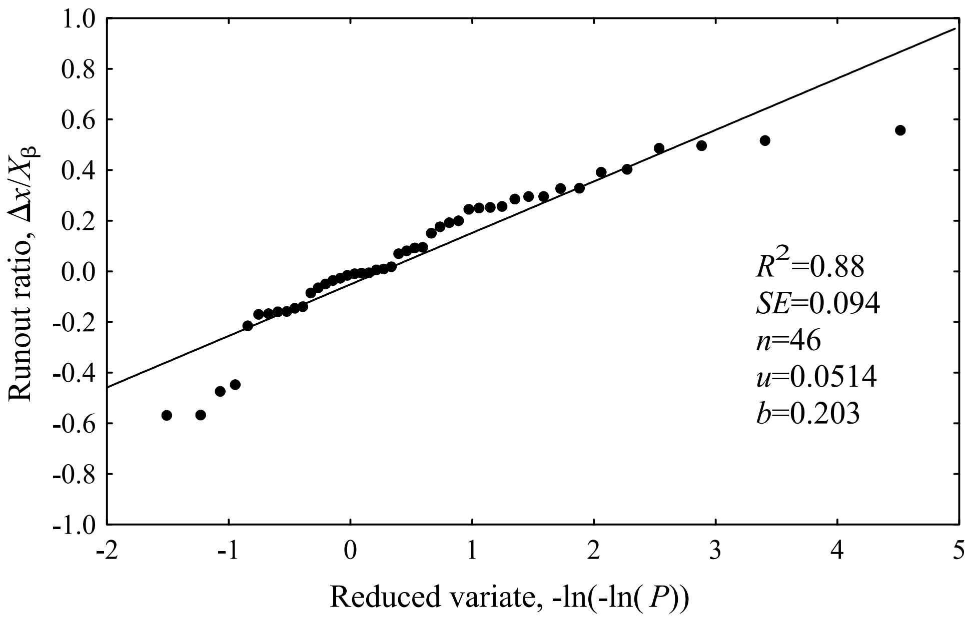

Figure 4.3 Runout ratio fitted to an extreme value (Gumbel) probability distribution for 46 avalanche paths in the combined mountain ranges. β point defined at 10º.

would be expected considering that many of the paths did not reach slope angles of 10º in the runout zone. The regression line has similar characteristics to that developed by McKittrick and Brown (1993) for the mountains of southwest Montana, in that there appears to be a "flattening" of the data at higher values of the runout ratio and a "steepening" of the data at lower values of the runout ratio. This "flattening" of the data at the upper-right end of Figure 4.3 is known as a "heavy-tail" and indicates that the runout ratio increases only slightly for reduced variates approximately greater than three, which corresponds to a non-exceedance probability of 0.95. A Gumbel distribution would only provide a good fit to the data if the extreme (high P) values in the dataset fell on or near the regression line, indicating increasing runout at higher non-exceedance probabilities.

Although alternative distributions may be used for analyzing the data shown on Figure 4.3, it is the intention of this study to apply previously developed methods to the data. As an example, an Extreme Value Type II, or Frechet, distribution (Watt et al., 1989) provides a better fit to the data with runout ratios exceeding zero than the fit shown for a Gumbel distribution (Figure 4.3). Fitting such a distribution to the data would require a transformation, or shifting of the y-axis, to allow for the inclusion of all of the data (i.e. ln $[\Delta x/X_\beta]$ is defined only for $\Delta x/X_\beta$, > 0). Also, a better fit of the data is obtained when the data is censored at lower values of P, similar to the findings of McClung and Mears (1991) who censored their data at $P = e^{-1}$. Censoring the data in this manner results in a less than ideal subset of data ($n = 29$) for the analyses. McClung and Mears (1991) also explored the use of log-normal distributions for their data but found the "extreme value distribution to be as good or better than other ones and consequently recommend its use for the least-squares procedure". In keeping with existing methods for statistical runout modelling, subsequent analyses are conducted by exploring the use of alternate definitions of the β point and using existing statistical methods.

Based on the poor fit of the regression line to the data with the β point defined at 10º, additional linear regressions were conducted by varying the β point definition from 10º through 27º. McKittrick and Brown (1993) found that using a reference point of 18º provided a better fit to their data, which included mostly shorter slopes. Although they did not develop a physical basis for this definition, there is some basis for using a β point as high as 25º, since this is where large, dry avalanches begin a deceleration and compressive phase (McClung and Mears, 1995). Figure 4.4 shows the results of the fit of regression lines to the data for varying β points from 10º through 27º, and that the best fit of the data to a Gumbel distribution occurs when the β point is defined at 24º. Using this definition of the β-point, both the R^2 is maximized at 0.98 and the standard error, SE, is minimized at 0.080.

Figure 4.5 shows the runout ratio for the combined ranges plotted as a function of the reduced variate, -ln(-ln(P)) with the β point defined at 24º. The linear regression line fit to the 46 data points has a coefficient of determination, R^2, of 0.98 and a standard error of 0.080. This is a large improvement over the model with the β point defined at 10º, and has a good fit to the data using rank order statistics. The resulting regression equation relating the runout ratio to the non-exceedence probability is:

$$(\Delta x / X_\beta)_P = 0.494 - 0.441 \ln(-\ln(P)) \tag{4.7}$$

This regression equation (Equation 4.7) is hereafter referred to as the 4-Range model.

4.4.4 Runout ratio model for individual mountain ranges

All previous work in the field of statistical avalanche runout estimation has had, as one of its underlying assumptions, that each region or mountain range constitutes a

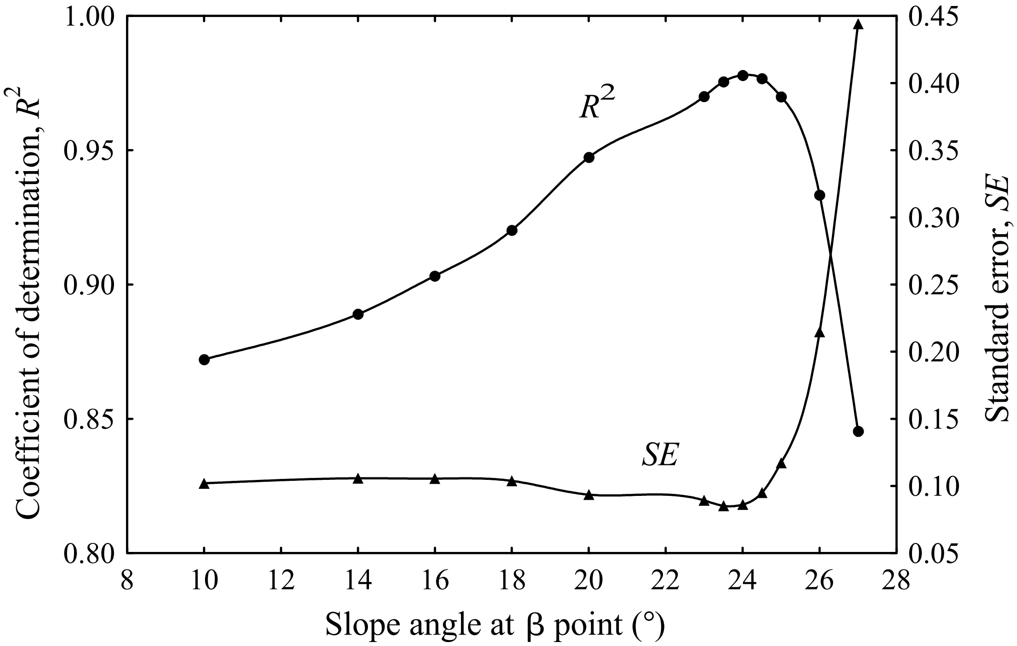

Figure 4.4 Plot of coefficient of determination, R^2, and standard error, SE, for regression lines from fitting an extreme value (Gumbel) distribution to the data using variable β point definitions

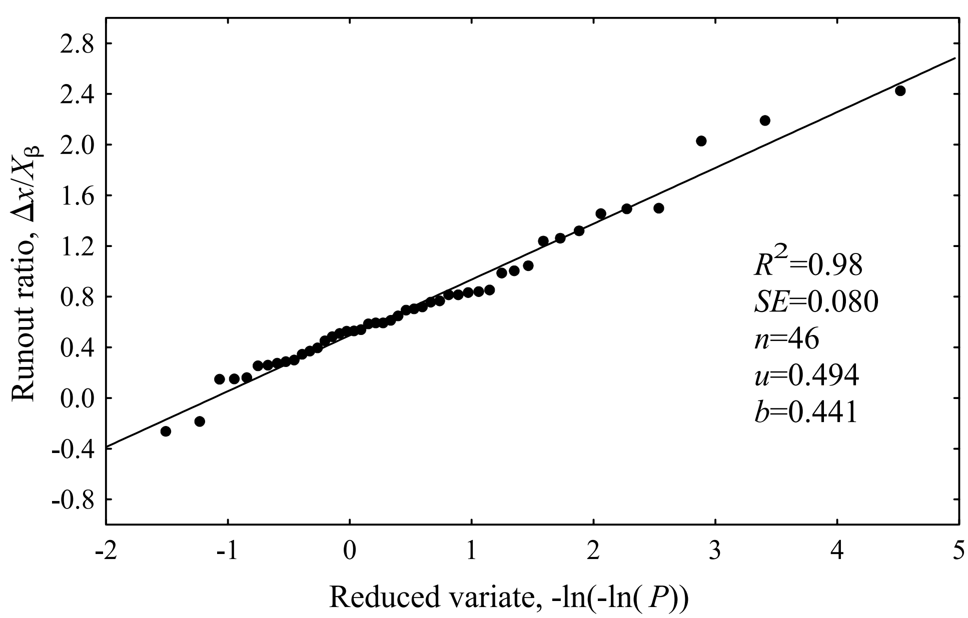

Figure 4.5 Runout ratio fitted to an extreme value (Gumbel) probability distribution for 46 avalanche paths in combined mountain ranges. β point defined at 24º.

separate population of extreme runout distances, and that each region must be analyzed separately (Mears, 1992, p. 26). The analyses in Section 4.4.3 show that a suitable model can be developed to represent short slopes in several mountain ranges. The four mountain ranges used in this study have very different climate characteristics, and represent all three of the basic snow climate regimes: Maritime, Continental and Intermountain (McClung and Schaerer, 1993, pp. 17-18).

Runout ratio models for individual ranges are developed in this section to determine the affect of the climate regime in the different mountain ranges on runout distance. By looking at individual mountain ranges, however, it must be noted that the sample size is generally not considered adequate for conducting statistical analyses within reasonable confidence intervals. From the central limit theorem (Kennedy and Neville, 1986, pp. 117-121), if $N \geq 30$, the normal approximation for the mean and variance of the runout ratio can be used with good precision even for an extreme value distribution. For the combined dataset, $n = 46$, so the normal approximation can be applied. The number of paths for the Coast, Columbia, Rocky Mountain and the Quebec mountain ranges are 15, 10, 15 and 6, respectively (Table 4.3). Thus, all the samples for individual ranges are well below the recommended sample size of $N \geq 30$. While considering this limitation, the following analyses show the results from the development of runout ratio models for individual ranges, and illustrates the effect of different ranges on the combined model.

Table 4.3 shows the results of regression analyses for the four individual mountain ranges in the study, with the β point defined at 24°. For the Columbia, Rockies and Quebec mountain ranges, the fit of a Gumbel distribution to the data is poor

Table 4.3 Results of regression analyses for runout ratio for individual mountain ranges, β point defined at 24°

Mountain Range	***n***	**Coefficient of determination, R^2**	**Standard error, *SE***
Coast	15	0.98	0.072
Columbia	10	0.90	0.141
Rockies	15	0.80	0.230
Quebec	6	0.89	0.286

(i.e. $R^2 \leq 0.90$) , especially when compared to the model for the combined ranges ($R^2 = 0.98$, Figure 4.5). The Coast Range has a comparable fit to the 4-Range model, with a slightly lower standard error (Figure 4.6). However, having a third of the number of data points when compared to the 4-Range model shows that the fit of the 4-Range model must be considered a better model. The individual model for the Coast Range is promising and, with the addition of more data, could prove to be a useful model. The resulting location parameter, *u*, for the Coast Range is 0.562 and the scale parameter, *b*, is 0.423, both of which are very close to the values for the 4-Range model. The resulting regression equation for the Coast Range, hereafter called the Coast Range model, can be written as

$$(\Delta x / X_\beta)_P = 0.562 - 0.423 \ln(-\ln(P)) \tag{4.8}$$

and has a coefficient of determination of 0.98 and a standard error of 0.072.

There are no obvious reasons why the Coast Range should give more consistent results than the other ranges. There probably is no less variation in climate regime within the Coast Range when compared to the other ranges. It may even be the case that there is more variation in climate regime considering that the sites included in the Coast Range include relatively maritime sites near the Pacific coast (e.g. Mt. Seymour, Brohm Ridge), sites within the dryer Cascade Range (Zum Peak, Zopkios Ridge), and arguably intermountain sites near Penticton (Apex Mountain) that were included in the Coast Range

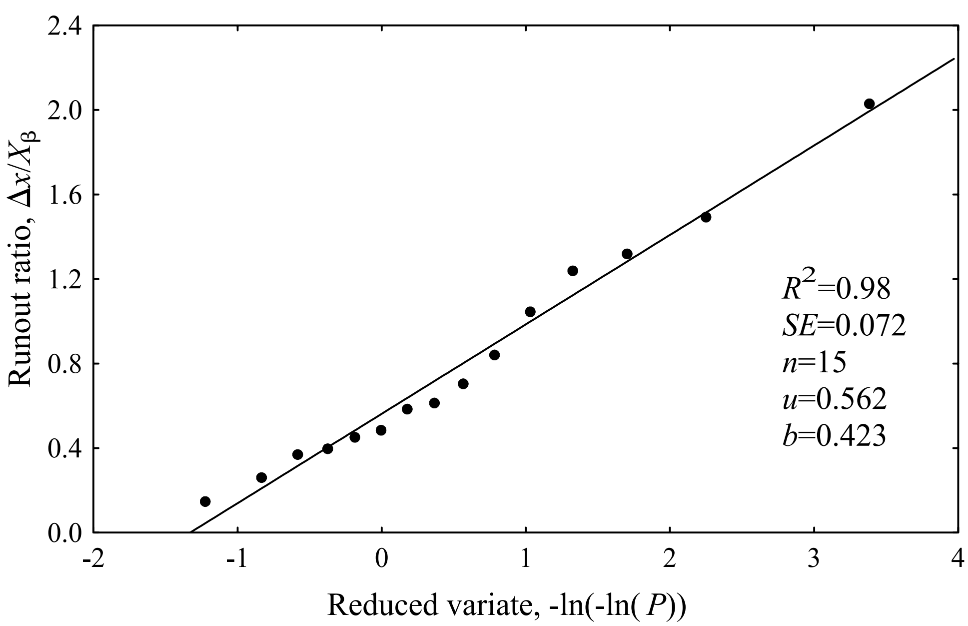

Figure 4.6 Runout ratio fitted to an extreme value (Gumbel) probability distribution for 15 avalanche paths in the Coast Mountain range. β point defined at 24°.

primarily because they are closer to the Coast Range than to the other ranges. A strong argument could also be made for including these sites in the Columbia Mountains but, for this project, they are classified as part of the Coast Range.

4.4.5 Length-scale effects for runout models

Similar to previous studies (e.g. McClung and Mears, 1991), the combined range dataset for short slopes exhibits a scale effect when the runout ratio is used to define runout distance. The Spearman rank correlation coefficients of H_β and X_β with the runout ratio, $\Delta x/X_\beta$, are both -0.55 (n = 46), which are highly significant ($p < 10^{-4}$) for both of the scale parameters. This indicates that the scale of the paths has a significant effect on runout distances. The negative correlations with runout ratio show that proportionately longer runout distances are associated with the shorter paths in the dataset which is consistent with the findings of McClung and Mears (1991).

Previous studies have found that partitioning the data into subsets provides a way to assess the length-scale effects on the model. Both McClung and Lied (1987) and McClung and Mears (1991) found that slopes with a vertical drop of less than 350 m did not fit well into their dataset, and consequently trimmed these paths from their dataset. In this study, the majority of the slopes have vertical drops of less than 350 m and, by developing a model for this dataset, the scale effect between larger slopes and slopes less than 350 m high is likely being addressed. However, within this dataset, there is also a scale effect, and it is important to estimate an upper limit for which a “short slope” model may be most applicable.

With the β point defined at 24º and using the 4-Range dataset, a series of regression analyses were conducted to assess the fit of a Gumbel distribution to the data for slopes with a vertical fall height, H_α, of less than a range of maximum values. The results of these regression analyses (Figure 4.7) show that the best fit linear regression is found when the dataset is limited to slopes with a vertical fall height of less than 275 m. Using this limit, the coefficient of determination, R^2, is maximized at 0.99 and the standard error is minimized at 0.063. This is an improvement in model fit over the 4-Range model developed in Section 4.4.3, with a 25 % reduction in the standard error. It should be noted, however, that this refined model is based on approximately 25 % fewer paths (n = 33)

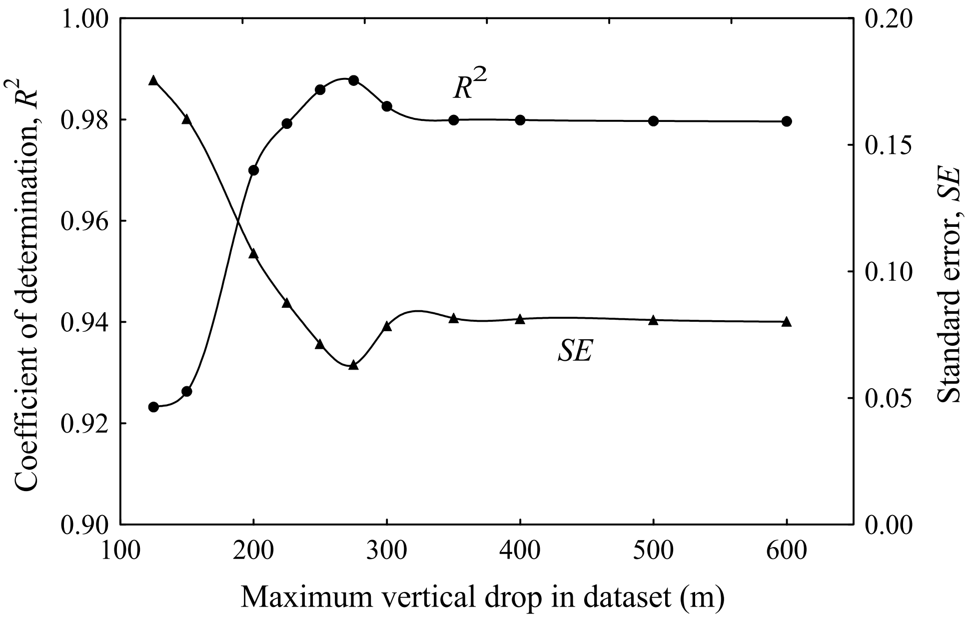

Figure 4.7 Plot of coefficient of determination, R^2, and standard error, SE, for regression lines fitting an extreme value (Gumbel) distribution to the data for variable maximum vertical fall height, H_α definition

compared to the 4-Range model for all the paths ($n = 46$). The preference for the minimum number of data points to exceed 30 (see Section 4.4.4) is achieved by this model and thus it can be considered to a statistically useful result. The data and linear regression line for this model are shown on Figure 4.8, and the resulting regression equation for slopes with a vertical fall height of less than 275 m, hereafter called the H275 model, is

$$(\Delta x/X_\beta)_P = 0.534 - 0.451\ \ln(-\ln(P)) \tag{4.9}$$

4.4.6 Residual analysis

The models developed in Sections 4.4.3 (4-Range model), 4.4.4 (Coast Range model) and 4.4.5 (H275 model) using the runout ratio method were accepted as potentially useful models based primarily on the resulting fit of estimated values to observed values in terms of the coefficient of determination and standard error. In this section, the statistical validity of these models is assessed using residual analyses.

A regression *residual* is the observed value of the dependent variable minus the predicted value (Mendenhall and Sincich, 1996, p. 378). In the following analyses, residuals for the runout ratio, $\Delta x/X_\beta$, are calculated by comparing the observed values, those calculated from the fitted parabolic curves and the observed runout positions, with

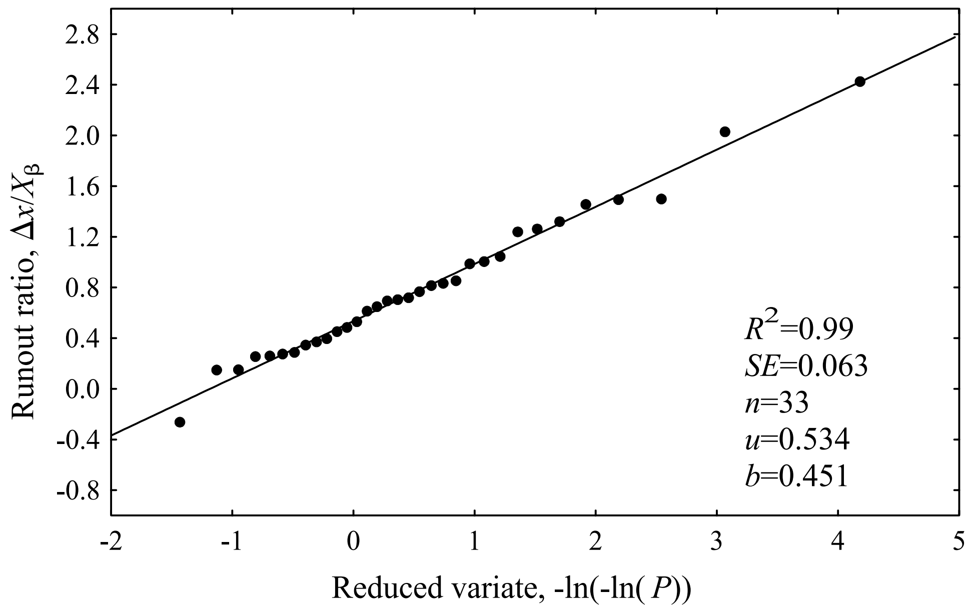

Figure 4.8 Runout ratio fitted to an extreme value (Gumbel) probability distribution for 33 avalanche paths in combined mountain ranges with $H_\alpha \leq 275$ m. β point defined at 24°.

the runout ratios estimated by the models.

Plots of the standard residuals for the three models are shown on Figures 4.9, 4.10 and 4.11. The abscissa represents the number of standard deviations of the residuals about the mean. By comparing these plots to the expected normal distributions, none of the three figures show obvious non-normality. To assess the normality of these residuals, the distributions are compared to the expected normal distributions using the Kolmogorov-Smirnov (K-S) and Lilliefors tests of normality (Neave and Worthington, 1988, pp. 149-159; 100-103). The results of this comparison are shown on Table 4.4. The hypothesis of normality was not rejected for the K-S test for all three models, and was rejected for the Lilliefors test at the 1% significance level only for the H275 model. Regression is robust

Table 4.4 Normality tests for residuals for runout ratio models

Model	**K-S**		**Lilliefors**
	d	***p***	***p***
4-Range, n = 46	0.119	> 0.20	< 0.10
Coast Range, n = 15	0.161	> 0.20	> 0.20
H275, n = 33	0.180	> 0.20	< 0.01

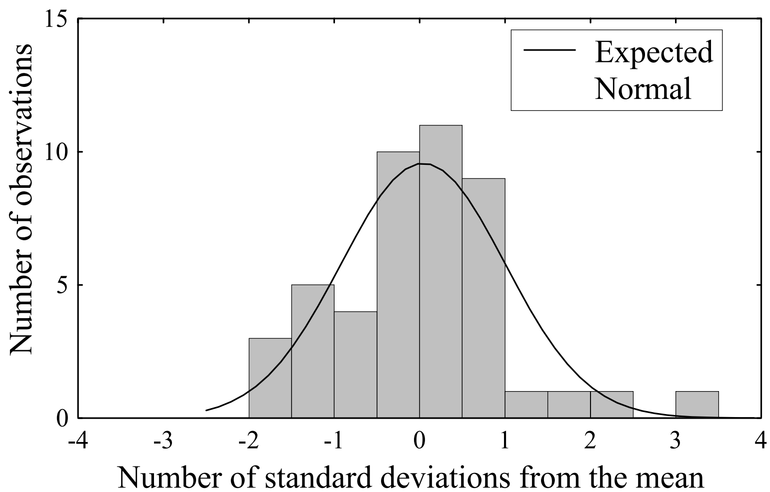

Figure 4.9 Distribution of standard residuals, 4-Range model, n = 46

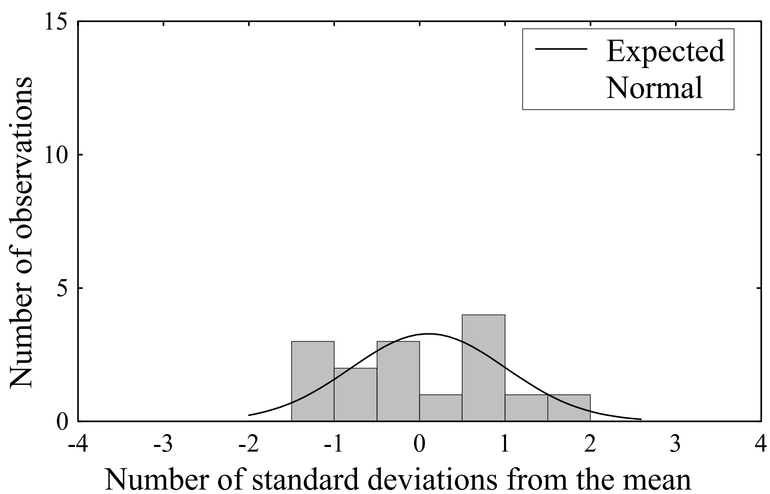

Figure 4.10 Distribution of standard residuals, Coast Range model, n = 15

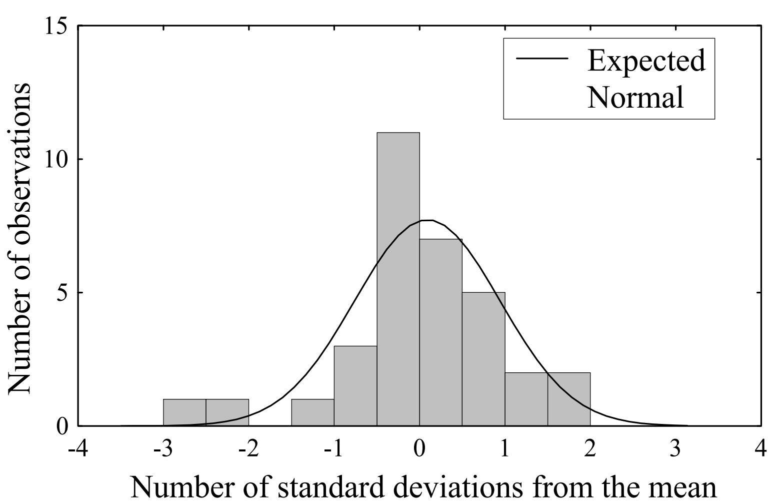

Figure 4.11 Distribution of standard residuals, H275 model, n = 33

with respect to non-normal residuals (Mendenhall and Sincich, 1996, p. 412), and consequently, these three models can be considered to have normal or near-normal distributions of the residuals.

It is common practice to define statistical *outliers* as observations with residuals that are greater than approximately three standard deviations from zero (Mendenhall and Sincich, 1996, p. 414). These outliers are often removed from the model dataset in order to improve the model fit using regression techniques. Examination of Figures 4.9 through 4.11 show that the 4-Range (n = 46) model has one outlier with a residual greater than three standard deviations from the mean. Another datapoint has a value of approximately 2.5 standard deviations from the mean. These two points correspond to the Brohm Ridge path in the Coast Range and the Harvey Bowl path in the Rockies, respectively.

It is important to understand why these two points may be considered outliers, and that these outliers may belong to populations different from other paths in the dataset (Mears, 1992, p. 25). Examination of the statistical distribution of the data shows that the Brohm Ridge and Harvey Bowl paths have α angles of 18.8º and 19.8º, respectively, which are significantly lower than the mean value of 26.5º, but within typical ranges for extreme avalanches observed in other studies (e.g. Lied and Bakkehøi, 1980; Martinelli, 1986; Nixon and McClung, 1993; Jóhannesson, 1998). One similarity between these two paths is that they reached relatively gently sloping areas of 10º, and continued past these areas onto slightly steeper slopes below and within partly confined stream channels. By concentrating the avalanche flow within a channel in the runout zone, it is possible that greater runout distances were achieved when compared to an open slope where avalanche material would disperse (Mears, 1984). McClung (2001a, p. 1262) also points out that "sometimes paths are highly confined in the runout zone resulting in unusually long running distances on slopes at or below 10º".

While it is tempting to reject these two paths based on the above argument, the purpose of these models is to estimate extreme runout distances. Consequently, one needs to be cautious about rejecting long-running avalanche paths as this may result in a model that underestimates runout distances for the tail events on a Gumbel distribution (Figure 1.10), which is the area of interest for engineering and planning purposes. Doing so may result in a model that is less conservative for the most extreme avalanches within the dataset. For this reason, these two outlier paths are left in the dataset and analyses.

The assumption of constant variance about zero can be tested by examining scatter plots of residual values for random scatter about zero. The plots shown in Figures 4.12, 4.13 and 4.14 show random scatter of data around zero for the Coast Range and the H275 models, which satisfies the assumption of constant variance. There are linear trends discernable for runout ratios between 0 and 0.8 in Figures 4.12 and 4.13 In this range of runout ratios, the models make a transition from under-estimating to over-estimating the runout ratio, but the residuals still scatter about zero. This trend, known as *serial correlation* or *residual correlation* (Mendenhall and Sincich, 1996, pp. 350, 430), is most important when data are in a time series, but may also be relevant in this case because the data have been ranked.

The Durbin-Watson test (Mendenhall and Sincich, 1996, p. 430) is used to test for the presence of residual correlation. Applying this test to the three models, only the H275 model has a Durban-Watson d-statistic of 2.0, which implies the residuals are not correlated with the runout ratio. The 4-Range model has a d-statistic of 1.23 and the Coast Range model has a value of 0.61 implying that these residuals are positively correlated. A positive correlation of residuals with the runout ratio implies that larger runout estimate errors are associated with higher runout ratios, or those paths with relatively longer runout distances. Thus, larger errors are associated with the paths in the dataset with the most extreme runout distances and, conversely, smaller errors are associated with the paths in the dataset with less extreme runout distances.

4.4.7 Summary of models developed using runout ratio methods

Several models were developed in the preceding sections using the runout ratio method. After analysis of the residuals, it is possible to summarize and propose uses and limitations for these models. Table 4.5 shows a summary of the regressions of the runout ratio on non-exceedance probability, P, and gives values of b and u for each model. The 4-Range model includes the greatest number of data and therefore best represents runout ratios for short slopes in Canada. The coefficient of determination for the 4-Range model is comparable to that of the other models, while the standard error is slightly higher. While the H275 model showed randomly distributed residuals and no serial correlation among

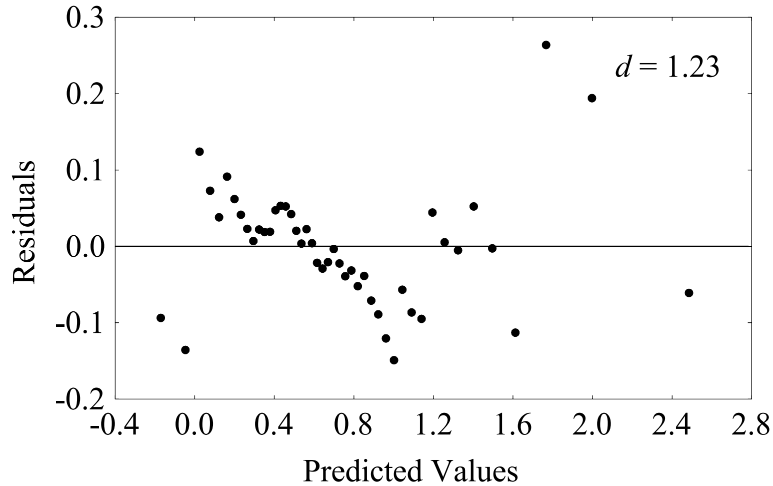

Figure 4.12 Scatter of residuals, 4-Range model, n = 46

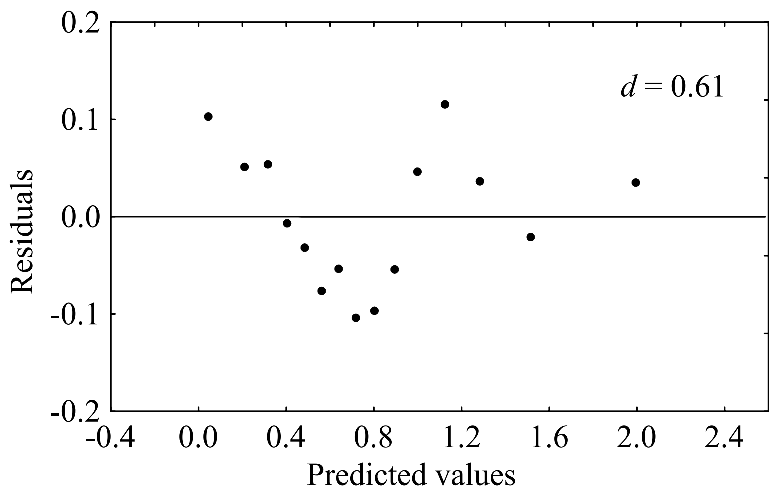

Figure 4.13 Scatter of residuals, Coast Range model, n = 15

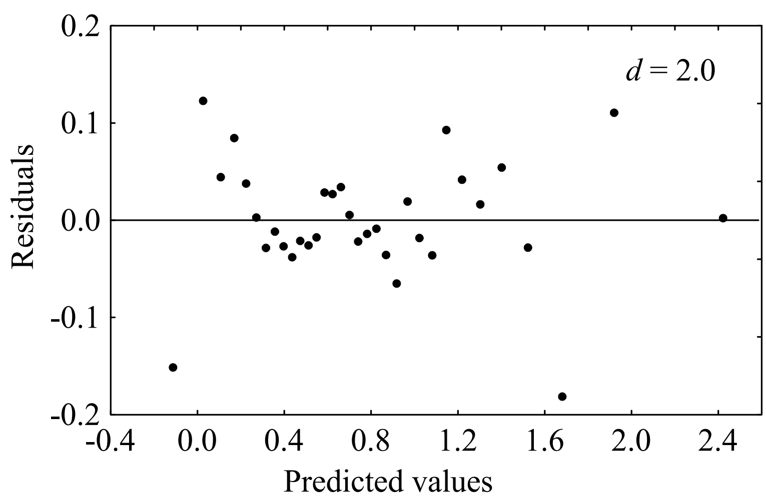

Figure 4.14 Scatter of residuals, H275 model, n = 33

Table 4.5 Extreme value scale and location parameters (b, u) for the three proposed runout ratio models					
Model	***n***	***R^2***	***SE***	***u***	***b***
4-Range	46	0.98	0.080	0.494	0.441
Coast Range	15	0.98	0.072	0.562	0.423
H275	33	0.99	0.063	0.534	0.451

the residuals, the 4-Range model displayed serial correlation in the middle range of data.

A comparison of the estimated and observed values for the 4-Range and Coast Range models shows that there is an average of 0.4 % difference between the estimated and observed values, which is an inconsequential amount when compared to the potential errors introduced in data field measurements. Field measurement errors were estimated to be approximately 2 % (Sections 3.3 and 3.7), which is an order of magnitude higher than the average residual error of 0.4 %. Based on this, the residual errors in the models can be overlooked and the 4-Range model is the preferred model because it incorporates the highest number of paths for model development. This model may applied with the stipulation that it may be best suited to avalanche paths with vertical fall heights, H_α, of less than 275 m.

In developing the 4-Range model, two paths with relatively long runout distances were noted, having runout ratio residuals greater than 2.5 standard deviations from the mean. While using conventional statistical techniques these could be excluded from analyses as outliers, but with extreme value statistics one wishes to include extreme data in the dataset. These “extreme” points are actually the more important data in the sample, while paths with lower runout ratios are sometimes censored from the dataset (e.g. McClung and Mears, 1991). Thus, these two paths were included in the analyses. Both of these paths have partially channelized runout zones which may contribute to longer runout distances (McClung, 2001a). Therefore, it should be pointed out that one of the limitations of this model is that it may not apply well to avalanche paths with confined or partly confined runout zones.

Although the results of the regression for the Coast Range (Equation 4.8) appear to be good, this regression is based on 15 avalanche paths, and therefore the utility of this model is limited at present. Collection of additional data for this model could result in a model well suited to paths in the Coast Range.

It was demonstrated in Section 4.4.3 that a β point located where the slope first reaches 10º is not a suitable reference point for a dataset comprising short slopes. Previously, McKittrick and Brown (1993) showed that a β point located where the slope first reaches 18º was better suited to a dataset of paths in southwest Montana. In this study, it has been shown that the location where the slope first decreases to 24º is a more appropriate location for the β point for short slopes within Canada, and that there may be some physical basis behind choosing the β point at this location (McClung and Mears, 1995; Salm et al., 1990). Because the β point has been redefined in this study to the location where the slope first reaches 24º, there is little point in trying to compare the scale and location parameters from these models to the parameters from previously developed models.

4.5 Multiple regression method

4.5.1 Introduction

In this section, least squares linear regression techniques are used to relate the dependent (response) variable, α, to various independent (predictor) terrain variables. The predictor variables must satisfy the condition of independence from α. The regression model to be developed has the general form

$$\alpha = \beta_0 + \beta_1 x_1 + \beta_2 x_2 + \ldots + \beta_k x_k + \varepsilon \tag{4.10}$$

that is used to describe a linear relationship between one dependent variable α and k independent random variables $x_1, x_2, \ldots, x_k$. The term β_i determines the contribution of the independent variable x_i, and is not to be confused with the β angle. The term ε represents the random error component of the model that makes the model probabilistic rather than deterministic. This error should satisfy two basic assumptions: it has a normal probability distribution with a mean equal to zero and a variance equal to the square of the population standard deviation, σ^2; and the random errors are probabilistically independent (Mendenhall and Sincich, 1996, p. 175). Multiple regression involves fitting a general linear model to the dataset by estimating the coefficients β_i that appear in the model. The coefficients are chosen to minimize the error sum of squares (the differences between the observed α_i and estimated α_i). This approach of using multiple regression to estimate α using terrain parameters is similar to the methods of Bovis and Mears (1976) and Lied and Bakkehøi (1980).

It was shown on Table 4.2 that the runout ratio, $\Delta x/X_\beta$, can be considered a normally distributed variable, in addition to fitting an extreme value distribution. While multiple regression methods could also be used to estimate the runout ratio based on the normality of this variable, the intention of this project is to use existing methods for statistical runout modelling. Thus, multiple regression methods are only used to develop a model to estimate α, not the runout ratio.

4.5.2 Initial regression model

Possible predictor variables for α were chosen from the 25 distinct terrain variables shown in Table 4.1 by including only those variables that are not a function of the α angle. Ordinal variables were included since these may be utilized in linear regression models, provided the regression residuals are normally distributed. In order to optimize model construction, predictor variables that are significantly correlated with the predictor variable, α, were selected for model development.

Spearman rank correlations between the predictor variables and α are shown in Table 4.6. All calculations in Table 4.6 and subsequent analyses in this thesis are based on the β point defined where the slope first decreases to 24º. Significant variables ($p \leq 0.05$) are highlighted, and near-significant correlations ($p \approx 0.05$) are shown in italics. Six of the variables are significant at the 0.05 level and these are used for model development. Other predictor variables that showed correlations of borderline significance with α were the Starting zone inclination, θ, and the Terrain Profile, TP. A total of eight predictor variables were used to develop the regression model, including the two near-significant variables. Backward elimination multiple regression methods (Mendenhall and Sincich, 1996, p. 247) were used with these eight predictor variables to obtain the best fit of the estimated values of α to the observed values.

A plot of the estimated against the observed data in the early part of the analyses showed one significant outlier, Mount Seymour, which had a standard residual in excess of three standard deviations from the mean. This path has a very large vertical drop to the

Table 4.6 Spearman rank correlations between the response variable, α, and predictor variables. β point defined at 24°			
Variable	*n*	*R*	*p*[1]
Beta angle, β (°)	**46**	**0.482**	**7.00×10^{-4}**
Vertical height to β point, H_β (m)	**46**	**0.610**	**6.67×10^{-6}**
Horizontal reach to β point, X_β (m)	**46**	**0.568**	**3.81×10^{-5}**
Vertical height to low point on parabola, H_0 (m)	**46**	**0.651**	**9.50×10^{-7}**
Second derivative of the slope function, y'' (m^{-1})	46	-0.169	0.262
Scale parameter for path profile, H_0y''	**46**	**0.684**	**1.56×10^{-7}**
Starting zone inclination,θ (°)	*46*	*0.260*	*0.081*
Starting zone aspect, Aspect (°)	46	-0.081	0.591
Starting zone elevation, SZ Elev (m)	46	0.086	0.571
Runout zone elevation, RZ Elev (m)	46	0.025	0.868
Surface roughness, SR (m)	46	0.067	0.659
Wind Index, WI (ordinal data)	46	-0.237	0.112
Width of starting zone, *W* (m)	**46**	**-0.293**	**0.048**
Terrain Profile, TP (ordinal data)	*46*	*-0.276*	*0.063*
[1]Rows for which $p \leq 0.05$ are marked in bold. Rows for which $p \leq 0.10$ italicized			

alpha point (H_α = 593 m) far greater than H_α for other paths in the dataset (average H_α = 224 m). Excluding this outlier from the analysis results in a greatly improved fit of the regression to the data.

After removal of this outlier, variables were systematically removed from the regression model equation (backward elimination) when they were found to have a minimal effect on the model (i.e. variable *F*-values were less than a specified threshold at each step in the regression). *F*-values (Table 4.7) were computed at each step in the regression to help facilitate removal of variables from the regression equation. Using a threshold *F* value of 3.1 (1 % significance level, $\upsilon_1 = 8$, $\upsilon_2 = 36$; Mendenhall and Sincich,

Table 4.7 Eight predictor variables used in multiple regression analyses and corresponding backwards elimination F values	
Variable	*F to remove*[1]
Beta angle, β (°)	0.902
Vertical height to β point, H_β (m)	0.288
Horizontal reach to β point, X_β (m)	**3.433**
Vertical height to low point on parabola, H_0 (m)	**11.759**
Scale parameter for path profile, H_0y''	**31.800**
Starting zone inclination,θ (°)	2.472
Width of starting zone, *W* (m)	0.785
Terrain Profile, *TP* (ordinal data)	**6.442**
[1] Rows for which $F \geq 3.1$ (1% significance level) are in bold	

Table 4.8 Results of multiple regression analysis for α			
Adjusted R^2 = 0.79, SE = 1.9°, $p < 10^{-4}$	**Coefficient β_i**	**Standard error of β_i**	***p***
Intercept	22.42 °	1.38 °	1.9×10^{-19}
H_0y''	22.11 °	2.63 °	1.9×10^{-10}
TP	-2.60 °	0.59 °	8.1×10^{-5}
H_0	0.01 °·m^{-1}	0.003 °·m^{-1}	5.0×10^{-4}

1996, p. 235, 821), all variables but H_0y'', H_0, TP and X_β were eliminated from the regression equation. Additional analyses showed that X_β could also be removed from the regression equation with minimal effect on the results. Thus, X_β was removed and the remaining three predictor variables for α were H_0y'', TP and H_0. Removal of any of these three variables had a large effect on the model, with R^2 values going from 0.79 with all three predictor variables to 0.72 or less when any one of the three variables were removed. The resulting regression equation is

$$\hat{\alpha} = 22.42 + 22.11\ H_0 y'' - 2.60\ \mathrm{TP} + 0.01\ H_0 \tag{4.11}$$

This model has an adjusted R^2 of 0.79, a standard error of 1.9° and utilizes 45 of the avalanche paths for model development. It can be observed that all three predictor variables are topographic parameters derived from the slope profile (Figure 4.1) and that all three are statistically significant (Table 4.8) in the regression equation. A summary of the results of regression, including the standard error and significance levels for each predictor variable is shown in Table 4.8.

4.5.3 Simplified regression model

As in previous studies, the goal is a simple regression equation for estimating α with reasonable accuracy that uses a limited number of variables. Previous studies (e.g. McClung and Lied, 1987; McClung and Mears, 1991) found that predictor variables other than β were not statistically significant in regression analyses of slopes mostly over 300 m in vertical fall height. Results in Section 4.5.2 showed that, although the β angle is significantly correlated with α, it is not one of the most useful predictors for multiple regression for this dataset of short slopes. For this dataset, H_0y'' is the most statistically significant variable in the regression equation, followed by TP and then H_0 (Table 4.8). Removing TP from the regression analysis results in an adjusted R^2 of 0.69 and a standard error of 2.3°. Removing H_0 from the regression analysis results in an adjusted R^2 of 0.72 and a standard error of 2.2°. Removal of both TP and H_0 results in an adjusted R^2 of 0.46 and a standard error of 3.1°. It can thus be observed that the regression may best be simplified by removing H_0 from the regression, and the resulting regression equation is

$$\alpha = 25.46 + 26.93\ H_0 y'' - 3.74\ \mathrm{TP} \tag{4.12}$$

with an adjusted R^2 of 0.72 and a standard error of 2.2°. However, simplifying the equation to this form may not be very beneficial, considering that the variable H_0 must also be calculated as part of the variable H_0y''. The regression equation developed in Section 4.5.2 (Equation 4.11) is preferred since it has a higher adjusted R^2 and lower standard error than Equation 4.12.

4.5.4 Residual analysis

The regression model developed in Section 4.5.2 was accepted as a promising model based primarily on the resulting fit of the estimated values to observed values in terms of the adjusted R^2 and standard error values. Before acceptance of this regression model, the residuals of regression are analysed, as in Section 4.4.6, to determine the statistical validity of the model.

The assumption of constant variance is tested by examining a plot of standard residuals for random scatter about zero. Visual inspection of Figure 4.15 shows that the assumption of constant variance is satisfied.

The distribution of the standard residuals is shown in Figure 4.16 along with the expected normal distribution. The K-S test for normality has a d value of 0.09 ($p > 0.20$) which, along with the Lilliefors test ($p > 0.20$), show that the hypothesis of normality of the residuals is not rejected. Thus, the assumption of normality of the residuals about a mean of zero is satisfied.

The third assumption to be tested is that the residuals are not serially correlated. The Durban-Watson statistic has a value of 2.0, indicating that the residuals are not correlated.

Since the above three assumptions for multiple regression have been satisfied, it is concluded that the regression equation developed for estimating α (Equation 4.11) is

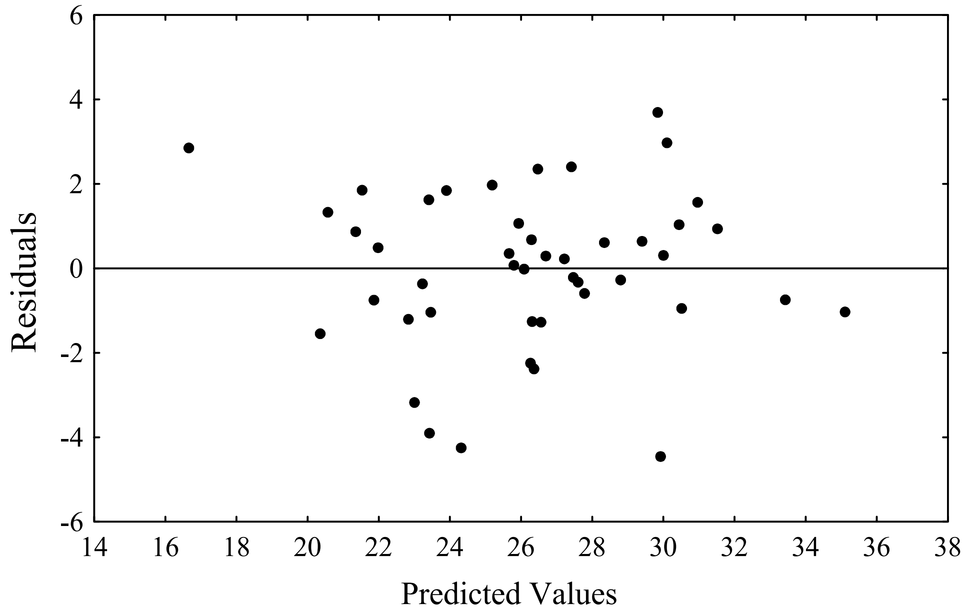

Figure 4.15 Scatter of residuals, multiple regression model (Equation 4.11)

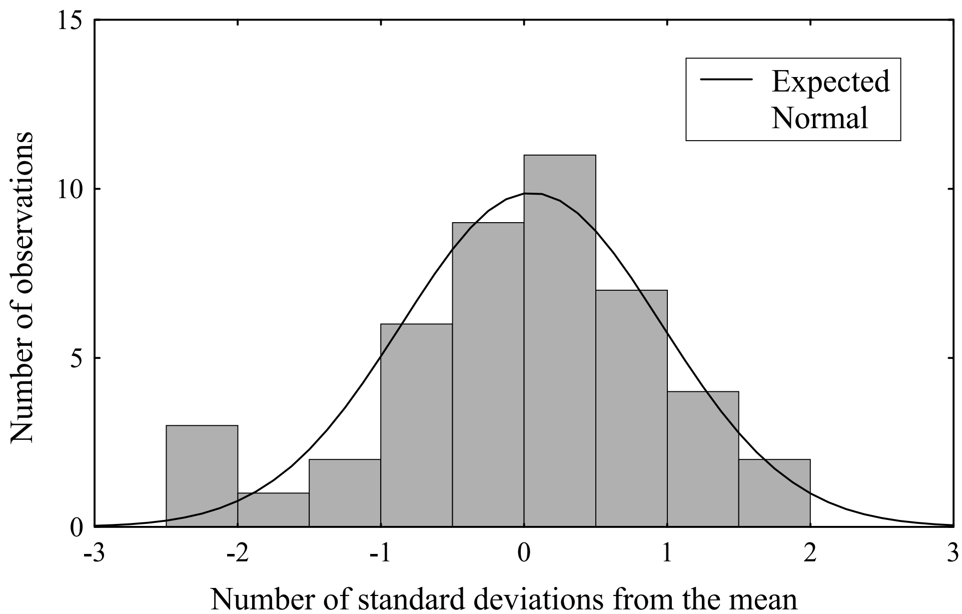

Figure 4.16 Distribution of residuals, multiple regression model (Equation 4.11)

statistically valid.

These three basic assumptions were also tested for the simplified model presented in Section 4.5.3 (Equation 4.12) using similar methods. The K-S test for normality has a *d* value of 0.14 ($p > 0.20$), while the Lilliefors test has a significance value of $p < 0.05$. Thus, the hypothesis of normality of the residuals is not rejected based on the K-S test but

Table 4.9 Spearman rank correlations of predictor variables to test for multicollinearity in regression models			
Variables	**Spearman *R***	***p***	***n***
$H_0y''$and TP	0.298	0.0467	45
H_0y'' and H_0	0.329	0.0275	45
TP and H_0	-0.365	0.0136	45

is rejected based on the Lilliefors test. The Durban-Watson statistic has a value of 2.0, indicating that the residuals are not correlated for the simplified model (Equation 4.12).

Analyses were conducted to assess if the variables used to develop the models (Equation 4.11 and 4.12) are significantly cross-correlated. When two or more independent variables in the regression are correlated, a condition called *multicollinearity* exists (Mendenhall and Sincich, 1996, p. 355-357). Highly significant correlations among the predictors can lead to problems with multiple regression, including increasing the likelihood of rounding errors in the calculation of β_i coefficients, and obtaining confusing and misleading results. Based on Spearman rank correlations of the three predictor variables with each other (Table 4.9), all three variables used in the analyses, H_0y'', TP and H_0 are significantly cross-correlated with each other at the 5 % significance level ($p < 0.05$) but are not highly significant at the 1 % significance level ($p < 0.01$). Problems may arise in regression analysis when *serious* multicollinearity is present (Mendenhall and Sincich, 1996, p. 355), which is not the case with these variables.

4.5.5 Effects of different mountain ranges on regression models

Figure 4.17 shows the standard residuals from the analysis in Section 4.5.2 (Equation 4.11) for estimating the α angle. Distinct symbols are marked for each mountain range. All values are within three standard deviations of zero, indicating the absence of any statistical outliers, and the majority of residuals fall within two standard deviations of zero. All of the residuals for the Coast mountain range are within approximately one standard deviation of zero indicating that the Coast range accounts for the least amount of

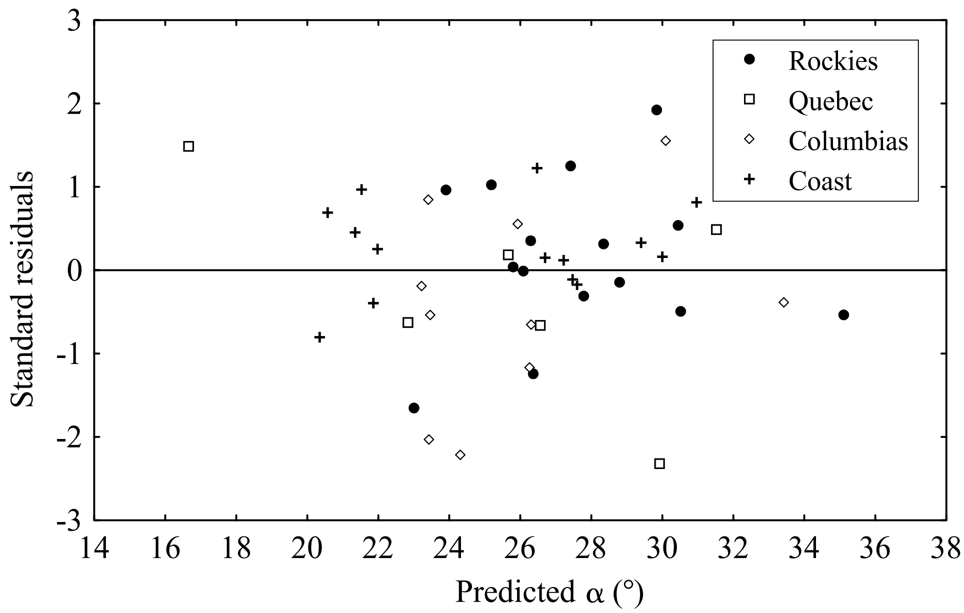

Figure 4.17 Distribution of residuals by mountain range

error in the model. The other three mountain ranges, the Rockies, Columbias and Quebec mountains, have residuals mostly less than two standard deviations. This is consistent with the results of Section 4.4.4, in which the Coast mountain range was found to have more consistent results than the other mountain ranges. This also implies that, with additional data points (i.e. $n \geq 30$), a suitable regression model could be developed for the individual Coast Range, while the advantage of such an approach for short slopes in the other three ranges is not apparent in this dataset

4.5.6 Scale effects on regression models

The standard residuals in the regression model are plotted versus the vertical fall height, H_α, in Figure 4.18. The standard residuals are randomly scattered about zero for all paths. A similar result for standard residuals plotted versus the total horizontal distance to the α point, X_α, is shown on Figure 4.19. Since there is no discernable scale effect in the regression model developed for estimating α, the model can be used for all vertical fall heights in the dataset (51 m to 440 m) and all horizontal lengths in the dataset (124 m to 852 m), excluding the Mount Seymour outlier path. As discussed in Section 4.4.5, the models developed using the runout ratio method may be best suited to the smaller slopes in the dataset (e.g. $H_\alpha \leq 275$ m), while scale effects are less apparent in the multiple

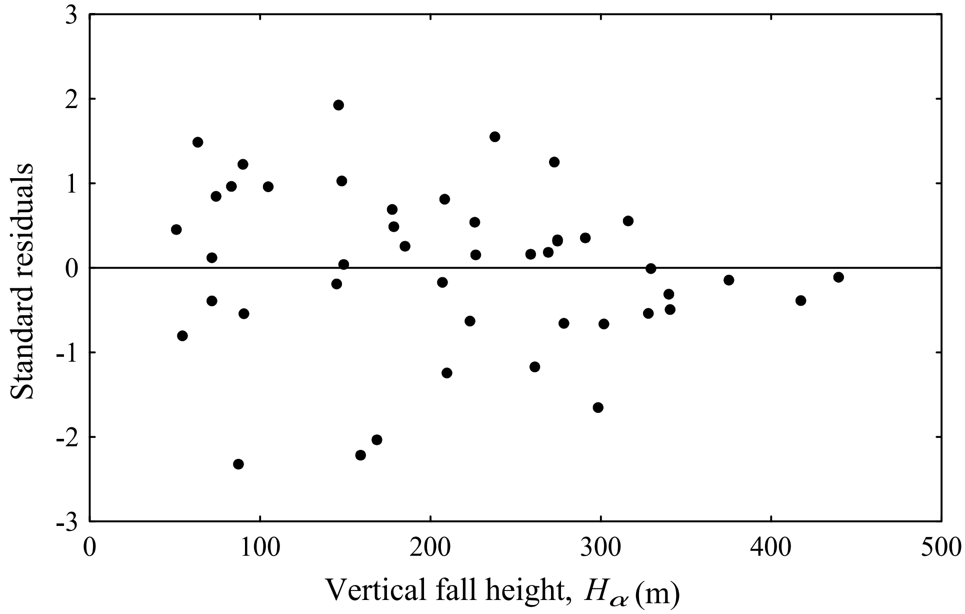

Figure 4.18 Distribution of standard residuals versus vertical fall height, H_α

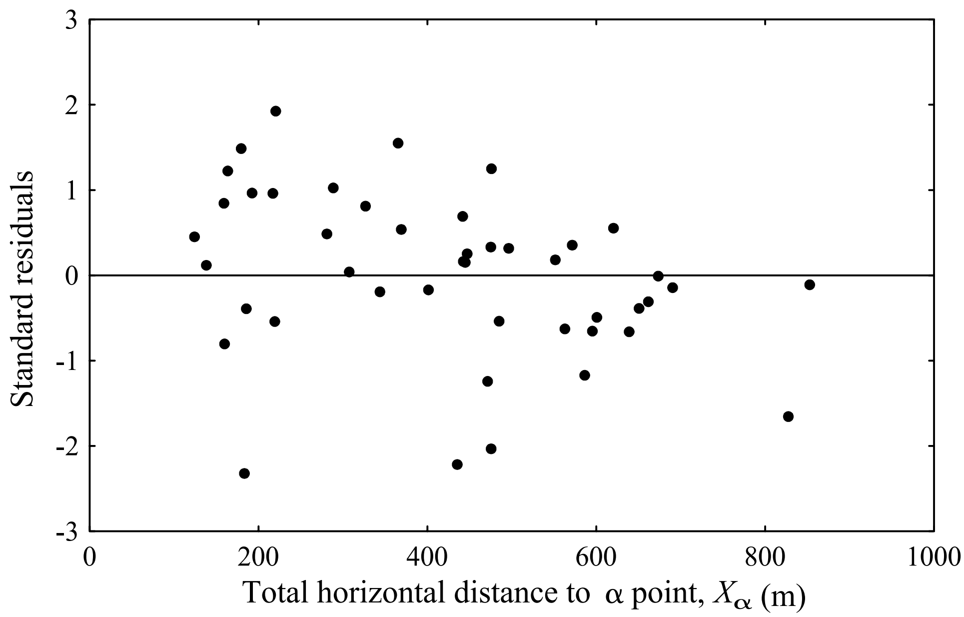

Figure 4.19 Distribution of standard residuals versus horizontal distance to α point, X_α

regression model.

4.5.7 Proposed physical effects of independent variables

The three independent variables used in the regression model, H_0y'', H_0 and TP are topographic parameters connected to the terrain profile for each path (Figures 4.1 and 4.2).

While all three variables are statistically important parts of the regression model, the physical effect of each variable runout should be discussed to evaluate their individual contribution to the model.

The variable H_0y'' was found to be statistically significant in studies for other mountain ranges (Lied and Bakkehøi, 1980; McClung and Lied, 1987; Lied et al., 1995; Jóhannesson, 1998). In all but the study by Lied et al. (1995), H_0y'' was subsequently left out of the regression equation for α since it did not substantially improve the model.

Lied and Bakkehøi (1980) argue that scaling the radius of curvature, y'', with H_0 makes the profile independent of the vertical fall height of the path. Their reasoning is that an avalanche path with a small vertical fall height should have a similar α to one with a large vertical fall height for a path with a similar shape (Lied and Bakkehøi, 1980).

H_0y'' is strongly and positively correlated with α (Table 4.6), which means that higher values of H_0y'' are associated with higher values of α, and consequently shorter runout distances.). Spearman rank correlations between H_0y'' and the scale variables X_β ($R = 0.293$, $p = 0.051$) and H_β ($R = 0.408$, $p = 0.0054$) show that, contrary to the discussion of Lied and Bakkehøi (1980), the variable H_0y'' is strongly scale dependent for the short slope dataset, even though it is a dimensionless variable.

H_0 is also strongly and positively correlated with α, while y'' is not significantly correlated with α (Table 4.6). Interpretation of these correlations shows that paths with higher values of y'' (highly curved) and higher values of H_0 (taller slopes) are associated with higher values of α, or relatively shorter runout distances. Conversely, low curvature (nearly planar), short paths are associated with lower values of α, or relatively longer runout distances.

In terms of avalanche dynamics, highly curved avalanche paths have higher energy losses associated slope angles that decrease markedly down the path and consequently reduced runout potential. The lowest amount of energy loss would be associated with a perfectly linear slope, for which $y'' \approx 0$.

The finding that H_0 is also strongly and positively correlated with α agrees with one of the original hypothesis of this study that shorter slopes have relatively longer runout distances than taller slopes in this dataset. While shorter slopes have relatively longer runout distances, as the strong and positive correlation with α suggests, there is also curvature effect in the model with respect to y''. Thus, H_0y'' is a more important predictor variable for α than either y'' or H_0 alone.

The variable TP, the terrain profile, is moderately and negatively correlated with α, but is not significant at the $p = 0.05$ level. Recalling from Section 4.2, TP = 1 represents a slope with a nearly linear transition in slope angle from the track to the runout zone, TP = 2 represents a path with a concave parabolic shape, and TP = 3 represents a path with a hockey-stick profile (Figure 4.2). This variable is highly related to the radius of curvature, y'', but accounts for the very abrupt change in slope associated with hockey-stick profiles. Based on the negative correlation of TP with α, paths with higher values of TP (i.e. hockey-stick profiles) are correlated with lower values of α, and consequently longer runout distances. This finding agress with Martinelli (1986) who observed unusually long runout distances associated with short-track, hockey-stick profile paths. One possible physical interpretation for this phenomenon is that fast moving snow may become partly fluidized upon reaching an abrupt slope transition associated with paths with hockey stick profiles (Martinelli, 1986; K. Lied, personal communication, 2002). Thus, snow in these cases may flow greater distances due to the entrained air and reduced frictional forces past this transition location (Martinelli, 1986). Another explanation for this phenomenon is that there is a tendency for snow to be deposited at a sharp slope transition and for the remaining snow to overide the material trapped in the transition area (McClung and Mears, 1995). The material trapped at the transition may serve to reduce frictional forces at the transition, resulting in relatively longer runout distances.

An important point to note is that the TP variable may simply be compensating for the quadratic fit of the curves to the hockey-stick profiles. It may be the case in these paths that the beta points for the fitted curves should be located farther upslope than the beta

Table 4.10 Summary of multiple regression models

Model	***n***	**adjusted R^2**	***SE***	**Model *p***	**Coefficient, β_i**			
					Intercept	**H_0y''**	**TP**	**H_0**
Initial model (Equation 4.11)	45	0.79	1.9 °	$< 10^{-5}$	22.42 °	22.11 °	-2.60 °	0.01 °·m^{-1}
Simplified model (Equation 4.12)	45	0.72	2.2 °	$< 10^{-5}$	25.46 °	26.93 °	-3.74 °	n/a

point at the transition of the hockey stick. Thus, when terrain parameters are taken from parabolas fitted to path profiles, avalanches in paths with hockey-stick profiles run farther in relation to paths with other profiles.

From a practical perspective, higher values of TP (i.e. TP = 3 for hockey-sticks) are associated with lower values of α, as shown by the negative contribution of TP to the regression model (Table 4.10). Therefore, for conservative estimates of runout one would have a preference to choose higher vaules of TP in the model if unsure of which category of TP to apply to the path profile.

If sufficient data were available, separate models could possibly be developed for each terrain profile class, or at least separate models for paths defined as hockey-sticks and other paths. However, there were only 10 paths classified as hockey-sticks in this study, which is not a sufficient number of data to conduct multple regression analyses for paths with TP = 3.

4.5.8 Summary of regression models

One avalanche runout model and a simplified version of this model were developed in the proceeding sections using multiple regression. The models were refined by excluding one outlier, and analyses of the residuals were performed. These models are summarized in Table 4.10 and below, and uses and limitations for the models are proposed.

The Initial model (Equation 4.11) has a slightly higher adjusted R^2 and lower standard error than the Simplified model (Equation 4.12). Considering that the variable H_0 must be calculated as part of the variable H_0y'', there is little reason to choose the simplified model over the initial model. Thus, the preferred regression equation relating α to terrain parameters is

$$\hat{\alpha} = 22.42 + 22.11\ H_0 y'' - 2.60\ \mathrm{TP} + 0.01\ H_0 \tag{4.11}$$

A comparison of residuals for individual mountain ranges (Section 4.5.5) showed that the Coast Range contributes the least amount of error to the proposed model and, with additional data, a regression equation might be developed for the Coast Range independent of the other ranges. A review of the standard residuals versus the vertical drop to the α point, H_α, and the total horizontal distance to the α point, X_α, shows that there is no discernable scale effect in the regression model developed for estimating α. This is in contrast to the models developed using the runout ratio method, in which there is a discernable scale effect in the dataset.

The physical effect of the three independent variables on the regression model was discussed to evaluate their individual contribution to the model.

4.6 Comparison of runout ratio and multiple regression methods

In the previous sections, avalanche runout models were developed using two different methods: the runout ratio method and the multiple regression method. Both methods yield models that provide reasonably good fits to the sample of avalanche paths from this study. To determine which of the models provide better estimates of runout distances, models based on the two methods are quantitatively compared in this section.

The models developed using the multiple regression method measure runout in terms of α, while models developed using the runout ratio method measure runout in terms of the runout ratio, $\Delta x/X_\beta$. With measured values of the predictor variables X_β and β, the runout can be estimated in terms of α and $\Delta x/X_\beta$ for model comparison. Because the model coefficients in the regression method have been chosen to minimize the sum of squared residuals in α, a bias is introducted when comparing these models to the models developed using the runout ratio method in terms of α (Jóhannesson, 1998). Similarily, the coefficients in the runout ratio method have been chosen to minimize the sum of squared residuals in the runout ratio, $\Delta x/X_\beta$, so comparing models in terms of Δx is biased toward the models developed using the runout ratio method. Thus, it is best to compare models in terms of both Δx and α. The following model comparison follows the approach of McClung (2001a).

Models developed using the multiple regression method contain the assumption that runout distances, measured in terms of α, are approximately normally distributed. This has been shown to be a valid assuption for the proposed regression model in Section 4.5. For a given avalanche path with a constant value of β, α decreases as the non-exceedence probability, P, increases with runout distance (measured from the β point) in the runout zone (McClung, 2001a). A chosen non-exceedence value of P ($0 < P < 1$) defines the number of α_P values for which $P \times 100$ % of the values in the normal distribution will not be less than the given value of α_P (McClung and Mears, 1991). A fit of the data using multiple regression methods allows for the estimation of α as a function of the non-exceedence probability, P, where the estimation interval for α_P is defined as (Walpole and Myers, 1985, p. 371):

$$\alpha_P = 22.42 + 22.11\ H_0 y'' - 2.60\ \mathrm{TP} + 0.01\ H_0 - z_P SE\,(1 + x_0' A^{-1} x_0)^{1/2} \qquad (4.13)$$

where z_P is the z-statistic representing standard deviations from the mean for a normal distribution, and the term $SE(1+x_0' A^{-1} x_0)^{1/2}$ represents the standard deviation of the sampling distribution for the estimator α_P using maxtrix operations, also called the standard error of estimation in many regression computer packages. The term x_0' is called the condition vector where $x_0' = [1, x_{10}, x_{20},\ldots,x_{k0}]$ for k predictor variables. A^{-1} is the inverse $(k + 1) \times (k + 1)$ matrix for the data used to build the regression model. The term $z_P SE(1+x_0' A^{-1} x_0)^{1/2}$ in Equation 4.13 provides a estimation interval for an individual α_P given a non-exceedance probability, P.

The term $1+x_0' A^{-1} x_0$ is complicated to calculate manually and is typically computed by computer packages using the regression model input data. Equation 4.13 can be simplified to

$$\alpha_P = 22.42 + 22.11\ H_0 y'' - 2.60\ \mathrm{TP} + 0.01\ H_0 - C_P SE \qquad (4.14)$$

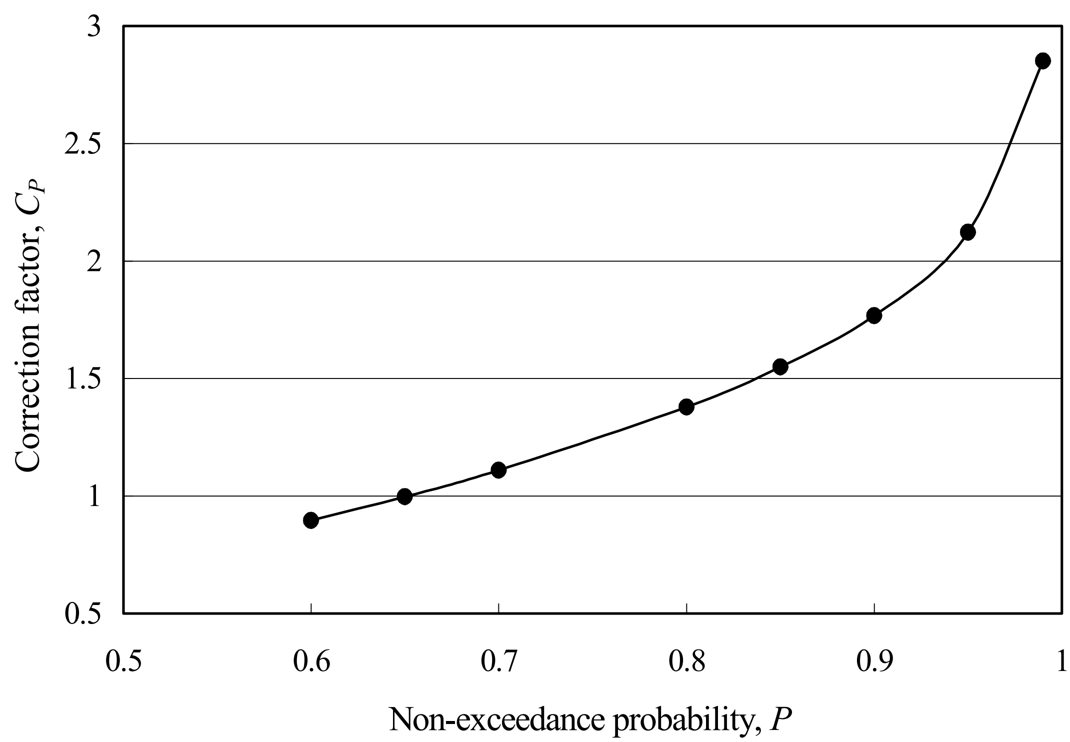

Figure 4.20 Prediction interval correction factor, C_P, in Equation 4.14

where C_P is a correction factor shown graphically in Figure 4.20 for a given non-exceedence probability, P, and SE is the standard error of regression of 1.9º. It can be observed in Figure 4.20 that the relationship between C_P and P increases non-linearly for P > 0.85.

The relationship between α_P and Δx_P can be expressed by the relationship

$$\frac{\Delta x_P}{X_\beta} = \frac{\tan\beta - \tan\alpha_P}{\tan\alpha_P - \tan\delta} \tag{4.15}$$

(McClung, 2001a) where Δx_P and α_P are the runout distance and α angle at a given value of P, and δ is the angle measured from the horizontal by sighting between the α and β points (Figure 4.1). Because X_β is a constant value for an individual avalanche path, the runout distance can be expressed as

$$\Delta x_P = \left(\frac{\tan\beta - \tan\alpha_P}{\tan\alpha_P - \tan\delta} \right) X_\beta \tag{4.16}$$

The δ angle is determined analytically rather than statistically (McClung, 2001a).

The runout ratio method assumes that runout distances can be represented by a Gumbel distribution. This was shown to be a valid assumption in Section 4.4. For a given avalanche path, the runout ratio, $\Delta x/X_\beta$, increases as the non-exceedence probability increases with runout distance measured from β in the runout zone. A chosen non-exceedence value of P ($0 < P < 1$) defines the number of $\Delta x/X_\beta$ values for which $P \times 100$ % of the values in the normal distribution will not exceed the given value of $\Delta x/X_\beta$. The equation representing the runout ratio, $\Delta x/X_\beta$, as a function of the non-exceedence probability, P, is (see Section 4.4.3):

$$(\Delta x/X_\beta)_P = 0.494 - 0.441 \ln(-\ln(P)) \tag{4.7}$$

Because X_β is a constant value for an individual avalanche path, Equation 4.10 can be re-written in terms of the runout distance, Δx_P

$$\Delta x_P = [0.494 - 0.441 \ln(-\ln(P))]\ X_\beta \tag{4.17}$$

This term may be compared with the expression for the runout distance as a function of non-exceedance probability for the multiple regression method (Equation 4.16).

Table 4.11 shows a comparison of the models developed using the runout ratio and multiple regression methods for two avalanche paths chosen randomly for each mountain

Table 4.11 Comparison of runout distances and α angles for eight paths for the regression model $\alpha_p = 22.42 + 22.11\ H_0y'' - 2.60\ TP + 0.01\ H_0 - C_PSE$ (Equation 4.14) and the 4-Range model $(\Delta x/X_\beta)_P = 0.494 - 0.441 \ln(-\ln(P))$ (Equation 4.7) (Table after Nixon and McClung, 1993)

Avalanche Path	***P***	**Regression model estimate**		**Runout ratio model estimate**			**Observed value** [1]	
		α_p	Δx_P	$(\Delta x/X_\beta)_p$	α_p	Δx_P	α	Δx
Wolverine Ridge	0.99 0.90 0.80 0.50	21.1 23.1 23.8 25.0	289 237 221 195	2.426 1.439 1.124 0.648	13.2 18.3 20.9 26.5	642 378 294 167	23.9	217
Shark Mountain	0.99 0.90 0.80 0.50	22.1 24.1 24.9 26.1	292 230 208 177	2.426 1.439 1.124 0.648	11.5 16.1 18.4 23.5	957 564 439 249	29.8	96
Apex Mountain East	0.99 0.90 0.80 0.50	24.7 26.7 27.4 28.7	240 191 176 150	2.426 1.439 1.124 0.648	12.8 17.9 20.4 25.8	815 480 373 212	30.3	115
Schroeder Shoulder	0.99 0.90 0.80 0.50	24.6 26.7 27.4 28.7	202 156 141 117	2.426 1.439 1.124 0.648	12.0 16.7 19.2 24.4	801 472 367 208	30.1	48
Brohm Ridge Col	0.99 0.90 0.80 0.50	16.7 18.7 19.4 20.6	417 347 326 292	2.426 1.439 1.124 0.648	14.7 20.4 23.3 29.2	504 279 231 131	22.5	247
Cornice Ridge North	0.99 0.90 0.80 0.50	18.1 20.1 20.9 22.1	322 267 248 222	2.426 1.439 1.124 0.648	13.9 19.3 22.0 27.7	488 288 224 127	19.5	282
Mont Jaques Cartier Saddle	0.99 0.90 0.80 0.50	17.5 19.5 20.5 21.5	459 381 348 317	2.426 1.439 1.124 0.648	14.3 19.8 22.6 28.4	628 370 288 163	21.6	314
Mont de la Passe West	0.99 0.90 0.80 0.50	21.1 23.2 23.9 25.2	430 352 329 289	2.426 1.439 1.124 0.648	13.7 19.0 21.7 27.4	889 524 407 231	25.3	287

[1] Observed values of α and Δx were estimated from vegetation damage during field studies, corresponding to return periods of 30 - 100 + years

range, for a total of eight avalanche paths. In order to compare the models in an unbiased manner, values for both the runout distance, Δx_P, and the equivalent α_P angle are presented. The results in Table 4.11 show that at higher values of *P* (0.90 and 0.99), the runout ratio method estimates longer runout distances than the regression method for most paths, with the exception of the Brohm Ridge and Mont Jaques Cartier Saddle paths at $P = 0.90$. This is consistent with the findings of Nixon and McClung (1993), and is explained by the fact that runout estimates based on the assumption that runout follows an extreme value distribution should be higher than estimates based on runout following a normal distribution. High non-exceedance probabilities (e.g. $P = 0.90$) are important in engineering applications such as land use planning, where one must account for avalanche events with longer return periods, and consequently higher non-exceedance probabilities.

Another important observation is that at very high values of *P* ($P = 0.99$), the runout ratio method estimates α values that appear to be unreasonably low (Table 4.11). A review of the literature (Lied and Bakkehøi, 1980; Mears, 1984; Martinelli, 1986; McClung and Mears, 1991; Nixon and McClung, 1993; Jóhannesson, 1998; Tremper, 2001, p. 70) shows that for most studies of avalanche runout, which include hundreds of avalanche paths, minimum observed α values are in the range of 14º to 20º. Exceptionally low values are in the range of 14º to 16º, with only one recorded α angle of 14º in the Colorado Rocky Mountains (Martinelli, 1986). The lowest observed α angle from the short slope dataset is 18.8º. Table 4.11 shows that for $P = 0.99$, the runout ratio model estimates α_P angles in the order of 12º to 15º. This implies that this model may be overly conservative at high non-exceedence probabilities. The regression model estimates more realistic α_P angles in the order of 17º to 24º for a non-exceedence probability of 0.99.

McClung (2001a) compared models developed using the runout ratio and regression methods and noted several important differences between the models, including:

- The runout ratio method provides more conservative (longer runout distance) estimations for flat terrain in the runout zone ($\delta = 0^\circ$) and the regression method is more conservative for sloping terrain ($\delta = 5^\circ$ and $\delta = 10^\circ$) in the runout zone.
- The runout ratio method has little dependence of the runout distance on runout zone steepness, while runout distance estimations using the regression method are strongly influenced by the runout zone steepness.

Table 4.12 Runout distances calculated using the runout ratio and regression methods, as a function of the non-exceedance probability, P, and the slope steepness in runout zone, δ (After McClung, 2001a)					
		Runout distance (m)			
P	Method	δ = 0º	δ = 5º	δ = 10º	δ = 15º
0.50	Runout ratio	188	188	188	188
0.50	Regression	98	120	155	222
0.80	Runout ratio	326	326	326	326
0.80	Regression	120	148	195	291
0.90	Runout ratio	417	417	417	417
0.90	Regression	134	167	223	340
0.99	Runout ratio	704	704	704	704
0.99	Regression	177	227	317	537

The results of similar analyses to those of McClung (2001a) for the models developed in this study are shown in Table 4.12. For comparison, mean values from the data (Table 4.1) are assumed for the input variables (McClung, 2001a), including $\beta = 32.8^{\circ}$, $X_{\beta} = 290$ m, $H_0 = 216$ m, $H_0 y'' = 0.332$ and TP = 2. The slope angle in the runout zone, δ is varied from 0º to 15º, and four non-exceedance probabilities are used: 0.5, 0.8, 0.9 and 0.99. The results in Table 4.12 indicate that there is a strong dependence of the runout distance on δ for any *P* value for the regression method, while the runout ratio method is independent of δ for a given *P*. This agrees with the findings of McClung (2001a). The runout distances estimated by the runout ratio method are comparable to values from the regression method for values around δ = 15º, which is also the mean value of δ for the dataset. McClung (2001a) found the runout distances to be comparable near δ = 5º, which is the mean value for their dataset. This result is not entirely unexpected considering that he defines the β point where the slope decreases to 10º, while the β point is defined in this study of short slopes where the slope first decreases to 24º. Thus, based on this modified definition of the β point, steeper slope angles beyond the β point (higher δ) are expected for the short slope dataset.

Contrary to the findings of McClung (2001a) for taller slopes, however, both Δx and

$\Delta x/X_\beta$ are negatively correlated with δ. The Spearman rank correlation of Δx with δ is -0.50 ($p = 4 \times 10^{-4}$) and the correlation of $\Delta x/X_\beta$ with δ is -0.57 ($p = 4 \times 10^{-5}$). This implies that longer runout distances are associated with gentler slopes in the runout zone, which contradicts the findings shown in Table 4.12. A possible explanation for this result is the presence of numerous paths with hockey-stick profiles in the dataset. Ten of the 46 paths (22 %) used in the analyses were classified as having hockey-stick profiles. As discussed in Section 4.5.7, paths with hockey-stick profiles are associated with lower α values, and consequently longer runout distances. This relationship can also be observed in the multiple regression Equation 4.11, whereby the negative regression coefficient for TP (β_i = -2.60) means that high values of the predictor variable TP (i.e. hockey-sticks) tend to reduce the response variable α and therefore increase the runout. By definition of a hockey-stick profile, the slope angle in the runout zone is close to 0º (Martinelli, 1986). Thus, paths that have hockey-stick profiles have low values of δ, and these paths are also associated with longer runout distances. This argument agrees with the results shown in Table 4.12.

Based on the above results, paths with hockey-stick profiles may have a very strong affect on the statistical models developed in this thesis, and the number of hockey-stick profiles found in the dataset may be proportionately higher than in other datasets. From a terrain perspecitve, it may be the case that hockey-stick profiles are more common for short slopes than with taller slopes, and such profiles can have a profound effect on extreme runout distances.

Perhaps the most important finding observed in Table 4.12 is that the runout ratio model is more conservative than the regression model except for P = 0.5 and δ = 15º. This agrees with the results in Table 4.11. This result is most profound for the highest non-exceedance probability analysed (P = 0.99), where the runout ratio method estimates runout distances between 1.5 and 4 times the distance estimated with the regression method for δ = 0º to δ = 15º.

4.7 Summary

In this chapter, several models were developed to estimate runout distance based on terrain parameters measured during field studies. Two survey sites with very steep runout zones were removed from the analysis, leaving 46 paths available to develop the runout models.

Several models were developed using the runout ratio method, which is based on the assumption that runout distances obey an extreme value (Gumbel) distribution. The 4-Range model was first developed using a β point defined where the slope first decreases to 10º, similar to previous studies, although this definition provided a poor fit of the data to a Gumbel distribution. Further analyses showed that a better fit was obtained when the β point was defined where the slope first decreases to 24º. This model included data from the four mountain ranges, implying that there is little observed difference in runout distances from short slopes between the four Canadian mountain ranges included in this study.

The runout ratio method was used to develop separate models for individual ranges, of which only the Coast Range data provided a good fit to a Gumbel distribution. The small number of data for this analysis ($n = 15$) limits the utility of this model, but the good fit of data to a Gumbel distribution ($R^2 = 0.98$, $SE = 0.072$) shows promise that an individual range model could be developed for the Coast Range with additional data. Scale effects were analysed by developing a number of models using variable upper limits on the vertical fall height of the avalanche paths. These analyses showed that the best results were obtained when the model was limited to paths with a vertical fall height of less than 275 m ($R^2 = 0.99$, $SE = 0.063$). This indicates that there is a scale effect in this dataset of short slopes with respect to runout ratio methods.

Two long-running avalanche paths were noted during analyses using the runout ratio method. These paths both had runout zones that were within partly confined stream channels and had high values of runout ratio. This channelization of the avalanche flow in the runout zone may have contributed to longer runout distances. These paths were included in subsequent analyses since the runout ratio models are most useful for estimating extreme runout associated with long running avalanche paths.

Models were then developed using a different technique based on multiple regression on terrain parameters. Eight potential predictor variables were chosen to estimate the α angle, all of which had to be geometrically independent of α. A model was developed using three of these variables, H_0y'', TP and H_0, providing a highly significant fit of the data to a normal distribution (adjusted R^2 = 0.79, SE = 1.9º). Attempts were made to simplify this model to one with only one or two predictor variables. A simplified model using the variables H_0y'', TP was developed (adjusted R^2 = 0.72, SE = 2.2º), but since H_0 needs to be calculated as a part of the variable H_0y'', the original model was deemed a more useful model. Scale effects and the proposed physical explanations of the independent variables on the regression model were discussed.

The final section of this chapter included a comparison of models developed using the runout ratio and regression methods for the short slope data. It was found that the runout ratio method estimates more conservative (longer) runout distances than the regression method for most non-exceedance probabilities. This effect is very pronounced for the higher non-exceedance probabilities (e.g. P = 0.99), where the runout ratio method estimates runout distances up to four times that estimated using the regression method. The α angles calculated using the runout ratio method based on the runout distance for non-exceedance probabilities of 0.99 appear to be unreasonably low (i.e. in the range of 12º to 15º), while those calculated using the regression method appear to be within a similar range of low α values found in the literature and in field measurements (i.e. in the range of 17º to 24º).

Further analyses indicated that runout estimated by the regression method depends strongly on δ (slope in the runout zone) for any non-exceedance probability value, while the models developed using the runout ratio method are independent of δ for all given non-exceedance probabilities. The runout distances estimated by the runout ratio method are comparable to values from the regression method for values around δ = 15º, which is also the mean value of δ for the dataset. Again, it was found that the runout ratio method is consistently more conservative than the regression method for variable P and δ values, and is most pronounced for non-exceedance probabilities of P = 0.99, where the runout ratio model estimates runout distances between 1.5 and 4 times the distance estimated with the regression method for δ between 0º and 15º.

The importance of hockey-stick profiles in the short slope dataset was recognized and discussed. When terrain parameters are taken from parabolas fitted to path profiles, avalanches in paths with a hockey-stick profile run father in relation to paths with other profiles. This has very important implications for estimating runout distances for short

5. DYNAMICS RUNOUT MODEL

5.1 Introduction

Models developed for estimating avalanche runout distances using statistical methods were presented in Chapter 4. These models relate runout distance to simple terrain variables using either the runout ratio or multiple regression methods. Another method commonly used for estimating avalanche runout is to apply avalanche dynamics models. These models are based on the physical modelling of avalanche motion, often with friction parameters chosen to fit observed avalanche runout distances. In practice, statistical models are often used to define the extreme runout position in an avalanche path and dynamics models are subsequently used to estimate avalanche velocities and impact pressures in the runout zone.

The friction values used in avalanche dynamics models are physically based parameters that can vary as a function of numerous factors, including snow properties and path characteristics such as slope angle and surface roughness. True values of friction coefficients for moving snow are difficult to determine using lab experiments (McClung, 1990). Because of this, and the large variability between avalanche paths and types of snow involved in an avalanche, friction coefficients are often estimated by back calculating values based on observed avalanche runout distances, or values are assigned based on a range of values given within the literature (e.g. Buser and Frutiger, 1980) and interpreted with the experience of the practitioner. Transference methods are also sometimes used, whereby information from avalanche paths with known runout distances is used to estimate friction parameters for the path of interest by systematically comparing topographical parameters between paths (e.g. Sigurðsson et al., 1998).

Mears (1992, p. 27) remarks that “statistical analysis has shown that the assumed friction parameters cannot be correlated to measurable terrain variables, such as path size or shape”. Bakkehøi et al. (1981) found that scaling the friction parameter, *M/D,* in the PCM model (Perla et al., 1980) with the vertical fall height of the path allowed them to narrow the possible range of the other friction parameter, μ. However, they found that friction parameters could not be directly associated with topographic variables, and using the vertical fall height in analyses merely narrowed the range of possible friction coefficient estimates.

It is proposed that, by selecting a simple avalanche dynamics model best suited to a dataset of short slopes, terrain parameters may be used to narrow the range of friction coefficient values and possibly provide a first estimate, or average value, of the friction coefficients to be used in the model. Such a model could help reduce some of the uncertainty associated with avalanche dynamics modelling by providing a first estimate of the friction parameters. These values could then be refined by the practitioner based on the knowledge of variables such as terrain characteristics, avalanche velocity and slope angle, and combined with expert judgment. Once an average friction value for a path was estimated, it could then be adjusted to provide more realistic values for various parts of the path (McClung, 1990).

5.2 Selecting the model

Of the avalanche dynamics models discussed in Chapter 2, very few can be considered useful for application to short slopes. Reasons for this include that many models include empirically based assumptions that were developed from a dataset of large avalanche paths, and that many models assume avalanche flow dynamics that may not be well suited to smaller slopes (e.g. avalanche motion as a turbulent fluid). The Swiss dynamics model (Salm et al., 1990) is an example of a model based on a physical description of avalanche flow that has subsequently been modified to fit a dataset of Swiss avalanches. Such models have limited utility for a dataset consisting entirely of short slopes. Thus, one seeks a simple avalanche dynamics model that does not include empirically derived assumptions, and has a relatively simple mathematical formulation. Three models that meet this criterion are the Leading Edge Model or LEM (McClung and Mears, 1995), PCM (Perla et al., 1982) and the PLK (Perla et al., 1984) models. All three models have different theoretical backgrounds and assumptions, but are all relatively simple models in terms of mathematics and application.

The PCM model, although mathematically simple, requires the input of two friction parameters, μ and M/D. The PLK model has the same two friction parameters, μ and M/D, but also has a random particle velocity parameter, for a total of three parameters that need to be estimated. The PCM and PLK models have previously been described in Sections

1.7 and 2.2. The presence of two or more friction parameters makes estimation of average values of the friction coefficients difficult when using regression methods based on terrain parameters. For this reason, these two models are not considered for analysis in this section.

The LEM has several qualities that make it the best candidate for application to a set of short slopes. First is that the simplified LEM requires input of only one basal friction parameter, μ, whereas most other models require at least two friction parameters. Thus, there is one unique solution when solving for a specified runout distance in a path. Models that use more than one friction parameter have non-unique solutions for a specified runout distance and typically require that one parameter be fixed while the second parameter is adjusted to fit a known runout distance in a path (e.g. Lied et al., 1995).

The second quality that makes the LEM model a good candidate for application to short slopes is that it calculates avalanche runout for the tip (leading edge) of the avalanche, rather than for the centre-of-mass of the deposit.

The third, and perhaps most important reason for selecting the LEM is that it treats avalanche motion as a granular flow (Dent, 1986; Dent, 1993). For short slopes, many avalanches would not have sufficient time, travel distance or velocity to fully break up a slab and form a mass that behaves predominantly as a turbulent fluid. A more probable situation is that avalanches on short slopes behave like a flowing granular material, without the substantial turbulence associated with larger avalanches, and especially with the powder cloud. Thus, the LEM likely models avalanche motion for short slopes more closely than the PCM, PLK or Swiss models.

Based on these three qualities, the LEM is chosen for analyses in the following sections.

5.3 Leading Edge Model

The Leading Edge Model calculates the stopping position of the tip of an avalanche by solution of one-dimensional momentum and continuity equations (McClung and Mears, 1995). This model assumes that the avalanche mass behaves as a dense granular material, and that basal drag is the dominant frictional force in the equation. Resistance at the top of the avalanche is also included in the model, but can be can be ignored in some cases of practical interest (McClung and Mears, 1995). This model also incorporates a passive snow pressure term that accounts for the slope angle dependence of basal resistance. The model was developed for use in the runout zone where granular flow is expected to be the dominant flow mechanism, and requires an incoming avalanche velocity be specified, usually at the top of the runout zone.

The LEM model assumes that avalanche discharge per unit width is constant, which is an approximation, but also a reasonable assumption in the runout zone (McClung and Mears, 1995). Many other models assume conservation of mass from the starting position to the runout position (e.g. Perla et al., 1980; Salm et al., 1990) which, due to entrainment and deposition of snow in different parts of the path, is likely to introduce larger errors into the model than one that only assumes constant mass in the runout zone.

The force-momentum equation for the Leading Edge Model is expressed as (McClung and Mears, 1995)

$$\frac{\mathrm{d}}{\mathrm{d}t}(vt) = -G_0 t + V - D_0 v^2 t \tag{5.1}$$

where

$$G_0 = g\,(\mu \cos\psi - \sin\psi) \tag{5.2}$$

$$V = v_0 \cos(\psi_0 - \psi)\left(1 + \frac{k_{\mathrm{p}} g h_0 \cos\psi_0}{2 v_0^{\,2}}\right) \tag{5.3}$$

and

$$D_0 = \frac{1}{2}\left(\frac{\rho_t}{\bar{\rho}}\right)\frac{C_D}{\bar{h}} \tag{5.4}$$

In the preceding equations, v is the speed of an avalanche along an incline at time t, g is the gravitational constant, μ is the basal frictional coefficient, ψ is the slope angle in the segment of interest, v_0 is the incoming velocity of the avalanche entering that segment, ψ_0 is the slope angle on entering a segment, h_0 is the flow depth on entering the runout zone, k_p is the coefficient of passive snow pressure, D_0 is the turbulent resistive force, ρ_t is the density of the snow-dust-air mixture, ρ is the average flow density, C_D is the drag coefficient and h is the average flow thickness measured perpendicular to the slope.

In the above equations, the term V is described as the momentum loss that is applied to the flow at the transition between slope segments with different average slope angles. In the interest of simplifying the model for practical application (McClung, 2001c), the passive pressure term in Equation 5.3 may be ignored, resulting in the momentum correction

$$V = v_0 \cos(\psi_0 - \psi) \tag{5.5}$$

Solving for Equation 5.1, the velocity at the end of a segment (Point B) can be related to the velocity at the beginning of the segment (Point A) by the simplified expression

$$v_B^{\ 2} = v_A^{\ 2} - G_0 x \tag{5.6}$$

where x is the length of the segment between Points A and B, measured along the slope, and G_0 is the expression shown in Equation 5.2. Thus, the velocity of the avalanche can be calculated at each point in the path with knowledge of the incoming velocity at the beginning of the segment, and by applying a momentum correction (Equation 5.5) at each slope transition. In the following segment, the velocity at Point B, v_B, becomes the initial velocity at Point A, v_A, for the next segment, and so on down the profile. All that is required to initiate and apply the model is an estimate of the incoming velocity, v_0, an estimate of the friction coefficient, μ, and a path profile divided into i segments of length x_i, each with an approximately constant slope angle, ψ_i.

In the runout zone, McClung and Mears (1995) argue that the $D_0 v^2 t$ term in Equation 5.1 can be ignored, which allows the equation to be solved analytically. Thus, the runout distance, X_R, measured in the last segment of the profile is

$$X_R = \frac{V^2}{G_0} \tag{5.7}$$

The above model simplifications result in a model that can easily be applied to individual avalanche paths and solved analytically. Equations 5.2, 5.5, 5.6 and 5.7 form the fundamental equations for the *Simplified LEM* (McClung, 2001c).

Because of the limited vertical fall height for short slopes, there is a strong argument for the case that granular flow is the appropriate description of the primary flow mechanism for these paths. The LEM is designed to be applied to the runout zone where granular flow is believed to be the dominant flow mechanism. The incoming velocity of an avalanche is estimated based on real velocity measurements of avalanches, for which the upper limit is typically assumed to be a function of the slope length, S_0 (McClung, 1990), or the vertical fall height, H_α (McClung and Schaerer, 1993, p. 110). Thus, conditions in the starting zone and track are not important in this model, and modelling typically is initiated in the lower part of the track or top of the runout zone (McClung and Mears, 1995).

5.4 Application of the dynamics model

Simplified Leading Edge Models were constructed for each of the 48 avalanche paths in the dataset. The two long-running paths that were noted in Section 4.4.6 (Monte Blanche LaMontagne and Blowdown Creek) were also included in these analyses as dynamics models may be used to model unusual paths, and typically work better than statistical runout models for these paths. Segments in the models represented the segments of constant slope angle that were measured during the field survey. The last segment in the LEM model was the last surveyed section of the path of which the downslope end of the segment corresponds to the interpreted extreme runout position. Each path typically had between 10 and 25 segments (Section 3.4).

It was decided that one of the fundamental assumptions of the model – that the model is initiated with an estimated initial velocity at the top of the runout zone – would need to be overlooked for two reasons. The first reason is that avalanche velocities are typically estimated from datasets of velocity measurements from avalanches around the world, and these datasets typically include few short slopes (McClung, 1990; McClung and Schaerer, 1993, p. 110). Some velocity measurements for shorter slopes do exist (e.g. Gubler et al., 1986), but are very limited in number. The second difficulty is where to define the starting point for the model. For many of the short slope paths, the track was either very short or not present, and thus defining the location to start the model was difficult. Also, the point from which to measure runout distances for short slopes (β point) is interpreted to be the location where the slope first decreases to 24º (Section 4.4.3), which many would argue is still part of the track.

In consideration of the above arguments, it was decided that the model would be initiated at the top of the starting zone (starting position), the only known boundary condition for velocity in the path other than the extreme runout position. At both these locations, the velocity of the extreme avalanche is assumed to be zero, and thus both these locations serve as suitable boundary conditions for the model. It is common practice to initiate other dynamics models at the top of the starting zone (e.g. Mears, 1992, pp. 27, 29, 31), and for practical purposes this assumption was also applied for the LEM, recognizing that entrainment and deposition are neglected.

After setting up the LEM for each path, the friction coefficient, μ, was adjusted until the stopping position of the model matched the extreme runout position interpreted from vegetation damage observed in the field. Thus, a unique value of μ was associated with the extreme runout position for each path. This is a very common technique for obtaining velocity estimates for extreme avalanches (Mears, 1992, p. 28). The calculated value of μ can be interpreted to be the mean friction coefficient for the entire path. McClung (1990) and McClung and Mears (1995) point out that the friction coefficient may need to be varied along the runout zone, as friction conditions at the base of the avalanche tend to increase with increasing distance in the runout zone and as the mass decelerates and stops (McClung and Mears, 1995). This correction was not applied for the avalanche paths, so only an average value of μ was calculated. It should be noted that the theoretical upper limit of the friction coefficient, μ_{max}, is $\tan\alpha$ (Scheidegger, 1973). Thus, based on the range of α in this dataset ($18.8^o < \alpha < 39.0^o$) from Table 4.1, initial estimates for μ_{max} should range between 0.34 and 0.80, with a mean μ_{max} of 0.49 corresponding to the mean α of 26.5º.

Table 5.1 shows the statistical distribution of the average friction coefficients and maximum velocity in the profile calculated using the LEM for each path. Additionally, statistics are presented for the theoretical upper limit for the friction coefficient, μ_{max},

Table 5.1 Statistical distribution of friction parameter, μ, and maximum velocity predicted by the Leading Edge Model

	Average μ	**$\mu_{max} = \tan(\alpha)$**	**Maximum velocity (m/s)**
N	48	48	48
Mean	0.49	0.50	33
Standard Deviation	0.11	0.10	8
Minimum, Q_0	0.29	0.34	18
Lower Quartile, Q_1	0.42	0.43	27
Median, Q_2	0.47	0.50	34
Upper Quartile, Q_3	0.56	0.57	39
Maximum, Q_4	0.80	0.81	56

based on the observed extreme runout position. As can be seen in Table 5.1, the values for average μ range between 0.29 and 0.80, which is in very close agreement with the range of values for the theorectical upper limit of μ_{max}, (0.34 to 0.80). This is not surprising since the LEM model is being fitted to observed values of α (the observed extreme runout position) and therefore these values should be very closely related.

The maximum velocity calculated by the LEM (Table 5.1) ranges from 18 to 56 m/s (mean of 33 m/s), and matches very closely the range of typical dry snow avalanche maximum velocity estimates provided by Mears (1992, p. 11) for slopes with a vertical fall height of between 100 and 500 m (20 to 55 m/s). Paths in the dataset with larger vertical fall heights (e.g. Mount Seymour, H_α = 593 m) are associated with avalanche velocities at the upper end of this range (e.g. maximum velocity of 56 m/s in the LEM simulation). Gubler et al. (1986) measured the velocity of several small (< 500 m^3) avalanches using doppler radar methods and recorded maximum velocities ranging between 13 and 28 m/s. Based on these two sources, the LEM model fitted to the observed extreme runout positions is believed to be providing a reasonable representation of avalanche velocity in these paths. These measured speed values are less than the mean value (33 m/s) estimates using the LEM probably because the measure avalanche speeds are not representative of extreme avalanches but, rather, represent avalanche speeds in smaller, artificially triggered avalanches.

5.5 Multiple regression model for estimating the friction parameter

Similar to the methods used in Section 4.5, multiple regression methods may be used to try to relate various independent predictor variables to a response variable, in this case the average friction coefficient, μ, in the LEM. Possible predictor variables for μ were chosen from the 25 distinct terrain variables shown in Table 4.1 by including only those variables that are not a function of μ and are not categorical variables. Since, μ is strongly related to α (Scheidegger, 1973), the same 14 potential predictor variables used in the regression for α (Section 4.5.2) were used as potential predictors for μ (Table 5.2).

Spearman rank correlations betweeen the predictor variables and μ are shown in Table 5.2. Significant variables ($p < 0.05$) are highlighted. Seven of the 14 variables are significant this level and these were used to build the regression model. Backward

Table 5.2 Spearman rank correlations between the response variable, μ, and the predictor variables used to develop the multiple regression model

Variable	*N*	*R*	*p*[1]
Beta angle, β (º)	**48**	**0.328**	**0.02**
Vertical height to β point, H_β (m)	**48**	**0.681**	**9.8×10^{-8}**
Horizontal reach to β point, X_β (m)	**48**	**0.662**	**3.0×10^{-7}**
Vertical height to low point on parabola, H_0 (m)	**48**	**0.724**	**5.9×10^{-9}**
Second derivative of the slope function, y'' (m^{-1})	**48**	**-0.340**	**0.02**
Scale parameter for path profile, H_0y''	**48**	**0.594**	**8.5×10^{-6}**
Start zone inclination,θ (º)	48	0.112	0.45
Start zone aspect, Aspect (º)	48	-0.0702	0.64
Start zone elevation, SZ Elev (m)	48	0.111	0.46
Runout zone elevation, RZ Elev (m)	48	0.0186	0.90
Surface roughness, SR (m)	48	0.0315	0.83
Wind Index, WI (ordinal data)	48	-0.104	0.48
Width of start zone, W (m)	48	-0.238	0.10
Terrain Profile, TP (ordinal data)	**48**	**-0.449**	**1.4×10^{-3}**

[1] Rows for which $p \leq 0.05$ are marked in bold

elimination multiple regression methods were used with these seven predictor variables to obtain the best fit of the predicted values of μ to the observed values.

A plot of the predicted against the observed data in the early part of the analyses showed one significant outlier, Mount Seymour, that had a standard residual in excess of three standard deviations from the mean. This is the same result found in Section 4.5.2 and consequently this path was excluded from subsequent analyses. After removal of this outlier from the regression model, variables were systematically removed from the regression equation (backward elimination) when they were found to have a minimal effect on the model (i.e. variable *F*-values were less than a specified threshold at each step in the regression). *F*-values (Table 5.3) were computed at each step in the regression to

Table 5.3. Seven predictor variables used in multiple regression analyses for μ and corresponding backwards elimination F values

Variable	*F to remove* [1]
Beta angle, β (º)	**10.489**
Vertical height to β point, H_β (m)	0.523
Horizontal reach to β point, X_β (m)	**7.575**
Vertical height to low point on parabola, H_0 (m)	0.0359
Scale parameter for path profile, H_0y''	**29.021**
Second derivative of the slope function, y''	1.039
Terrain Profile, *TP* (ordinal data)	**72.674**

[1] Rows for which $F \geq 3.1$ (1% significance level) are in bold

help facilitate removal of variables from the regression equation. Using a threshold *F*-value of 3.1 (1 % significance level, $\upsilon_1 = 7$, $\upsilon_2 = 39$; Mendenhall and Sincich, 1996, p. 235, 821), all variables but but H_0y'', *TP,* β and X_β were eliminated from the regression equation. Additional analyses showed that β and X_β could also be removed from the regression equation with minimal effect on the results. Thus, β and X_β were removed and the remaining two predictor variables in the regression equation were H_0y'' and *TP*. Removal of either of these two variables from the regression had a very large adverse effect on the model, with adjusted R^2 values going from 0.76 using both variables to less than 0.40 when either of these variables was removed. The resulting regression equation is

$$\mu = 0.515 + 0.578\ H_0 y'' - 0.107\ \mathrm{TP} \tag{5.8}$$

This model has an adjusted R^2 of 0.76 and a standard error of 0.052, and utilizes 47 of the 48 avalanche paths in the dataset for model development. The regression model has a significance level of 8.5×10^{-15}, which is highly significant. It can be observed that these two predictor variables are topographic parameters derived from the slope profile (Figure 4.1) and were also used in the regression model for estimating α (Section 4.5). The similarity of Equation 5.8 to the regression equation for α (Equation 4.12) is not unexpected considering the strong relationship between average μ and α. A summary of the regression model is shown in Table 5.4

Table 5.4 Results of multiple regression analysis for μ

Adjusted R^2 = 0.76, n = 47 **SE = 0.052, $p < 8.5 \times 10^{-15}$**	**Coefficient β_i**	**Standard error of β_i**	***p***
Intercept	0.515	0.0295	$< 10^{-19}$
H_0y''	0.578	0.0569	4.1×10^{-13}
TP	-0.107	0.0125	7.2×10^{-11}

5.6 Residual analysis

The regression model developed in Section 5.4 was accepted as a promising model based primarily on the fit of the predicted values to observed values of μ in terms of the adjusted R^2 and the standard error, *SE*. Before acceptance of this regression model, the residuals of regression are analysed assess the fit of the model to the data.

The assumption of constant variance is tested by examining a plot of standard residuals for random scatter about zero (Figure 5.1). Visual inspection of Figure 5.1 shows that the assumption of constant variance is satisfied.

The distribution of the standard residuals is shown in Figure 5.2 along with the expected normal distribution. The K-S test for normality has a *d* value of 0.15 ($p > 0.20$), while the Lilliefors test has a significance value of $p < 0.01$. Thus, the hypothesis of

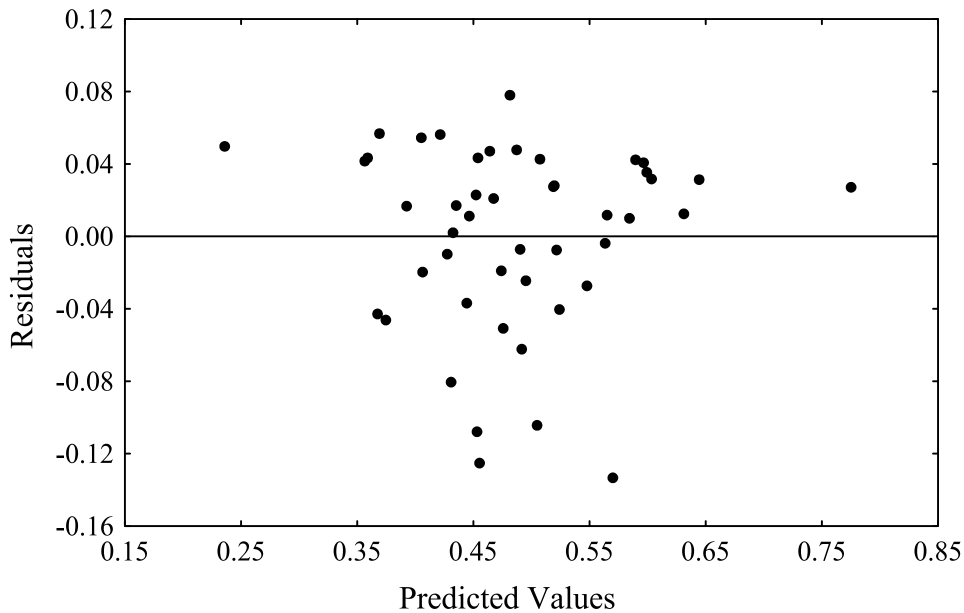

Figure 5.1 Scatter of residuals, multiple regression model for μ

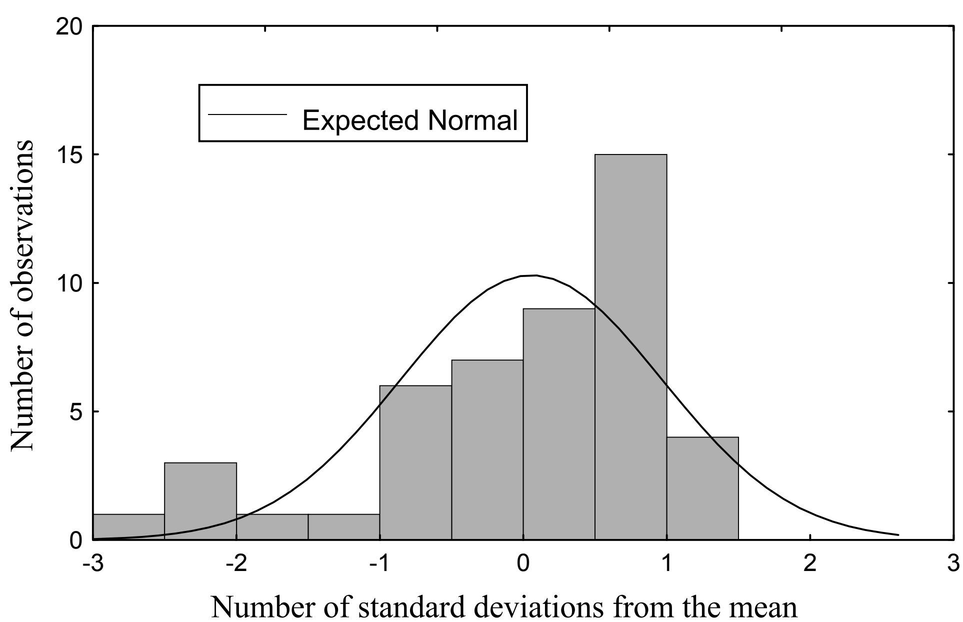

Figure 5.2 Distribution of residuals, multiple regression model for μ

normality of the residuals is not rejected based on the K-S test but is rejected based on the Lilliefors test. Nevertheless, the model is considered acceptable since the regression method is robust with respect to non-normal residuals (Mendenhall and Sincich, 1996, p. 412).

The Durban-Watson statistic for this regression has a value of 2.0, indicating that the residuals are not serially correlated for this model.

Based on Spearman rank correlations between H_0y'' and TP (Spearman $R = 0.21$, $p = 0.17$, $n = 47$), these two variables are not cross-correlated at the 10 % significance level ($p < 0.10$), indicating that strong multicollinearity does not exist in this model. Different values of Spearman rank correlations were obtained than those calculated between H_0y'' and TP in Section 4.5.4, in which it was found that they were correlated at the 5 % ($p < 0.05$) level. This difference may be explained by the inclusion of the two paths (Monte Blanche LaMontagne and Blowdown Creek) in the regression for μ, while these paths were excluded from the regression for α since they are atypical paths that do not fit well into the statistical runout estimation methods of Chapter 4. It must be concluded that these two paths have a large effect on the correlation between H_0y'' and TP.

Since the basic assumptions for multiple regression have largely been satisfied, it is concluded that the regression equation developed for estimating μ (Equation 5.8) is

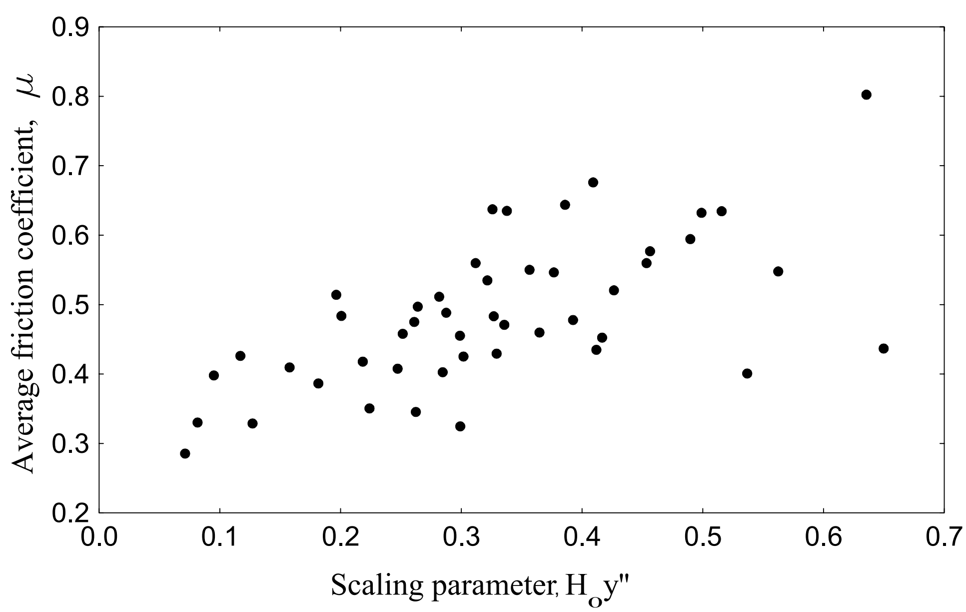

Figure 5.3 Relationship between the scaling parameter and average friction coefficient in the LEM analyses

acceptable.

5.7 Proposed physical effects of independent variables

The two independent variables used in the regression model in Section 5.4, H_0y'' and TP, are topographic parameters that are related to the terrain profile for each path (Figures 4.1 and 4.2). While both of these parameters are statistically important parts of the regression model, the physical effect of each variable should be discussed to evaluate their individual contribution to the model.

The scaling parameter, H_0y'' is strongly and positively correlated with μ (Spearman $R = 0.59$, $p = 8.5 \times 10^{-6}$), which means that higher values of H_0y'' are associated with higher friction coefficients in the LEM. Since higher friction coefficients provide more resistance in the dynamics model, they also contribute to shorter runout distances. This is consistent with the results discussed in Section 4.5.7. The relationship between the scaling parameter, H_0y'', and the average friction coefficient in the analyses using the LEM are shown on Figure 5.3. Reiterating the findings of Section 4.5.7, highly curved paths (high y'') have greater energy losses associated with decreasing slope angles and consequently reduced runout potential (higher μ). The lowest amount of energy loss would

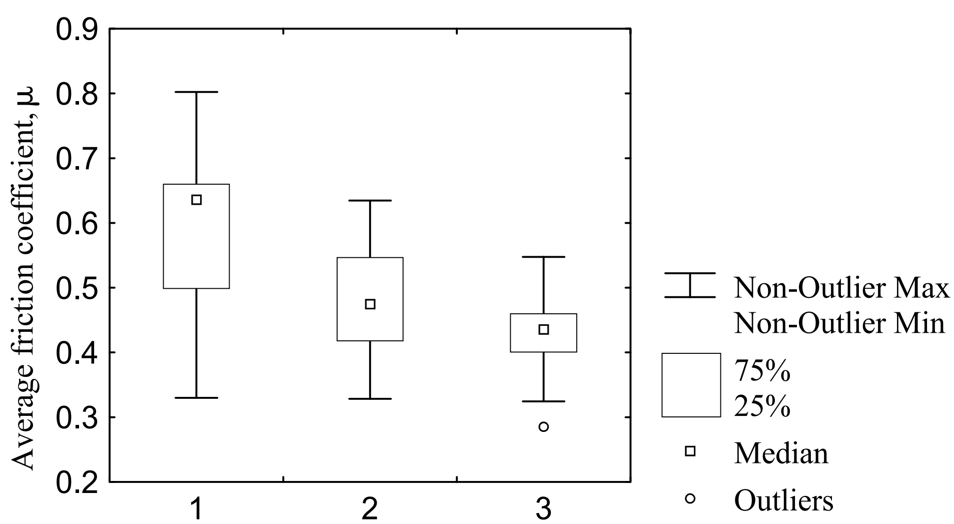

(1 = Nearly linear/planar; 2 = Concave parabola; 3 = Hockey-stick)

Figure 5.4 Box and whisker plot showing relationship between average μ in the LEM and the terrain profile variable, TP. Maximum, minimum, 25th and 75 percentiles, median and outliers are shown for each range of TP.

be associated with a perfectly linear slope, for which $y'' = 0$. This phenomenon is accounted for in the LEM by applying a momentum correction (Equations 5.3 and 5.5) at the transition between segments in the analysis. On a nearly linear slope $\psi_0 \approx \psi$ in Equation 5.5, and thus $\cos(\psi_0 - \psi) \approx 1$. Thus, no momentum correction is applied for a nearly linear slope.

The variable TP, the terrain profile (Figure 4.2), is strongly and negatively correlated with μ (Spearman $R = -0.45$, $p = 1.4 \times 10^{-3}$). Thus, when terrain parameters are taken from parabolas fitted to path profiles, avalanches in paths with hockey-stick profiles run farther in relation to paths with other profiles. This is consistent with the results of Section 4.5.7.

A box and whisker plot showing the relationship of TP with μ is shown in Figure 5.4. This figure clearly shows μ as a decreasing function of TP. What is most important to observe is that the range of friction coefficients associated with hockey-stick profiles (TP = 3) is quite limited, with the friction coefficient lying within the range of $0.29 < \mu < 0.55$. Fifty percent of these values (25th to 75th percentile) lie in the narrow range of $0.40 < \mu < 0.45$. It can be observed that a much larger range of friction coefficients are associated with linear (TP = 1) and concave parabola (TP = 2) profiles. The low values of μ associated with hockey-stick profiles further substantiates the argument that avalanches in these paths may flow greater distances – perhaps due to fluidization – upon reaching an abrupt slope transition (Martinelli, 1986; K. Lied, personal communication, 2002), and possibly also a result of the flow material over-riding snow trapped at the slope transition (McClung and Mears, 1995).

5.8 Summary

Multiple regression methods were used to develop a model to estimate the average friction coefficient, μ, in the LEM based on various terrain variables. Average values of the friction coefficient in a path were obtained by fitting the stopping position of an avalanche in the dynamics model to the interpreted extreme runout position surveyed during the field studies.

The regression model providing the best fit for the short slope dataset uses the terrain parameters H_0y'' and TP to predict μ, and is very similar in form to the regression model for α that was developed in Section 4.5. This result could be expected since μ is strongly related to observed α. The predictive model for μ has an adjusted R^2 of 0.76 and a standard error of regression of 0.052, and utilizes 47 of the 48 paths in the dataset. One path was excluded from the analysis as an outlier since it had residuals more than three standard deviations from the mean. Residual analyses show that the basic assumptions for multiple regression have largely been satisfied.

One of the fundamental assumptions of the LEM, that the model be initiated in the lower part of the track or upper part of the runout zone, was overlooked by initiating avalanche motion at the top of the starting zone. This can be justified when considering that the purpose of this analysis was to develop a useful tool for the practitioner to estimate extreme runout distances, and the very few maximum velocity estimates available for short slopes.

The regression equation developed provides an average value of the basal friction coefficient, μ, to be input into the LEM to model avalanche motion in short slopes. This value is only meant to be a first estimate of the friction coefficient, and may need to be subsequently modified based on the knowledge of other terrain and snowpack variables, and interpreted with expert judgment. Also, this value may need to be modified for various parts of the path to reflect changes in terrain and snowpack characteristics. The importance of hockey-stick profiles with respect to estimating μ was discussed, particularly with respect to hockey-stick profiles which were shown to be associated with lower values of the friction coefficient and consequently longer runout distances.

6. CONCLUSIONS AND RECOMMENDATIONS FOR FUTURE RESEARCH

6.1 Statistical runout models

- Runout ratios for 48 short slopes from four mountain ranges are well fit by a Gumbel distribution (R^2 = 0.99, SE = 0.059) when the β point is defined at 24º, rather than the conventional 10º.
- The 4-Range model includes data from all four mountain ranges in the study, implying that there is little difference between mountain ranges in terms of runout distances for short slopes when using the runout ratio method.
- The runout ratio method was used to develop separate models for individual ranges, of which only the Coast Range data were well fit (R^2 = 0.98, SE = 0.072) by a Gumbel distribution. This result shows promise that an individual range model might be developed for the Coast Range with additional data.
- The best results using the runout ratio method were obtained when the model was limited to paths with a vertical fall height of less than 275 m (R^2 = 0.99, SE = 0.063). This indicates that there is a scale effect in this dataset of short slopes with respect to runout ratio methods.
- Two long-running avalanche paths with runout zones within partly confined stream channels were noted in the analyses for the models developed using the runout ratio method. Channelization of the avalanche flow in the runout zone probably contributed to longer runout distances in these paths.
- The model developed using the multiple regression method uses three terrain variables (H_0y'', TP and H_0) to estimate the α angle for extreme runout (adjusted R^2 = 0.79, SE = 1.9º). Scale effects are less pronounced in models developed using the multiple regression method compared to the runout ratio models.
- A comparison of the two statistical methods shows that the runout ratio method estimates more conservative (longer) runout distances than the regression method for most non-exceedance probabilities. This effect is very pronounced for the higher non-exceedance probabilities (e.g. P = 0.99), where the runout ratio method estimates runout distances up to four times that estimated using the regression method.
- Runout estimated by the regression method depends strongly on δ (the slope angle

between the α and β points) for any non-exceedance probability value, whereas the runout ratio model is independent of δ for all given non-exceedance probabilities. The runout ratio method is more conservative than the regression method for most values of P and δ.

- When terrain parameters are taken from parabolas fitted to path profiles, avalanches in paths with hockey-stick profiles tend to run farther in relation to paths with parabolic or almost linear profiles. This has important implications for estimating runout distances for short slopes, particularily when applied to land-use planning.

6.2 Multiple regression model for μ in the Leading Edge Model (LEM)

- Multiple regression methods were used to develop a model to estimate the average basal friction coefficient, μ, in the LEM based on easily measured terrain variables. A regression model was developed for the short slope dataset that uses the terrain parameters H_0y'' and TP to estimate μ, with an adjusted R^2 of 0.76 and a standard error of 0.052.
- The regression model for μ provides an average value of μ to simulate avalanche motion on short slopes with the LEM. This value provides a first estimate of the friction coefficient, which can be modified based on knowledge of other terrain and snowpack variables, and interpreted with expert judgment. Also, this value can be modified for various parts of the path to reflect changes in terrain and snowpack characteristics.
- When terrain parameters are taken from parabolas fitted to path profiles, avalanches in paths with hockey-stick profiles are associated with lower values of the friction coefficient and consequently run farther in relation to paths with other profiles.
- Considering the limitation of statistical models for estimating runout in atypical paths, the regression model provides an important tool for estimating runout on short slopes.

6.2 Recommendations for future research

This study included 48 avalanche paths which was sufficient to build models for combined mountain ranges, but was not sufficient data for properly assessing each range individually. Thus, a larger dataset could be developed that includes more sites in the individual ranges. Most notably, the Coast Range shows promise for having an individual model developed using the runout ratio method.

Since combined models could be developed for paths from four distinct mountain ranges in Canada, regional differences between ranges in the models are interpreted to be weak. However, there may be important climatic variations within these ranges that influence runout distances. Future studies could look into specific climate variables (e.g. 30-year maximum water equivalent of snowfall) and assess their affect on runout distances.

The models developed in this thesis could be verified by applying them to other short slopes both within Canada and internationally. It may be possible to extrapolate this model for use in other regions of the world, and refine the models by inclusion of paths from other regions. Verification of the models was not performed in this study due to the limited number of data. Analyses with additional data to verify the models would improve the reliability of these models.

The upper limit on the slope height for the regression model could be determined with more data for taller slopes.

Since the regression model developed for short slopes with the three terrain variables, H_0y'', TP and H_0, applies across mountain ranges, this approach could be tried for taller slopes. It might provide a means of estimating runout across ranges for taller slopes, especially in areas for which there are no regional datasets and parameters for existing tall slope models.

While a model for estimating the average basal friction coefficient was developed, the effect on this coefficient of distance from the starting position, ground roughness, confinement, velocity and snow properties was not studied. Analyses of these effects could lead to refined friction coefficients for various segments of an avalanche path, and to improved calculations of runout, velocity and impact pressures.

REFERENCES

Bakkehøi, S., Cheng, T., Domaas, U., Lied, K., Perla, R. and Schieldrop, B. 1981. On the computation of parameters that model snow avalanche motion. *Canadian Geotechnical Journal*, 18, 121-130.

Bakkehøi, S., Domaas, U., and Lied, K. 1983. Calculation of snow avalanche runout distance. *Annals of Glaciology*, 4, 24-29.

Barbolini, M., Gruber, U., Keylock, C.J., Naaim, M. and Savi, F. 2000. Application of statistical and hydraulic-continuum dense-snow avalanche models to five real European sites. *Cold Regions Science and Technology*, 31(2), 133-149.

Bartelt, P.A. and Stöckli, V. 2001. The influence of tree and branch fracture, overturning and debris entrainment on snow avalanche flow. *Annals of Glaciology*, 32, 209-216.

Bartelt, P.A. and Gruber, U. 1997. Calibration of a dense snow avalanche model using a Galerkin finite element method. Eidgenossisschen Institutes für Schnee und Lawinenforsschung, Interner Bericht 715. Davos, Switzerland.

Benjamin, J.R. and Cornell, C.A. 1970. *Probability, Statistics and Decision for Civil Engineers*. McGraw-Hill Inc., New York.

Blikra, L.H. and Saemundsson, T. 1998. The potential of sedimentology and stratigraphy in avalanche hazard research. In: Hestnes, E., (Ed.) *Proceedings of the Anniversary Conference 25 Years of Snow Avalanche Research, Voss, 12-16 May 1998*. Oslo, Norwegian Geotechnical Institute, Publication 203, 60-64.

Boucher, D., Hétu, B. and Filion, L. 1999. Late-holocene development of a snow avalanche path in Mount Hog's Back, Gaspé Peninsula, Quèbec. CANQUA-CGRC meeting 1999, University of Calgary, Calgary AB.

Bovis, M.J. and Mears, A.I. 1976. Statistical prediction of snow avalanche runout from terrain variables in Colorado. *Arctic and Alpine Research*, 8(1), 115-120.

Burrows, C.J. and Burrows, V.L. 1976. Procedures for the study of snow avalanche chronology using growth layers of woody plants. Boulder, CO: Institute of Arctic and Alpine Research, University of Colorado, Occasional Paper No. 23.

Buser, O. 1983. Avalanche forecast with the methods of nearest neighbours: an interactive approach. *Cold Regions Science and Technology*, 8(2) 155-163.

Buser, O. and Frutiger, H. 1980. Observed maximum runout distance of snow avalanches and the determination of the friction coefficients μ and ξ. *Journal of Glaciology,* 26(94), 121-130.

Canadian Avalanche Association, 2000. Course manual for Introduction to Snow Avalanche Mapping. Course co-sponsored by the Canadian Avalanche Association and the Forestry Continuing Studies Network, 26 September - 1 October, 2000, Nelson, BC. Canadian Avalanche Association, Revelstoke, BC, Canada.

Canadian Avalanche Association. 2002a. *Land Managers Guide to Snow Avalanche Hazards in Canada* (Jamieson, J.B., Stethem, C.J., Schaerer, P.A. and McClung, D.M., eds.). Canadian Avalanche Association, Revelstoke, BC, Canada.

Canadian Avalanche Association, 2002b. *Guidelines and Standards for Avalanche Risk Determination and Mapping in Canada* (McClung, D.M., Stethem, C.J., Jamieson, J.B. and Schaerer, P.A., Eds.). Canadian Avalanche Association, Revelstoke, BC, Canada.

Caterino, P. 1998. Reconstructing ancient avalanches of the Sierra Nevada Range. In: Proceedings of the International Snow Science Workshop, Sunriver Oregon, September 27-October 1, 1998. Stevens Pass Skia Area, P.O. Box 98, Skykomish, WA.

Dent, J.D. 1986. Flow properties of granular materials with large overburden loads. *Acta Mechanica*, 64, 111-122.

Dent, J.D. 1993. The dynamic friction characteristics of a rapidly sheared granular material applied to the motion of snow avalanches. *Annals of Glaciology*, 18, 215-220.

Government of Quebec. 2000. Report: Public Inquiry into the Causes and Circumstances Surrounding the Deaths in Kangiqsualujjuaq, Nouveau-Québec on January 1, 1999. Le Coroner en chef, Ste-Foy, Québec.

Gubler, H., Hiller, M., Klausegger, G. and Suter, U. 1986. Messungen an Fliesslawinen. Zwischenbericht 1986. Mitteilungen des Eidgenössischen Institutes für Schnee- und Lawinenforschung (EISLF), 41. Davos, Switzerland.

Gubler, H. 1994. Swiss avalanche-dynamics procedures for dense flow avalanches. Report 51, Swiss Federal Institute for Snow and Avalanche Research. Davos, Switzerland.

Gumbel, E. J. 1958. *Statistics of Extremes*. New York, Columbia University Press.

Harbitz, C.B., Issler, D. and Keylock, C.J. 1998. Conclusions from a recent survey of avalanche computational models. In: Hestnes, E., (Ed.), *Proceedings of the Anniversary Conference 25 Years of Snow Avalanche Research, Voss, 12-16 May 1998*. Oslo, Norwegian Geotechnical Institute, Publication 203, 128-135.

Hansen-Bristow, K. and Birkeland, K. 1989. Applications of dendrochronology in avalanche studies. *The Avalanche Review*, 7(4), January 1989. The American Association of Avalanche Professionals, Salt Lake City, Utah.

Hoeller, P. and H. Schaffhauser. 2001. The avalanches of Galtuer and Valzur in Feb. 1999. Proc. International Snow Science Workshop, Oct. 1-6, 2000, Big Sky, Montana: 514-518.

Jamieson, B. 2001. Snow Avalanche Dyanamics and Hazard Mitigation. ENCI 751 course notes, Fall 2001. Department of Civil Engineering, University of Calgary. Calgary, Canada.

Jamieson, B. and Geldsetzer, T. 1996. *Avalanche Accidents in Canada, Vol. 4: 1984-96*. Canadian Avalanche Association, PO Box 2759, Revelstoke, BC, V0E 2S0.

Jamieson, J.B. and Stethem, C. 2002. Snow avalanche hazards and management in Canada: Challenges and Progress. *Natural Hazards* 26(1), 35-53.

Jóhannesson, T. 1998. A topographical model for Icelandic avalanches. Veðurstofa Íslands Report, VÍ-G98003-ÚR03, January 1998. Reykjavík, Iceland.

Jóhannesson, T. 1998. Icelandic runout models compared with topographic models used in other countries. In: Hestnes, E., (Ed.), *Proceedings of the Anniversary Conference 25 Years of Snow Avalanche Research, Voss, 12-16 May 1998*. Oslo, Norwegian Geotechnical Institute, Publication 203, 43-52.

Jónasson, K., Sigurðsson, S.T., and Arnalds, T. 1999. Estimation of avalanche risk. Rit Veðurstofu Íslands VÍ-R99001-ÚR01.

Judson, A. and B.J. Erickson. 1973. Predicting avalanche intensity from weather data: a statistical analysis. United States Department of Agriculture Forest Service Research Paper RM-112.

Judson, A. and King, R.M. 1984. Effect of simple terrain parameters on avalanche frequency. In: Proceedings of the International Snow Science Workshop at Aspen, October 1984. ISSW Workshop Committee, C/O Mountain Rescue-Aspen, Inc., P.O. Box 4446, Aspen, CO, 81612, USA, 12-20.

Kennedy, J.B. and Neville, A.M. 1986. *Basic Statistical Methods for Engineers and*

Scientists, Third Edition. Harper and Row Publishers, Inc., New York.

Keylock, C.J., McClung, D.M. and Magnússon, M.M. 1999. Avalanche risk mapping by simulation. *Journal of Glaciology*, 45(150), 303-314.

Keylock, C.J. and Barbolini, M. 2001. Snow avalanche impact pressure – vulnerability relations for use in risk assessment. *Canadian Geotechnical Journal*, 38, 227-238.

Kristensen, K., Harbitz, C. and Harbitz, A. 2000. Significance of historical records for avalanche hazard zoning in Norway. In: Proceedings of the International Snow Science Workshop, Big Sky, Montana, October 1-6, 2000. American Avalanche Association, P.O. Box 1032, Bozeman, MT, 59771, USA, 475-479.

Lied, K. and Bakkehøi, S. 1980. Empirical calculations of snow-avalanche runout distance based on topographic parameters. *Journal of Glaciology*, 26(94), 165-177.

Lied, K. and Toppe, R. 1989. Calculation of maximum snow-avalanche run-out distance based on topographcial parameters. *Journal of Glaciology*, 26(94), 165-177.

Lied, K., Weiler, C., Bakkehøi, S., and Hopf, J. 1995. Calculation methods for avalanche run-out distance for the Austrian Alps. Norwegian Geotechnical Institute, Report 581240-1, Oslo.

Martinelli, M. 1974. Snow avalanche sites, their identification and evaluation. United States Department of Agriculture, Forest Service Agriculture Information Bulletin, 360.

Martinelli, M. 1986. A test of the avalanche runout equations developed by the Norwegian Geotechnical Institute. *Cold Regions Science and Technology*, 13(1), 19-33.

McClung, D.M. 1990. A model for scaling avalanche speeds. *Journal of Glaciology*, 36 (123), 188-198.

McClung, D.M. 1999. The encounter probability for mountain slope hazards. *Canadian Geotechnical Journal*, 36, 1195-1196.

McClung, D.M. 2000. Extreme avalanche runout in space and time. *Canadian Geotechnical Journal*, 37(1), 161-170.

McClung, D.M. 2001a. Extreme avalanche runout: a comparison of empirical models. *Canadian Geotechnical Journal* 38, 1254-1265.

McClung, D.M. 2001b. Characteristics of terrain, snow supply and forest cover for avalanche initiation caused by logging. *Annals of Glaciology*, 32, 223-229.

McClung, D.M. 2001c. Course manual for Avalanche Hazard Mapping Beta Course. Canadian Avalanche Association development course, 18-22 June, 2001, Revelstoke, BC. Canadian Avalanche Association, Revelstoke, BC, Canada.

McClung, D.M. and Lied, K. 1987. Statistical and geometrical definition of snow avalanche runout. *Cold Regions Science and Technology*, 13(2), 107-119.

McClung, D.M., Mears, A.I., and Schaerer, P.A. 1989. Extreme avalanche runout: data from four mountain ranges. *Annals of Glaciology*, 13, 180-184.

McClung, D.M. and Mears, A.I. 1991. Extreme value prediction of snow avalanche runout. *Cold Regions Science and Technology*, 19, 163-175.

McClung, D.M., Nettuno, L. and Savi, F. 1994. One dimensional modelling for flowing avalanche runout and runup. In: Proceedings of the International Symposium on Snow and Related Manifestation. Snow & Avalanche Study Establishment, Manali (HP), India.

McClung, D.M. and Schaerer, P.A. 1993. *The Avalanche Handbook*. The Mountaineers, Seattle, WA.

McClung, D.M. and Mears, A.I. 1995. Dry flowing avalanche run-up and run-out. *Journal of Glaciology* 41(138), 359-372.

McKittrick, L.R. and Brown, R.L. 1993. A statistical model for maximum avalanche run-out distances in southwest Montana. *Annals of Glaciology*, 18, 295-299.

Mears, A.I. 1984. Climate effects on snow avalanche travel distances. In: Proceedings of the International Snow Science Workshop at Aspen, October 1984. ISSW Workshop Committee, C/O Mountain Rescue-Aspen, Inc., P.O. Box 4446, Aspen, CO, 81612, USA, 1984, 80-83.

Mears, A.I. 1988. Comparisons of Colorado, Eastern Sierra, coastal Alaska, and Western Norway runout data. Proceedings of the International Snow Science Workshop, Whistler, BC, October 12-15, 1988, 232-238.

Mears, A.I. 1989. Regional comparisons of avalanche-profile and runout data: *Arctic and Alpine Research*, 21(3), 283-287.

Mears, A.I. 1992. *Snow-Avalanche Hazard Analysis for Land-Use Planning and Engineering*. Colorado Geological Survey, Bulletin 49.

Mendenhall, W. and Sincich, T. 1996. *A Second Course in Statistics: Regression Analysis*. Prentice Hall, Inc., New Jersey.

Naaim, M. and Ancey, C. 1992. Dense avalanche model. European Summer University, Chamonix, CEMAGREF Publictions, Gap, France, 173-181.

Natale, L., Nettuno, L. and Savi, F. 1994. Numerical simulation of dense snow avalanche: an hydraulic approach. In: IASTED 1994, Proceedings of the 24th Annual Pittsburgh

International Conference on Modelling and Simulations, Pittsburgh, Pennsylvania, 233-236.

Neave, H.R. and Worthington, P.L. 1988. *Distribution-Free Tests*. Unwin Hyman, London, UK.

Nixon, D.J. and McClung, D.M. 1993. Snow avalanche runout from two Canadian mountain ranges. *Annals of Glaciology*, 18, 1-6.

Norem, H., Irgens, F. and Scheildrop, B. 1987. A continuum model for calculating snow avalanche velocities. In: Salm, B. and Gubler, H (Eds.) *Avalanche Formation, Movement and Effects*, International Association of Hydrological Sciences, Publication No. 162, 363-379.

Norem, H. Irgens, F., and Schieldrop, B. 1989. Simulation of snow-avalanche flow in runout zones. *Annals of Glaciology*, 13, 218-225.

Perla, R., Cheng, T.T. and McClung, D.M. 1980. A two-parameter model of snow-avalanche motion. *Journal of Glaciology* 26(94), 197-207.

Perla, R., Lied, K. and Kristensen, K. 1984. Particle simulation of snow-avalanche motion. *Cold Regions Science and Technology*, 9, 191-202.

President's Water Resources Policy Commission. 1950. Water Policy for the American People. Report. Washington, D.C. Vol. 1.

Salm, B. Burkard, A. and Gubler, H. 1990. Berechnung von Fliesslawinen eine Anleitung für Praktiker mit Beispielen: Mitteilungen des Eidgenossischen Instituts für Schnee-und Lawinenforschung. No. 47, Davos, Switzerland.

Salm, B. 1997. Principles of avalanche hazard mapping in Switzerland. In: Ixumi, M., Nakamura, T. and Sack, R.L. (Eds) *Snow Engineering: Recent Advances*. Balkema, Rotterdam, The Netherlands, 531-538

Salway, A. 1976. Statistical estimation and prediction of avalanche activity from meteorological data for the Rogers Pass area of British Columbia. PhD thesis, Faculty of Forestry, The University of British Columbia.

Savage, S.B. and Hutter, K. 1989. The motion of a finite mass of granular material down a rough incline. *Journal of Fluid Mechanics*, 199, 177-215.

Schaerer, P.A. 1972. Terrain and vegetation of snow avalanche sites at Rogers Pass, British Columbia. Mountain Geomorphology: Geographical Processes in the Canadian Cordillera., B.C. Geographical Series No. 14, 215-222.

Schaerer, P.A. 1977. Analysis of snow avalanche terrain. *Canadian Geotechnical Journal*, 14(3), 281-287.

Schaerer, P.A. 1987. *Avalanche Accidents in Canada III. A Selection of Case Histories 1978-1984*, National Research Council of Canada, NRCC Publication 27950.

Schaerer, P.A. 1991. Suggestions for snow research. In: CSSA 1991 Symposium, Center for Snow Science at Alta. April 20, 1991.

Scheidegger, A.E. 1973. On the prediction of the reach and velocity of catastrophic landslides. *Rock Mechanics*, 5(4), 231-236.

Sigurðsson, S., Jónasson, K. and Arnalds, T. 1998. Transferring avalanches between paths. In: Hestnes, E., (Ed.) *Proceedings of the Anniversary Conference 25 Years of Snow Avalanche Research, Voss, 12-16 May 1998*. Oslo, Norwegian Geotechnical Institute, Publication 203, 259-263.

Sovilla, B., Somavilla, F. and Tomaselli, A. 2001. Measurements of mass balance in dense snow avalanche events. *Annals of Glaciology*, 32, 230-236.

Stethem, C.J. and Schaerer, P.A. 1979. *Avalanche Accidents in Canada I. A Selection of Case Histories of Accidents, 1955-1976*. National Research Council of Canada, Division of Building Research Paper 834, NRCC Publication 17292.

Stethem, C.J. and Schaerer, P.A. 1980. *Avalanche Accidents in Canada II. A Selection of Case Histories of Accidents, 1943-1978*. National Research Council of Canada, Division of Building Research Paper 926, NRCC Publication 18525.

Switzerland. 1984. Richtlinien zur Beruecksichtigung der Lawinengefahr bei raumwirksamen Taetigkeiten. Bundesamt fuer Forstwesen, EISLF, EDMZ, Bern.

Tremper, B. 2001. *Staying Alive in Avalanche Terrain*. The Mountaineers Books, Seattle, WA.

Voellmy, A. 1955. Über die Zerstörungskraft von Lawinen [On the destructive forces of avalanches]. Schweizerische Bauzeitung, 73 (12/15/17/19): 159-162, 212-217, 246-249, 280-285. (United States Department of Agriculture, Forest Service, Alta Avalanche Study Center. Translation 2, 1964).

Walpole, R.E and Meyers, R.H. 1985. *Probability and Statistics for Engineers and Scientists*. Third Edition, Macmillan Publishing Co., Ltd., New York.

Watt, W.E., Lathem, K., Neill, C.R. and Richards, T.L. (Eds.). 1989. *Hydrology of floods in Canada, A guide to planning and design*. National Research Council Canada, Associate Committee on Hydrology, Ottawa, Ontario, Canada.

Weir, P. 2002, In press. *Handbook for Management of Snow Avalanche Prone Forest Terrain*. Victoria, BC, Ministry of Forests Research Branch.

APPENDIX A - EXAMPLE OF FIELD NOTES

An example of field notes taken during the survey of the Hector Ridge North avalanche path in the Rocky Mountains is shown in Figure A.1. Field notes were recorded in a field book on water-resistant paper. General terrain characteristics were recorded on the first page, and survey notes were recorded on subsequent pages. Field observations were recorded in a manner consistent with guidelines developed as part of the Canadian Avalanche Association's "Introduction to Snow Avalanche Mapping" course (Canadian Avalanche Association, 2000) and Martinelli (1974).

Columns for the survey notes include: *Pt.*, the survey point number; *Slope Down*, the slope angle measured with the clinometer down the slope; *Slope Up*, the slope angle measured up the slope; *Dist*, the slope distance measured from the starting position or the segment length between survey points; *Elev.*, the elevation measured with an altimeter; and *Comments*, a column reserved for any other observations. The comments column includes information on observations of vegetation in the path, including estimated return periods for large avalanches and the interpreted extreme runout position. Estimates of α and β are included in the field notes when they were measured during the field survey.

Hector Ridge South

Aug. 8/01
A. Jones

At bottom of steep B/R gully below Hector North Ridge. Too steep above for slab formation

sz. width = 55 m main part of sz. (40 m extra sz. to the south but has lots of trees) check at bottom to see if this should be included

SZ asp = 270° (W)
SZ elev = 2125 m
SZ veg. = grass, small shrubs, talus to 0.2 m Ø
SZ rough = 0.2 m

Photo 27 SZ from Pt. 11
28 Runout zone "
29 SZ. from Pt. 21.

Pt.	Slope Down	Slope Up	Dist.	Elev	Comments
1.	39.0	47.0	0.0	2125	Top of SZ. in gully feature.
2.	48.0	35.0	16.0	2125	
3.	38.0	46.0	34.0	2110	
4.	39.5	37.0	55.0	2100	
5.	44.0	38.0	68.0	2100	
6.	37.5	43.0	73.5	2085	
7	37.0	37.0	89.5	2085	still in gully
8	44.0	36.0	120.0	2055	
9.	33.0	45.0	125.5		End gully, onto open slope w. shrubs.
10	33.0	34.5	155.0	2045	
11.	32.0	33.5	184.0	2025	
12.	32.5	32.0	200.0	2010.	Flag. ~4 m on mature spruce in middle of path.

Figure A.1 Field notes for Hector Ridge South avalanche path

3 of 6

4 of 6

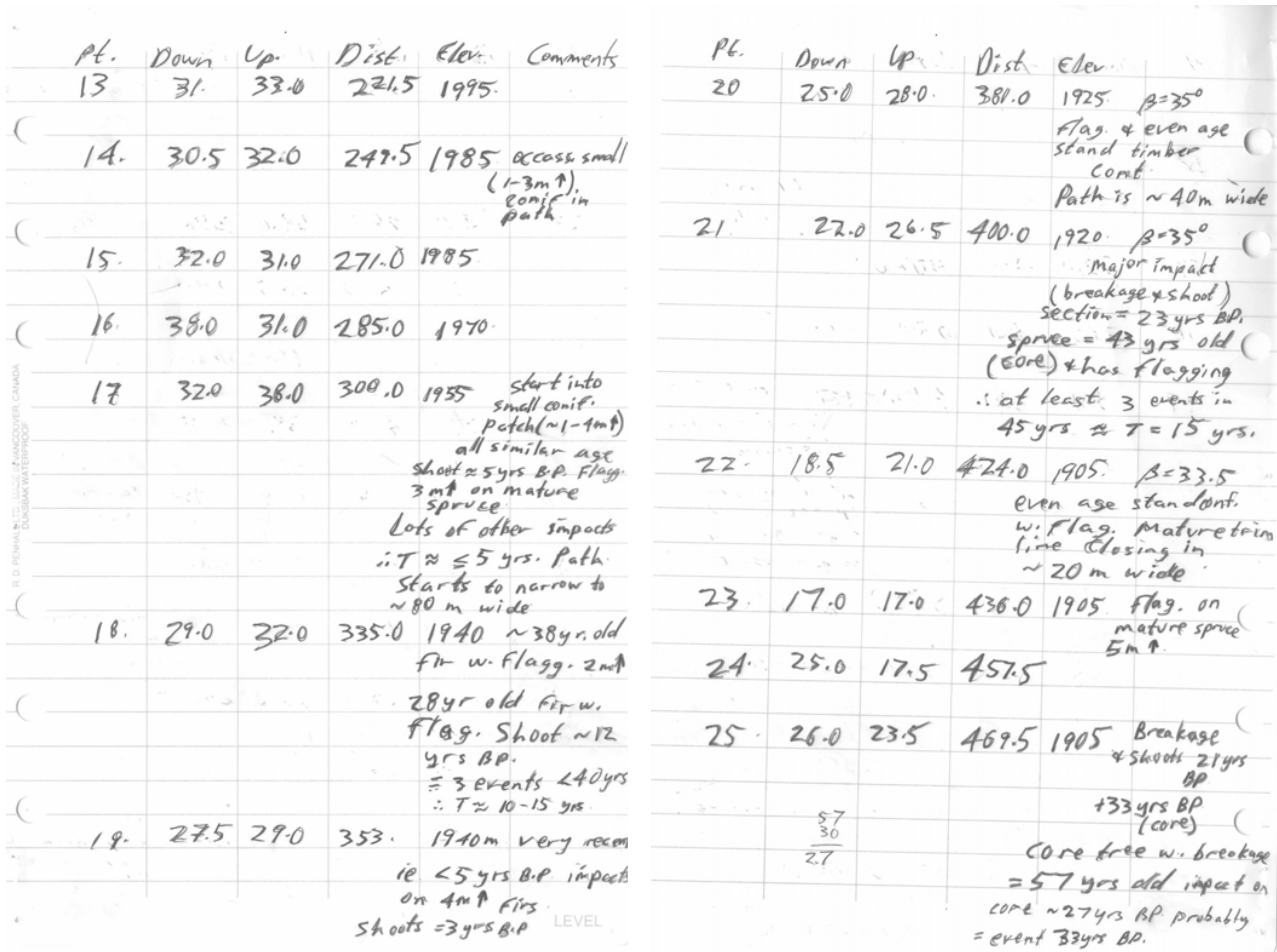

Pt.	Down	Up.	Dist.	Elev.	Comments
13	31.	33.0	221.5	1995.	
14.	30.5	32.0	249.5	1985	occass. small (1-3m↑) conif in path
15.	32.0	31.0	271.0	1985	
16.	38.0	31.0	285.0	1970.	
17	32.0	38.0	300.0	1955	start into small conif. patch(~1-4m↑) all similar age Shoot ≈ 5yrs B.P. Flagg. 3m↑ on mature spruce. Lots of other impacts ∴ T ≈ ≤ 5 yrs. Path Starts to narrow to ~80 m wide
18.	29.0	32.0	335.0	1940	~38yr. old fir w. Flagg. 2m↑ 28yr old Fir w. Flag. Shoot ~12 yrs BP. ⩧ 3 events <40yrs ∴ T ≈ 10-15 yrs
19.	27.5	29.0	353.	1940m	very recent ie <5yrs B.P impacts on 4m↑ firs Shoots = 3yrs B.P

Pt.	Down	Up.	Dist.	Elev.	
20	25.0	28.0.	381.0	1925.	β=35° Flag. & even age stand timber Cont. Path is ~40m wide
21.	22.0	26.5	400.0	1920.	β=35° major impact (breakage & shoot) section = 23yrs BP. Spruce = 43 yrs old (core) & has flagging ∴ at least 3 events in 45 yrs ≈ T = 15 yrs.
22.	18.5	21.0	424.0	1905.	β=33.5 even age stand cont. w. Flag. Mature trim line Closing in ~20 m wide
23.	17.0	17.0	436.0	1905.	Flag. on mature spruce 5m↑.
24.	25.0	17.5	457.5		
25.	26.0	23.5	469.5	1905	Breakage & shoots 21yrs BP +33yrs BP (core)
	57 30 27				Core tree w. breakage = 57 yrs old impact on core ~27yrs BP probably = event 33yrs BP.

Figure A.1 (Continued) Field notes for Hector Ridge South avalanche path

Pt.	Down	Up.	Dist.	Elev.
				∴ 3 events in 60 yrs
				$T \approx 20$ yrs.
26.	23.0	24.0	480.0	1885 Flagging on immature spruce 4 m ↑.
27	28.0	23.0	487.0	
28.	21.0	25.0	500.0	1875 Flag. on mature spruce 5 m ↑.
29.	7.0	22.0	512.5	1870. cont. immature Fir patch + flagging.
30.	8.0	7.5	533	start into mature spruce forest. Flag. 3 m ↑ on mature spruce
31.	13.0	9.0	547.0	$\beta = 30°$.
32.	19.5	15.0	564	1865 cont Flag. on mature spruce 4 m ↑
33	12.5	19.0	578.5	
34	13.0	12.0	600.0	$\beta = 28.5°$
35.	14.0	13.5	629.0	1855.
36.	14.0	14.0	651.5	1840 $\alpha = 27°$

pt. 36 End open patch within mature forest
Path closes up & only mature trees below.
∴ end extreme runout

Large spruce core = 109 yrs old
w. no impacts
∴ $T \approx 100$ yrs.

$$\begin{array}{r} 2125 \\ -\ 1840 \\ \hline 285 \end{array}$$

Figure A.1 (Continued) Field notes for Hector Ridge South avalanche path

APPENDIX B - SAMPLE PROFILE

An example of a profile for the Schroeder Shoulder avalanche path in the Columbia Mountains is shown in Figure B.1. This profile shows measurement points numbered from 1 in the starting position to 23 at the Trans-Canada Highway. Point 22 represents the interpreted extreme runout position interpreted from vegetation damage observed during the field survey. The coordinate system is measured from the origin in the lower left of the figure. It can be observed in Figure B.1 that the Schroeder Should path is a very good example of a hockey-stick profile, with an abrupt transition from the track to the runout zone at Point 18.

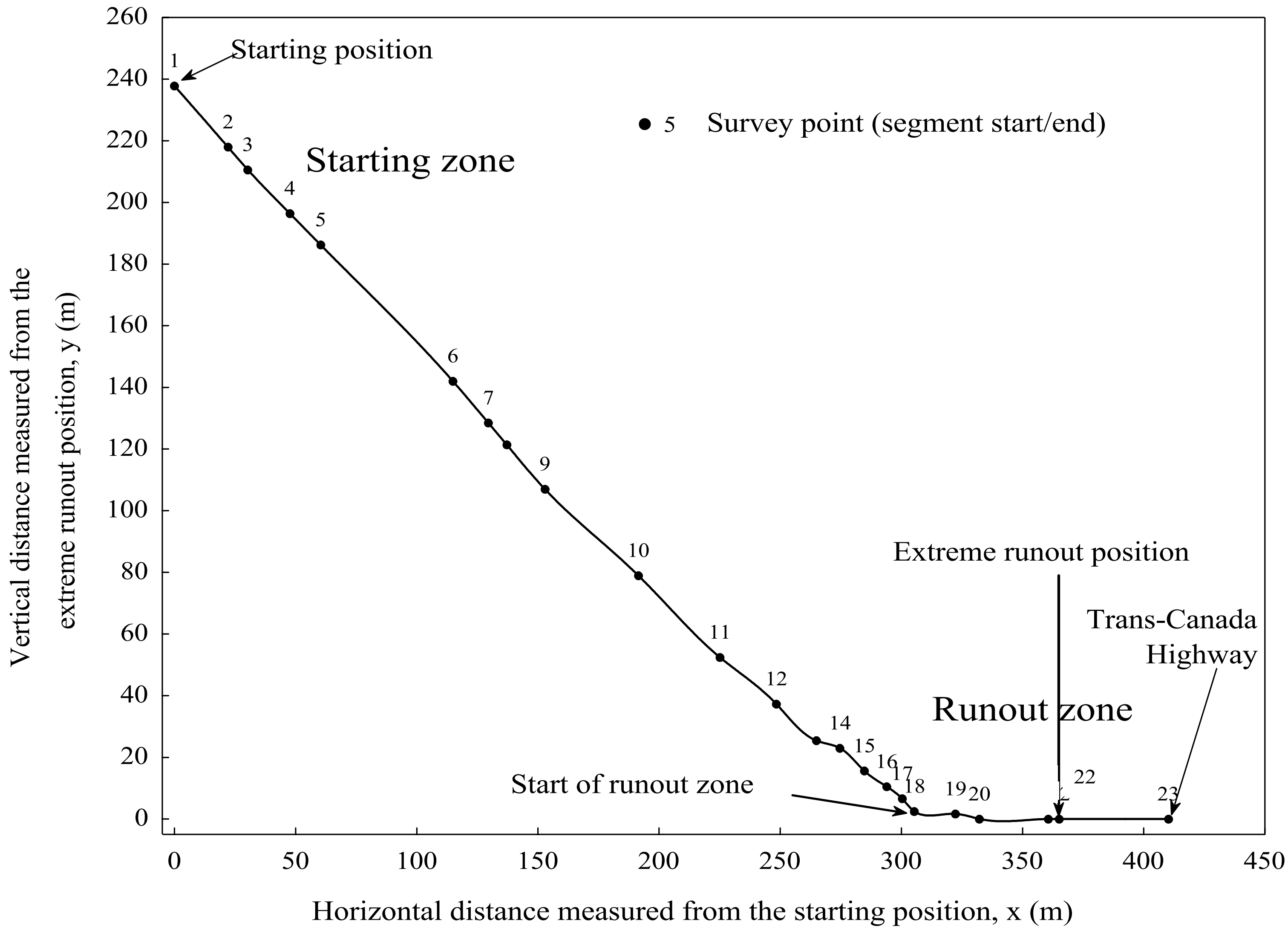

Figure B.1 Profile of Schroeder Shoulder path, Columbia Mountain Range